

# Prospects of GPD Measurements at EIC

TIDC Workshop at NCKU  
August 18, 2022

Po-Ju Lin  
Academia Sinica

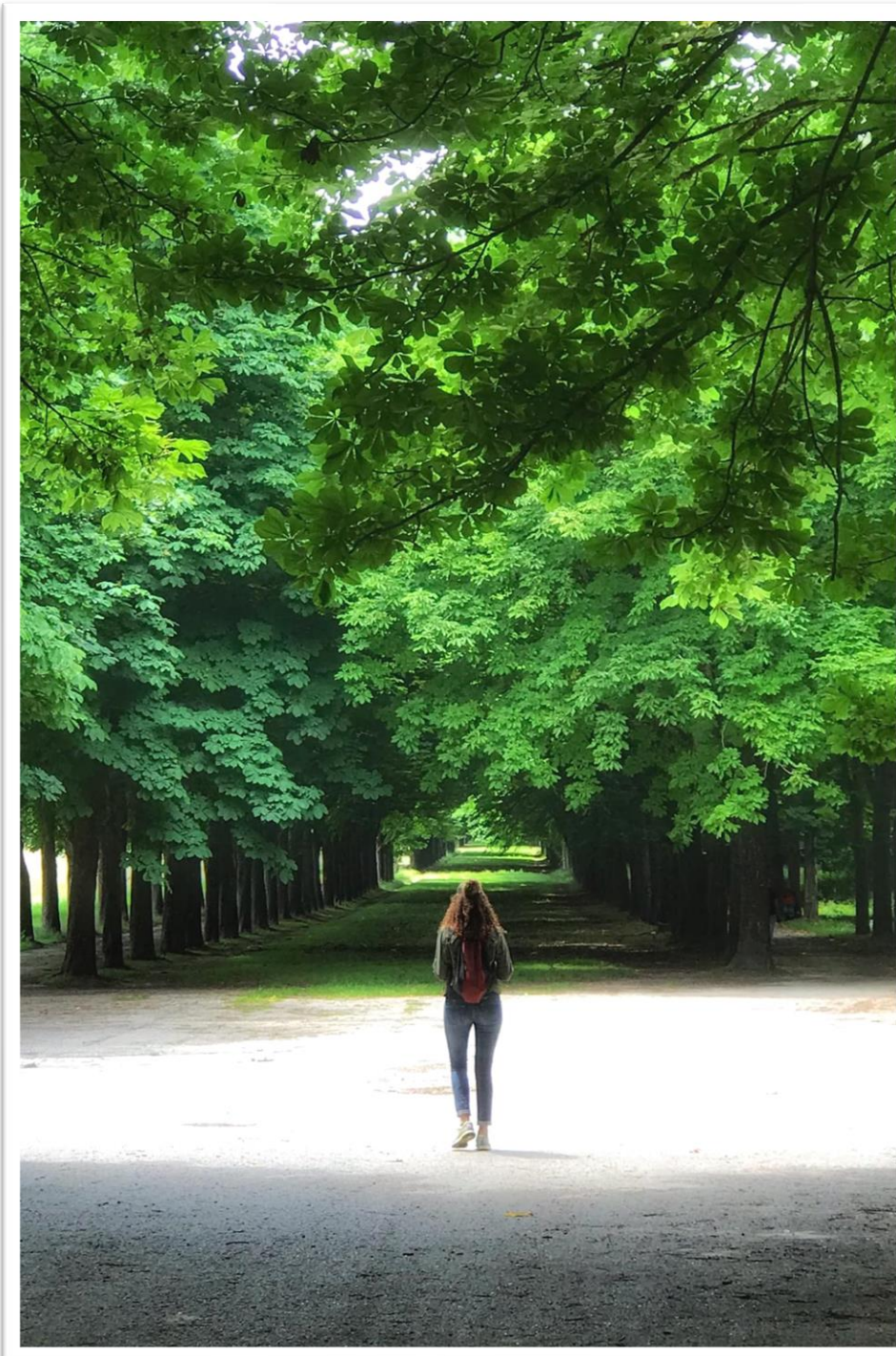
## **1. Review**

## **2. Outlook**

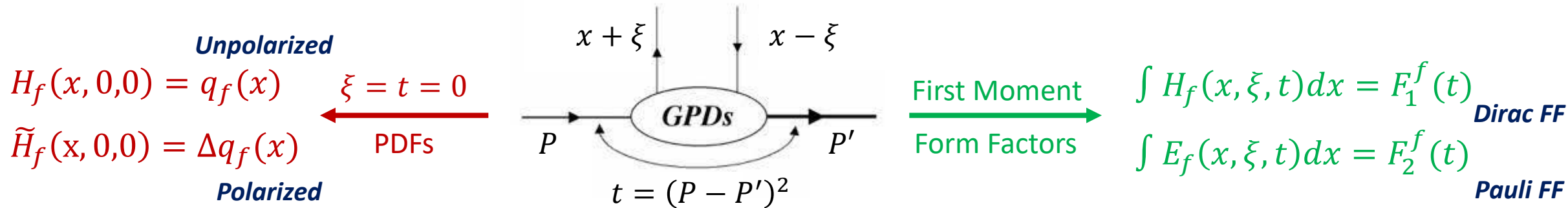
In this presentation, I blatantly took a lot of materials from:

- EIC white paper
- EIC yellow report
- Great talks presented by Andrey Kim, Dariah Sokhan, Stepan Stepanyan, Nicole d'Hose and many others

# Trodded paths & where we are



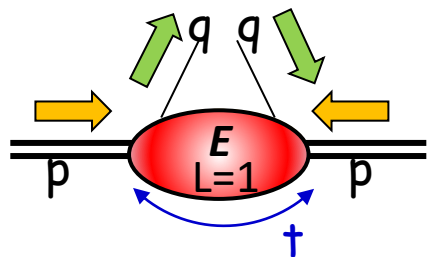
# Generalized Parton Distributions (GPDs)



➤ GPDs embody both PDFs and FFs

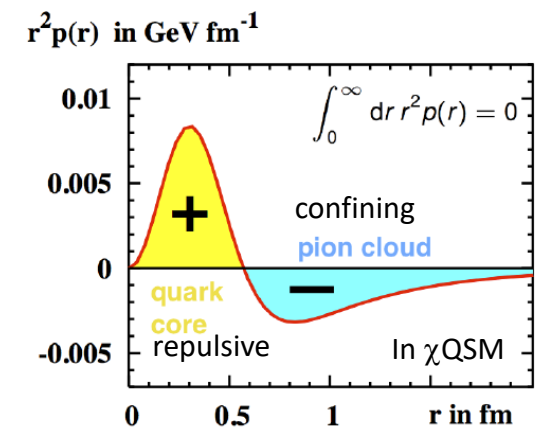
Provides information on the interesting properties of the nucleon.

- Mapping the transverse plane distribution of parton
- Pressure distribution inside nucleon
- Angular momentum of parton



$$J_q = \frac{1}{2} \int_{-1}^1 dx x [H^q(x, \xi, 0) + E^q(x, \xi, 0)]$$

*Ji's Sum Rule*



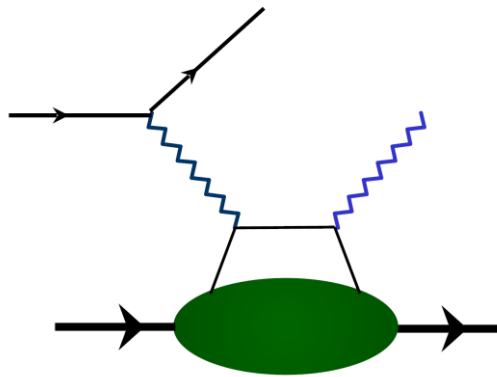


# Exclusive Process

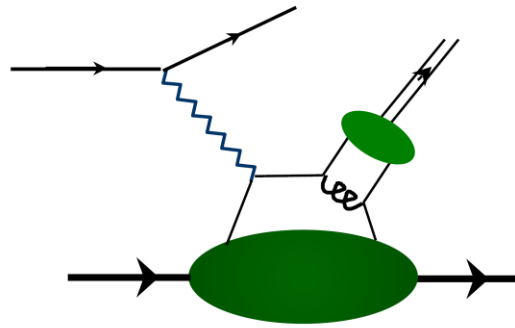
➤ Use **exclusive processes**, where all final state particles are “detected”, to access the multi-variable dependence of GPDs, and constrain the GPD parameterization with measurements in various phase space.

➤ Processes:

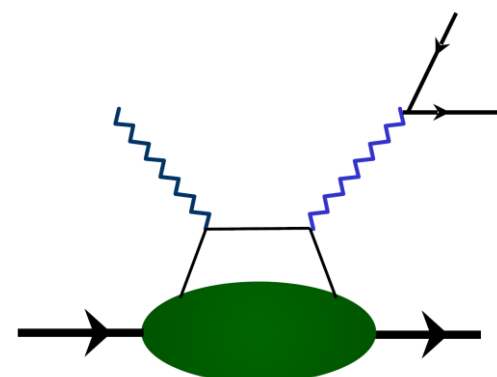
- **Deeply Virtual Compton Scattering (DVCS)**
- Deeply Virtual Meson Production (DVMP)
- Time-like Compton Scattering (TCS)
- Double DVCS (DDVCS)
- ...



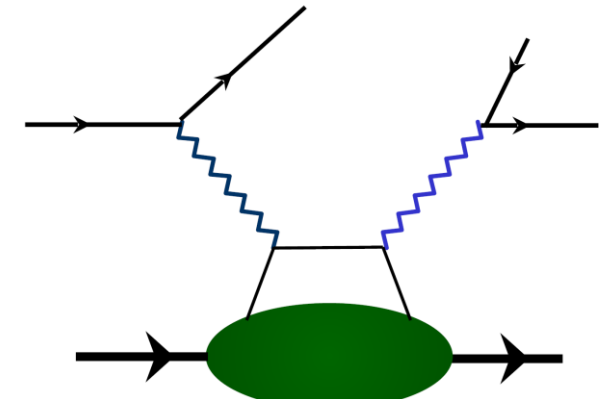
**DVCS**



**DVMP**

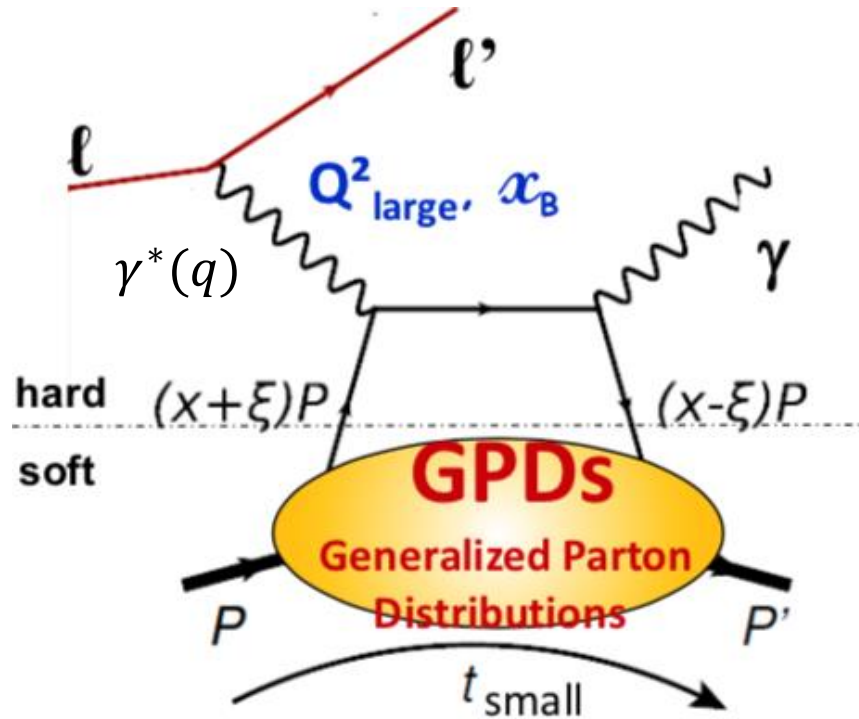


**TCS**



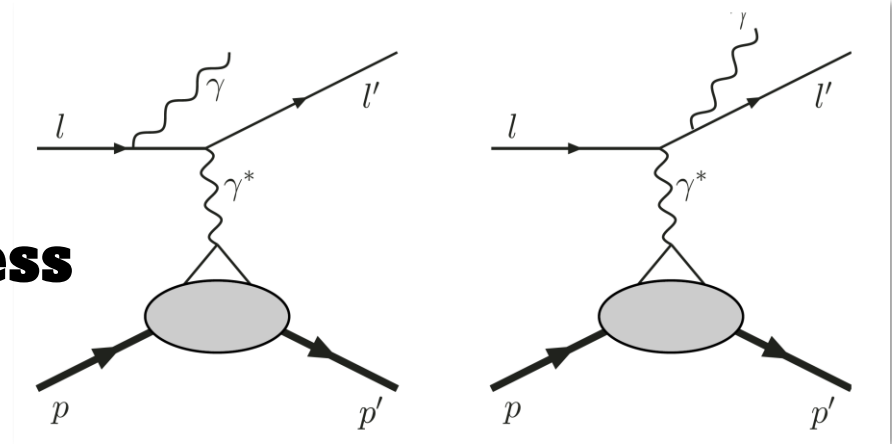
**DDVCS**

# Deeply Virtual Compton Scattering



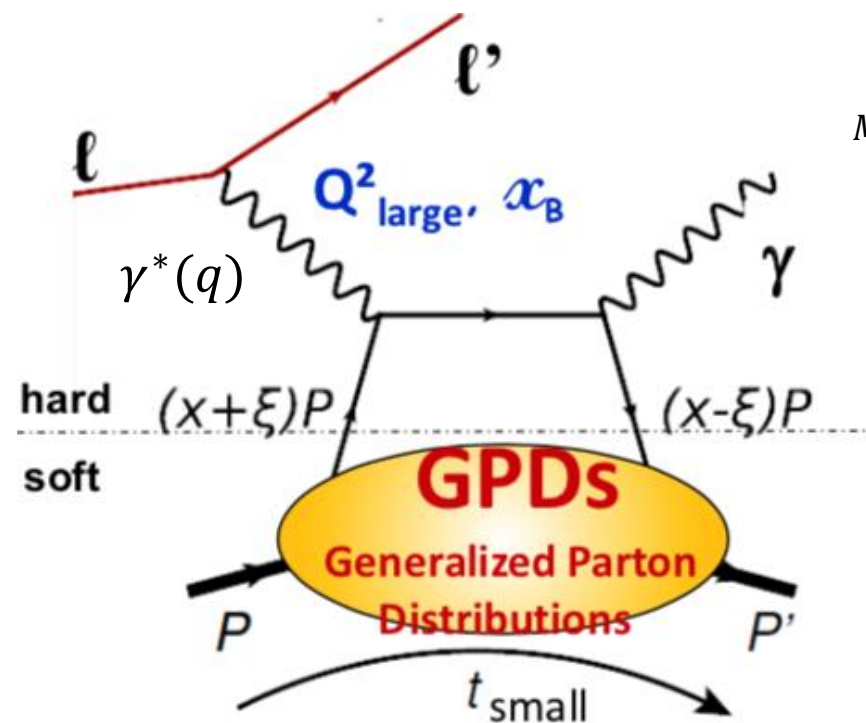
$$\text{DVCS: } l + p \rightarrow l' + p' + \gamma$$

**BH  
Process**



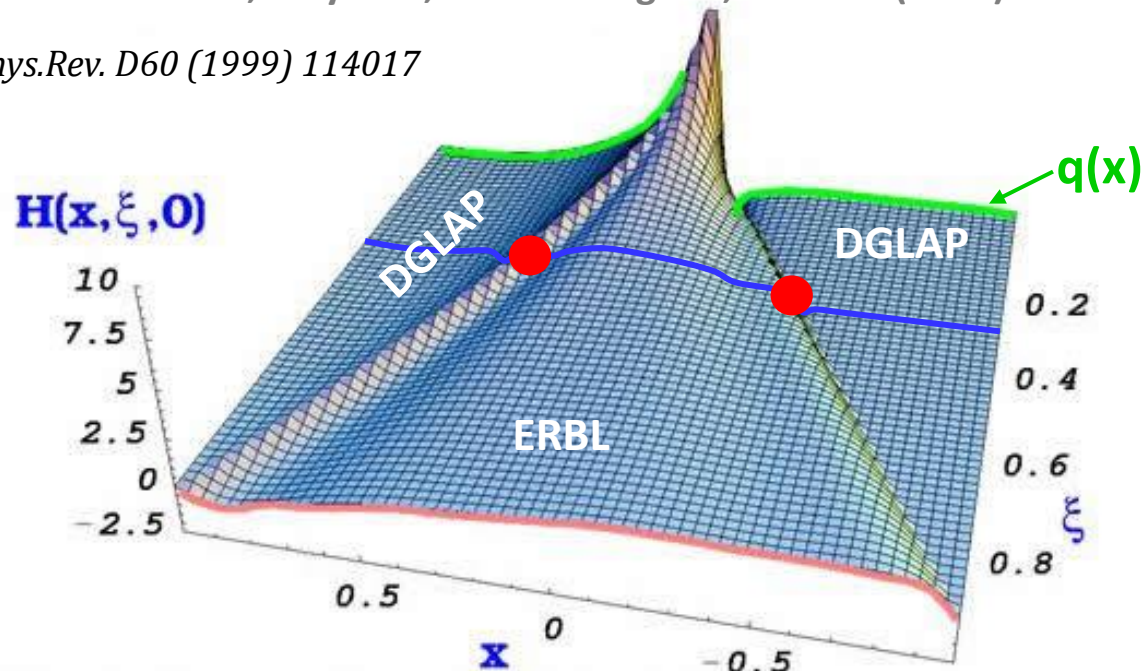
- DVCS is regarded as the golden channel and gives access to four chiral-even GPDs  $H, \tilde{H}, E, \tilde{E}(x, \xi, t)$ . Its interference with the well-understood Bethe-Heitler process gives access to more info.

# Compton Form Factors (CFFs)



From Goeke, Polyakov, Vanderhaeghen, PNPP47 (2001)

M. Polyakov, C. Weiss, Phys.Rev. D60 (1999) 114017



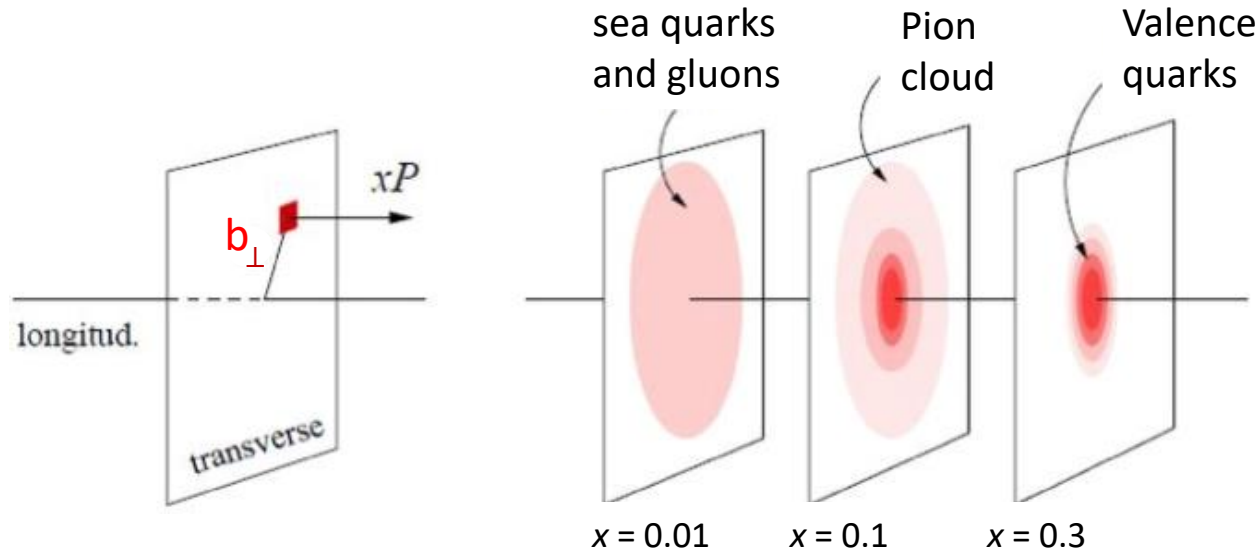
$$\overset{\text{CFF}}{\mathcal{H}(\xi, t)} \overset{\text{GPD}}{=} \int_{-1}^{+1} dx \frac{\mathbf{H}(x, \xi, t)}{x - \xi + i\epsilon} + \dots = \mathcal{P} \int_{-1}^{+1} dx \frac{\mathbf{H}(x, \xi, t)}{x - \xi} - i\pi \mathbf{H}(x = \pm \xi, \xi, t) + \dots$$

$$\text{Re } \mathcal{H}(\xi, t) = \mathcal{P} \int dx \frac{\text{Im } \mathcal{H}(x, t)}{x - \xi} + \Delta(t)$$

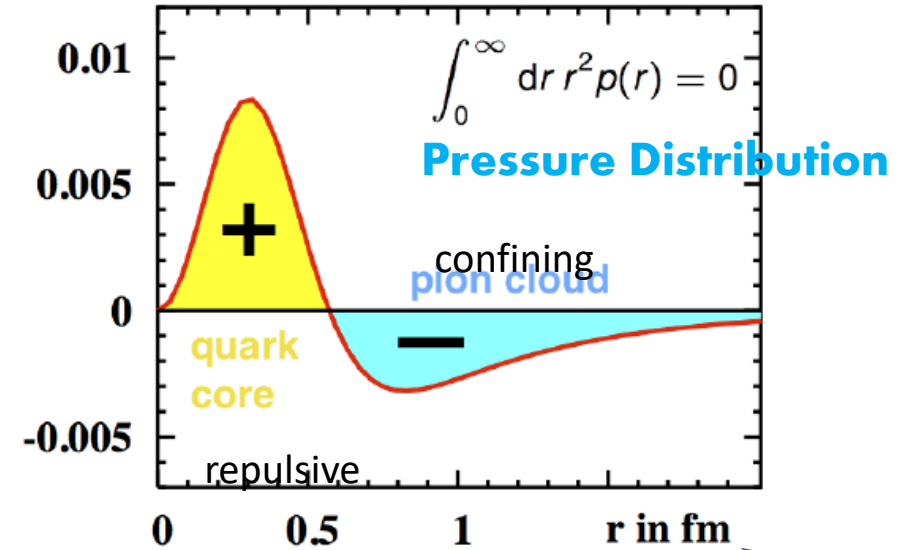
# Transverse Imaging and Pressure Distribution

M. Polyakov, P. Schweitzer, *Int.J.Mod.Phys. A33* (2018)

## Mapping in the transverse plane



$r^2 p(r)$  in  $\text{GeV fm}^{-1}$



CFP  $\mathcal{H}(\xi, t)$  GPD

$$\mathcal{H}(\xi, t) = \int_{-1}^{+1} dx \frac{\mathbf{H}(x, \xi, t)}{x - \xi + i\epsilon} + \dots = \mathcal{P} \int_{-1}^{+1} dx \frac{\mathbf{H}(x, \xi, t)}{x - \xi} - i\pi \mathbf{H}(x = \pm \xi, \xi, t) + \dots$$

REAL part

$$\text{Re } \mathcal{H}(\xi, t) = \mathcal{P} \int dx \frac{\text{Im } \mathcal{H}(x, t)}{x - \xi} + \Delta(t)$$

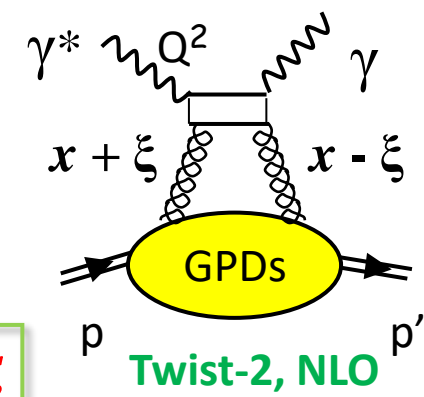
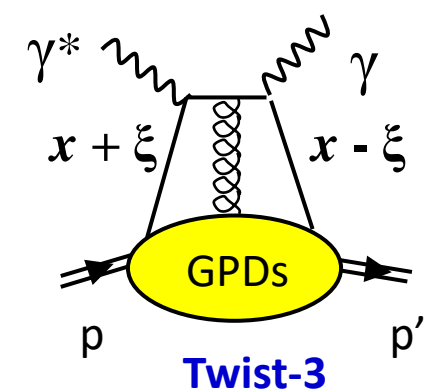
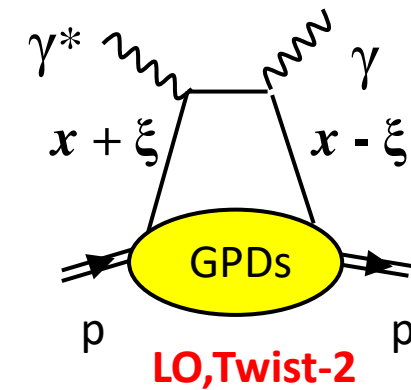
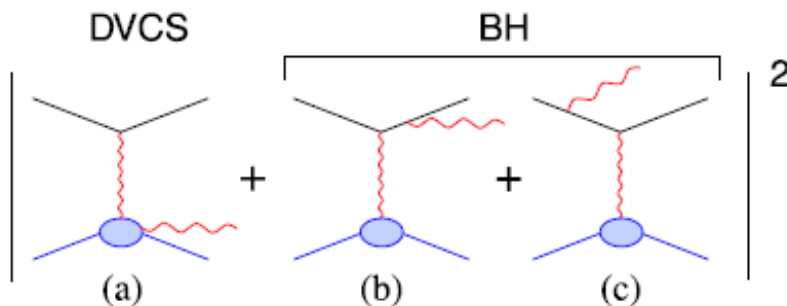
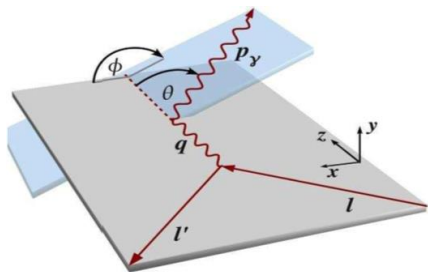
Imaginary part

FT of  $\mathcal{H}(x, \xi=0, t)$

D-term  $d_1(t)$

# Polarized Beam & Unpolarized Target

- Experimental access by cross-sections and spin asymmetries



$$\frac{d^4\sigma(\ell p \rightarrow \ell p \gamma)}{dx_B dQ^2 d|t| d\phi} = \underset{\text{Well known}}{d\sigma^{BH}} + \left( d\sigma_{impol}^{DVCS} + P_\ell d\sigma_{pol}^{DVCS} \right) + (e_\ell \text{Re } I + e_\ell P_\ell \text{Im } I)$$

$$d\sigma^{BH} \propto c_0^{BH} + c_1^{BH} \cos \phi + c_2^{BH} \cos 2\phi$$

$$d\sigma_{impol}^{DVCS} \propto c_0^{DVCS} + c_1^{DVCS} \cos \phi + c_2^{DVCS} \cos 2\phi$$

$$d\sigma_{pol}^{DVCS} \propto s_1^{DVCS} \sin \phi$$

$$\text{Re } I \propto c_0^I + c_1^I \cos \phi + c_2^I \cos 2\phi + c_3^I \cos 3\phi$$

$$\text{Im } I \propto s_1^I \sin \phi + s_2^I \sin 2\phi$$

Change  $P_\ell \rightarrow s_1^I = \text{Im } \mathcal{F}$

Change  $e_\ell, P_\ell \rightarrow c_1^I = \text{Re } \mathcal{F}$

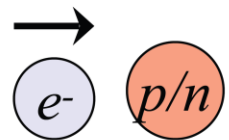
$$\mathcal{F} = F_1 \mathcal{H} + \xi(F_1 + F_2) \tilde{\mathcal{H}} + t/4m^2 F_2 \mathcal{E}$$



# Sensitivity to CFFs

➤ The target polarization can be explored as well.

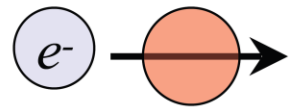
Beam, target  
polarisation



*For example:*

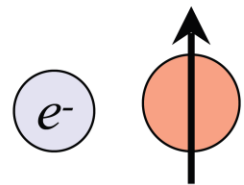
$$\Delta\sigma_{LU} \sim \sin\phi \Im(F_1 H + \xi G_M \tilde{H} - \frac{t}{4M^2} F_2 E) d\phi$$

Proton	Neutron
$\Im\{H_p, \tilde{H}_p, E_p\}$	$\Im\{H_n, \tilde{H}_n, E_n\}$



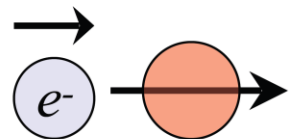
$$\Delta\sigma_{UL} \sim \sin\phi \Im(F_1 \tilde{H} + \xi G_M(H + \frac{x_B}{2} E) - \xi \frac{t}{4M^2} F_2 \tilde{E} + \dots) d\phi$$

$\Im\{H_p, \tilde{H}_p\}$	$\Im\{H_n, E_n, \tilde{E}_n\}$
---------------------------	--------------------------------



$$\Delta\sigma_{UT} \sim \cos\phi \Im(\frac{t}{4M^2}(F_2 H - F_1 E) + \dots) d\phi$$

$\Im\{H_p, E_p\}$	$\Im\{H_n\}$
-------------------	--------------



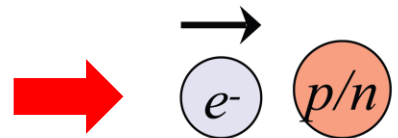
$$\Delta\sigma_{LL} \sim (A + B \cos\phi) \Re(F_1 \tilde{H} + \xi G_M(H + \frac{x_B}{2} E) + \dots) d\phi$$

$\Re\{H_p, \tilde{H}_p\}$	$\Re\{H_n, E_n, \tilde{E}_n\}$
---------------------------	--------------------------------

# Sensitivity to CFFs

➤ The target polarization can be explored as well.

Beam, target polarisation

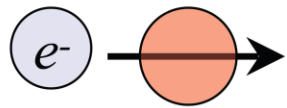


*For example:*

$$\Delta\sigma_{LU} \sim \sin\phi \Im(F_1 H + \xi G_M \tilde{H} - \frac{t}{4M^2} F_2 E) d\phi$$

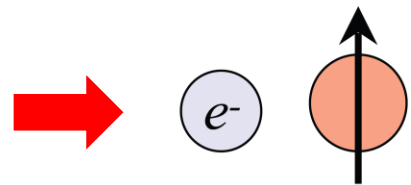
Proton      Neutron

$$\begin{aligned} & \text{Im}\{H_p, \tilde{H}_p, E_p\} \\ & \text{Im}\{H_n, \tilde{H}_n, E_n\} \end{aligned}$$



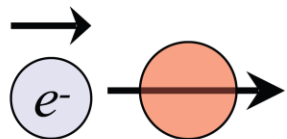
$$\Delta\sigma_{UL} \sim \sin\phi \Im(F_1 \tilde{H} + \xi G_M (H + \frac{x_B}{2} E) - \xi \frac{t}{4M^2} F_2 \tilde{E} + \dots) d\phi$$

$$\begin{aligned} & \text{Im}\{H_p, \tilde{H}_p\} \\ & \text{Im}\{H_n, E_n, \tilde{E}_n\} \end{aligned}$$



$$\Delta\sigma_{UT} \sim \cos\phi \Im(\frac{t}{4M^2} (F_2 H - F_1 E) + \dots) d\phi$$

$$\begin{aligned} & \text{Im}\{H_p, E_p\} \\ & \text{Im}\{H_n\} \end{aligned}$$

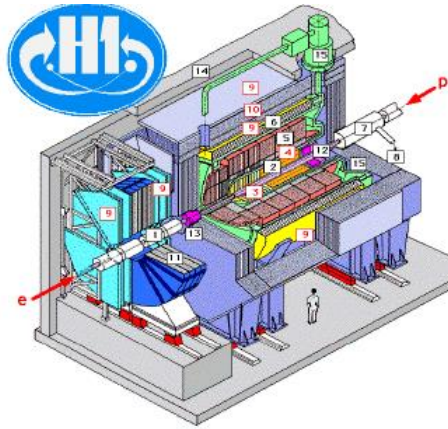


$$\Delta\sigma_{LL} \sim (A + B \cos\phi) \Re(F_1 \tilde{H} + \xi G_M (H + \frac{x_B}{2} E) + \dots) d\phi$$

$$\begin{aligned} & \text{Re}\{H_p, \tilde{H}_p\} \\ & \text{Re}\{H_n, E_n, \tilde{E}_n\} \end{aligned}$$

➤ **Neutron target: flavor decomposition & access to  $E$**

# The Past and Present Experiments

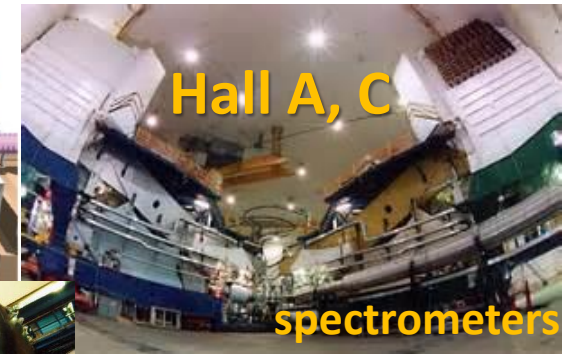


## e-p Collider forward fast proton

- **HERA: H1** and **ZEUS**  
Polarised **27 GeV** e-/e+  
Unpolarized **920 GeV** proton  
~ *Full event reconstruction*

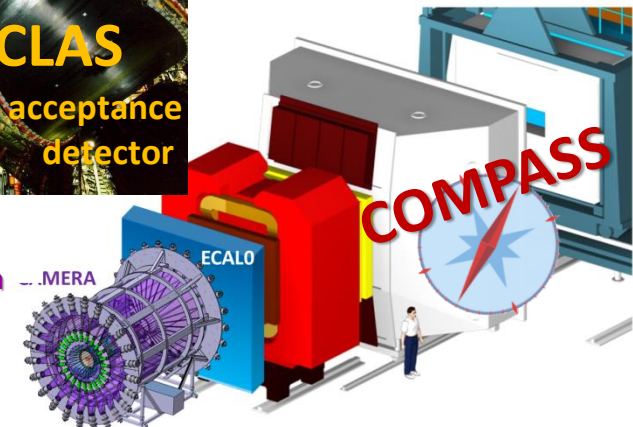
## Fixed target mode slow recoil proton

- **HERMES:** Polarised **27 GeV** e-/e+  
Long., Trans. polarised p, d target  
*Missing mass technique, 2006-09 with recoil detector*
- **Jlab: Hall A, C, CLAS** High Luminosity Polar. **6 & 12 GeV** e-  
Long., (Trans.) polarised p, d target  
*Missing mass technique (A,C) and complete detection (CLAS)*
- **COMPASS @ CERN:** Polarised **160 GeV**  $\mu^+/\mu^-$   
p target, (Trans.) polarised *target with recoil p detection*



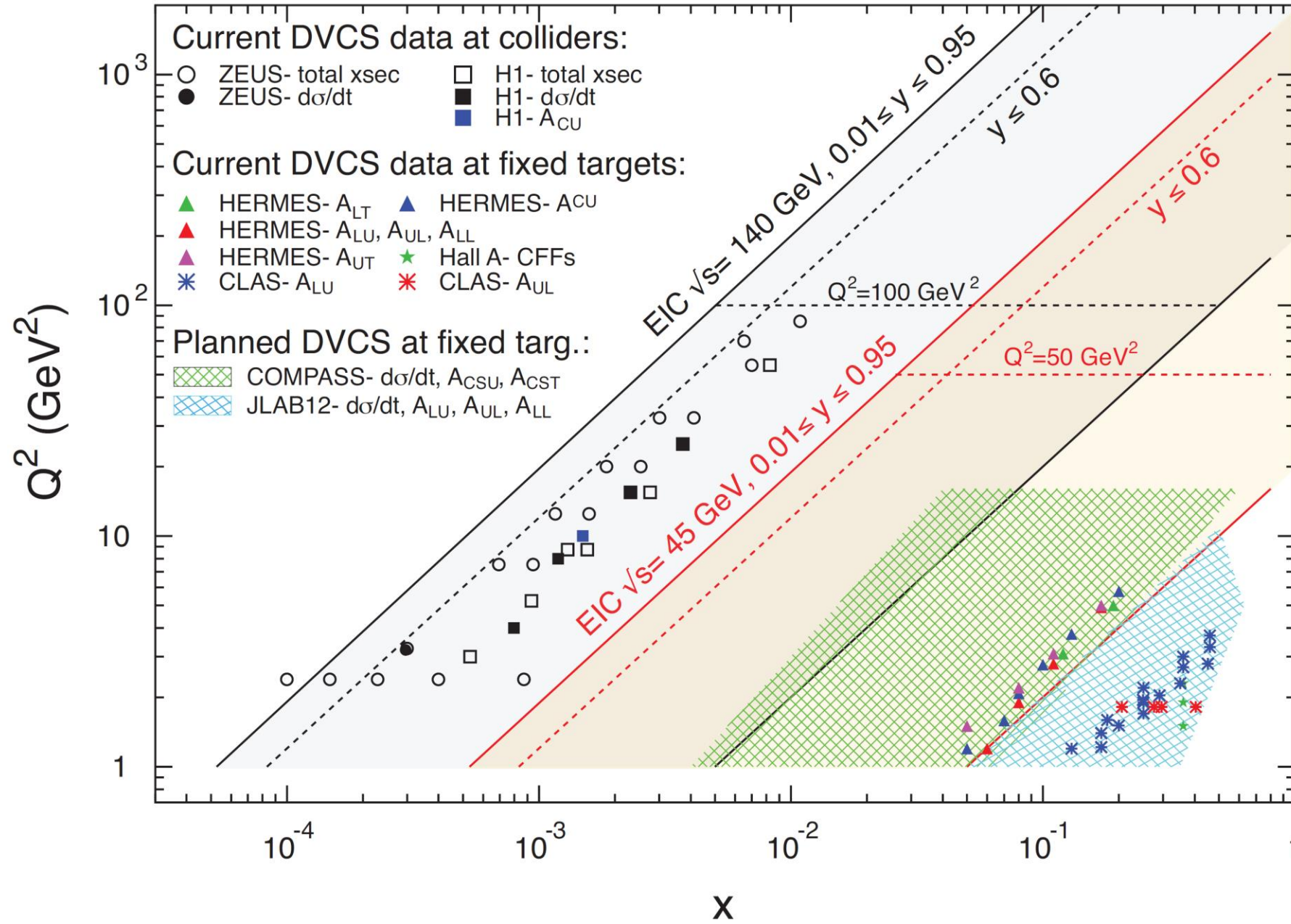
**CLAS**  
large acceptance detector

recoil proton detector CAMERA



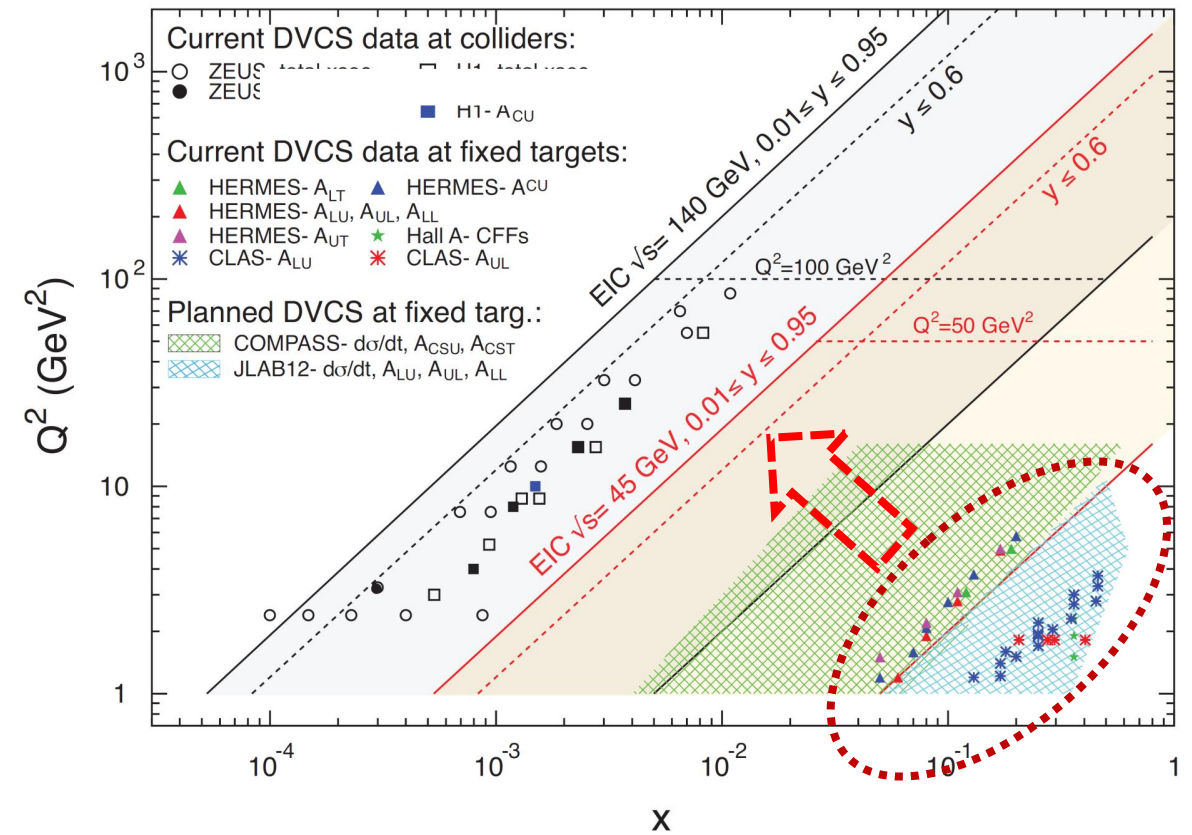


# Landscape – Global Programs of DVCS



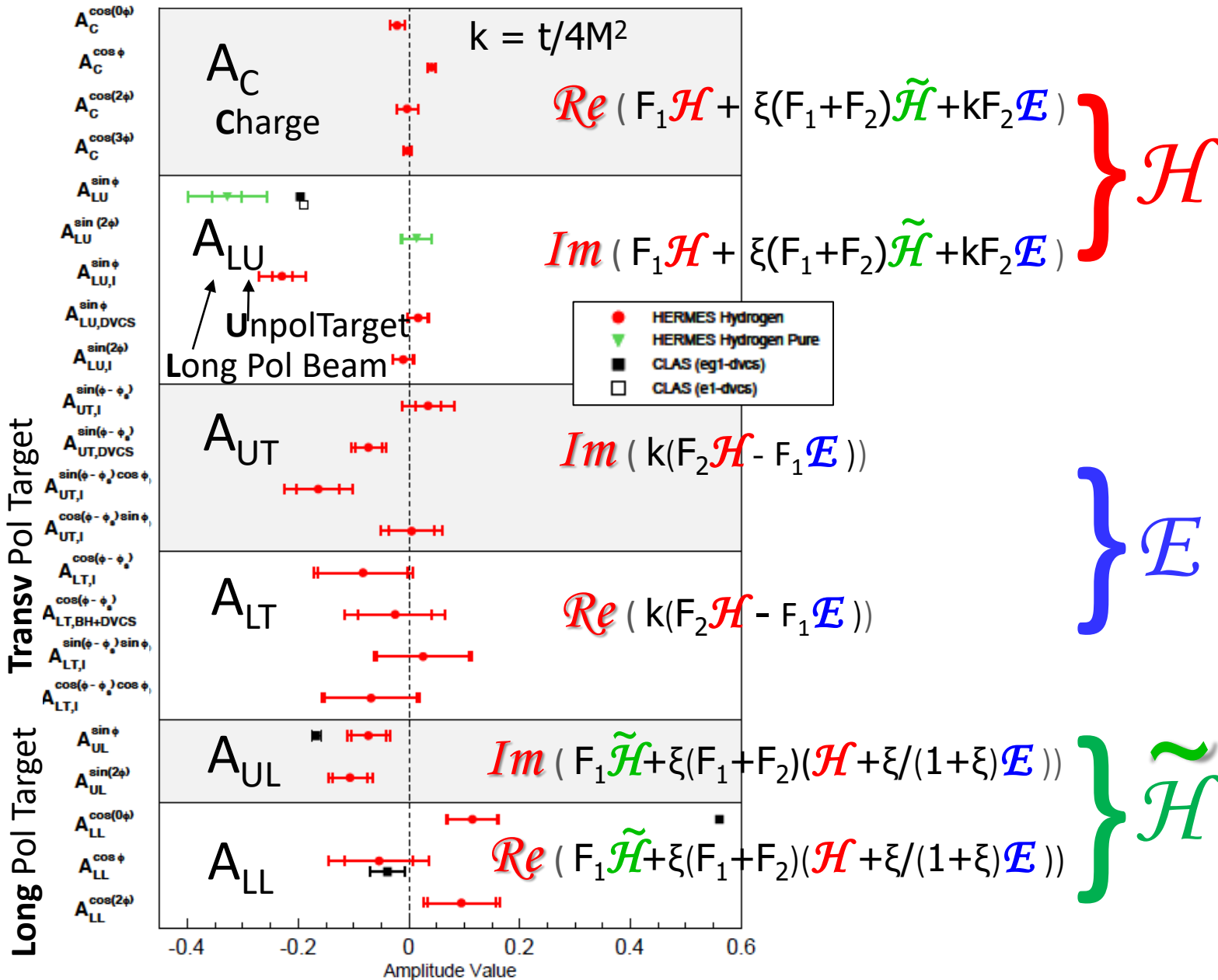
# DVCS Measurements

Starting with lower energy – intermediate to high  $x$





# A complete set of DVCS asymmetries at Hermes



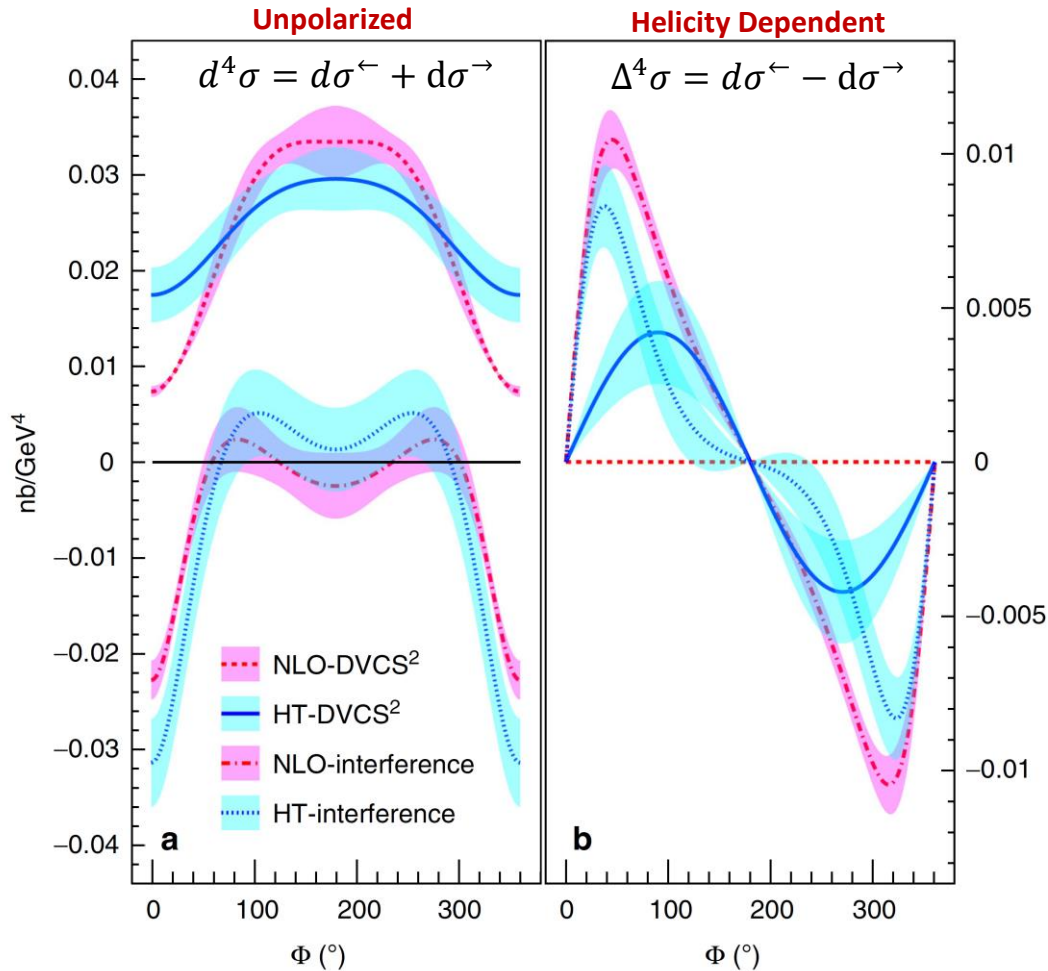
## HERMES provided a complete set of observables

- 2001: 1<sup>st</sup> DVCS publication as CLAS & H1
- 2007: end of data taking
- 2012: still important publications
  - JHEP 07 (2012) 032  $A_C$   $A_{LU}$
  - JHEP10(2012) 042  $A_{LU}$
  - with recoil detection (2006-7)

- Electron & positron beams on proton
- Beam energy of 27.6 GeV
- Luminosity  $\leq 10^{31} \text{ cm}^{-2} \text{ s}^{-1}$
- Most data within:
  - $0.05 \leq x_B \leq 0.2$
  - $2 \text{ GeV}^2 \leq Q^2 \leq 6 \text{ GeV}^2$

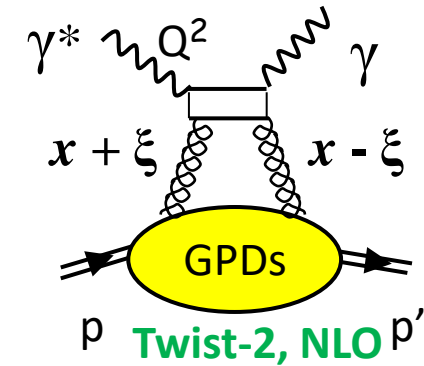
# Beam Spin Sum and Diff of DVCS at JLab Hall A

- After the pioneering E00-110 in 2004 at Hall-A, the E07-007 experiment in 2010
- High precision cross-section measurement in a small kinematic region: Generalized Rosenbluth separation of the DVCS<sup>2</sup> (scales as  $E_e^2$ ) and the BH-DVCS interference (scales as  $E_e^3$ ) terms. **NLO and/or higher-twist improve model agreement**



$$\vec{e} p \rightarrow e \gamma p$$

- $E_e$ : 4.5 & 5.6 GeV
- $Q^2$ : 1.5, 1.9, 2.3 GeV<sup>2</sup> at fixed  $x_B$ : 0.36

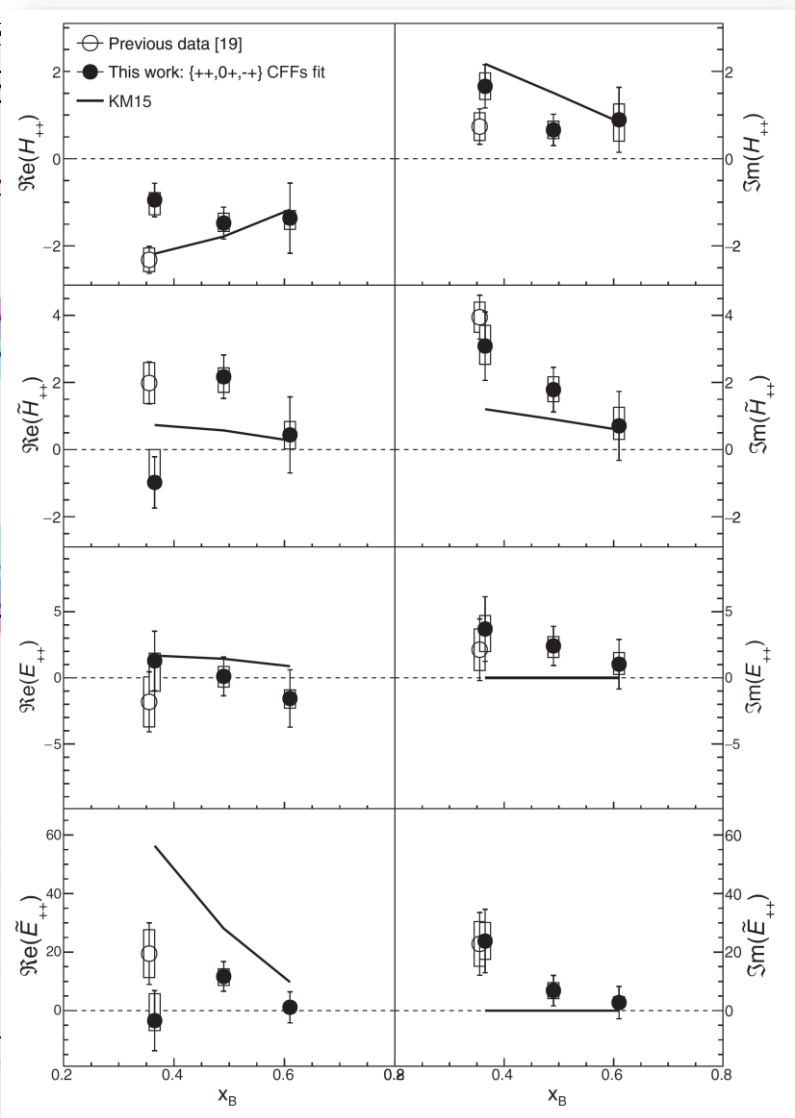
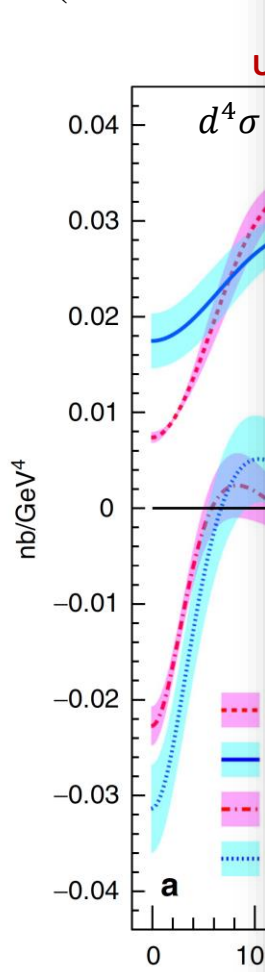


- Two scenarios: **higher-twist** or **next-to-leading order**
- Significant differences between pure DVCS and interference contributions.
- Sensitivity to gluons.
- Separation of HT and NLO effects requires scans across wider ranges of  $Q^2$  and beam energy  $\rightarrow$  JLab 12

# Beam Spin Sum and Diff of DVCS at JLab Hall A

➤ After the pioneering E00-110 in 2004 at Hall-A, the E07-007 experiment in 2010

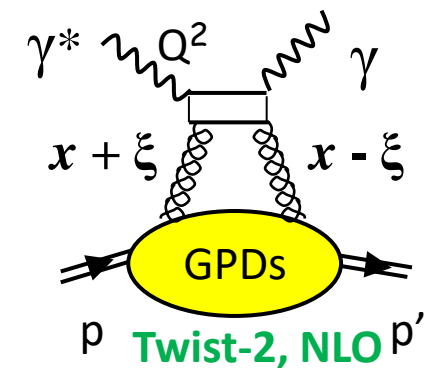
➤ High precision  
(scales as  $E_e^3$ )



kinematic region: Generalized Rosenbluth separation of the DVCS<sup>2</sup> as  $E_e^3$  terms. **NLO and/or higher-twist improve model agreement**

$$\vec{e} p \rightarrow e \gamma p$$

- $E_e$ : 4.5 & 5.6 GeV
- $Q^2$ : 1.5, 1.9, 2.3 GeV<sup>2</sup> at fixed  $x_B$ : 0.36



- Two scenarios: **higher-twist** or **next-to-leading order**
- Significant differences between pure DVCS and interference contributions.
- Sensitivity to gluons.
- Separation of HT and NLO effects requires scans across wider ranges of  $Q^2$  and beam energy → JLab 12

➤ **First experimental extraction of all four helicity-conserving CFFs**

F. Georges et al. (JLab Hall A Collaboration), Phys. Rev. Lett. 128, 252002 (June 2022)

# Nucleon Tomography in the Valence Domain with CLAS Data

Fit of 8 CFFs at **L.O.** and **L.T.**

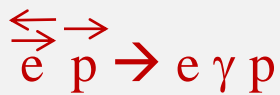
( $\text{Im}H$ ,  $\text{Re}H$ ,  $\text{Im}E$ ,  $\text{Re}E$ ,  $\text{Im}\tilde{H}$ ,  $\text{Re}\tilde{H}$ ,  $\text{Im}\tilde{E}$ ,  $\text{Re}\tilde{E}$ )

Better Constrained

- Wide kinematic coverage
- Carried out measurements with longitudinally polarized target as well



- Valence quarks at centre
- Sea quarks spread out towards the periphery.

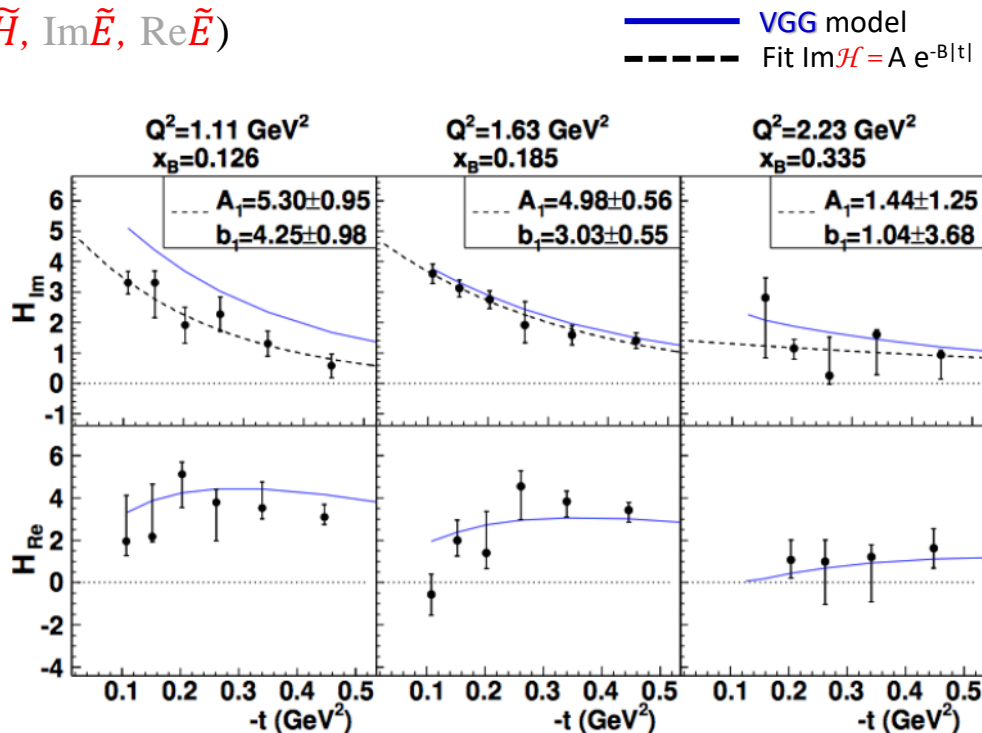


- Simultaneous fit to BSA, TSA & DSA → Information on relative distribution of quark momenta (PDFs) and quark helicity,  $\Delta q(x)$

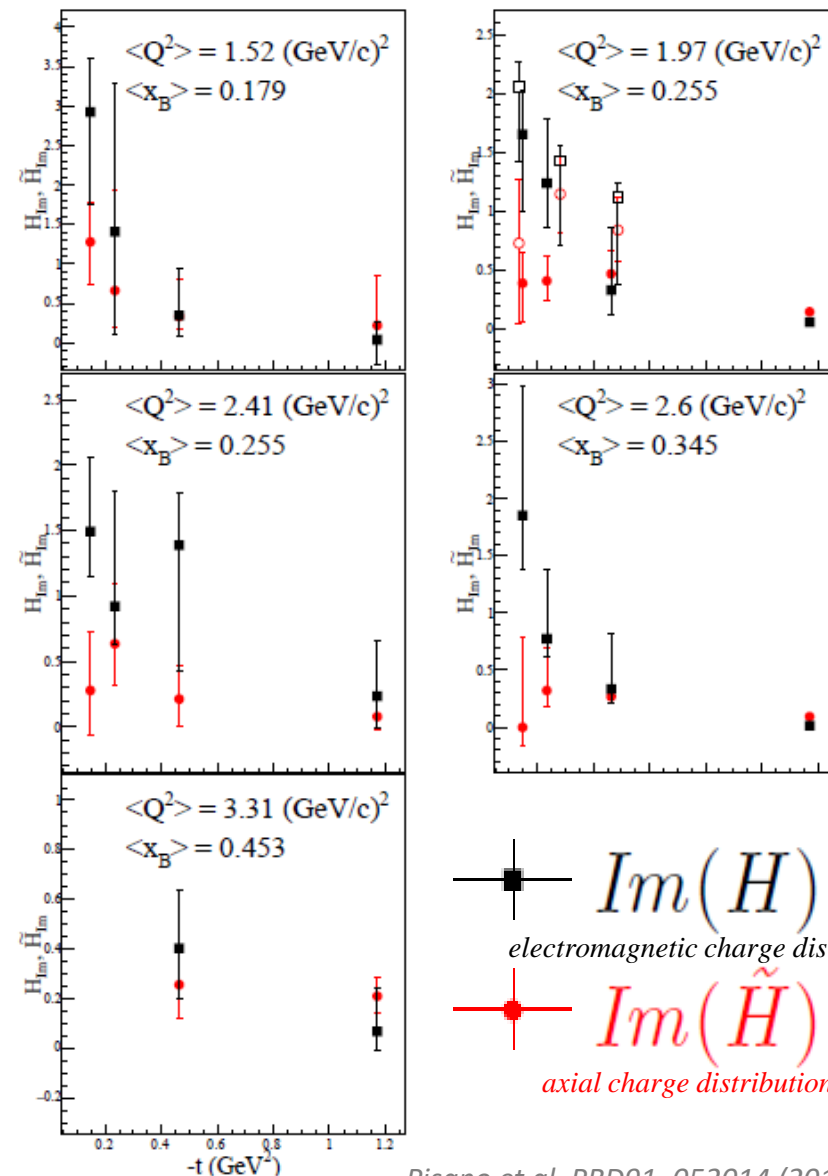
$$H(x, 0, 0) = q(x) \quad \tilde{H}(x, 0, 0) = \Delta q(x)$$

$$\int_{-1}^{+1} H dx = F_1 \quad \int_{-1}^{+1} \tilde{H} dx = G_A$$

- Indication that axial charge is more concentrated than electromagnetic charge



H.-S. Jo et al. (CLAS) PRL115, 212003 (2015) 212003  
N. Hirlinger Saylor et al (CLAS) PRC 98 (2018) 045203



$\blacksquare$   $\text{Im}(H)$   
electromagnetic charge distribution  
 $\bullet$   $\text{Im}(\tilde{H})$   
axial charge distribution

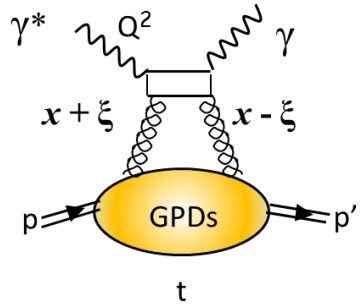
Pisano et al. PRD91, 052014 (2015)  
Seder et al. PRL114, 032001 (2015)

# Nucleon Tomography in the Gluon Domain at HERA

$$d\sigma^{DVCS}/d|t| \propto e^{-B|t|}$$

$B'$  related to the transversed size of the scattering object

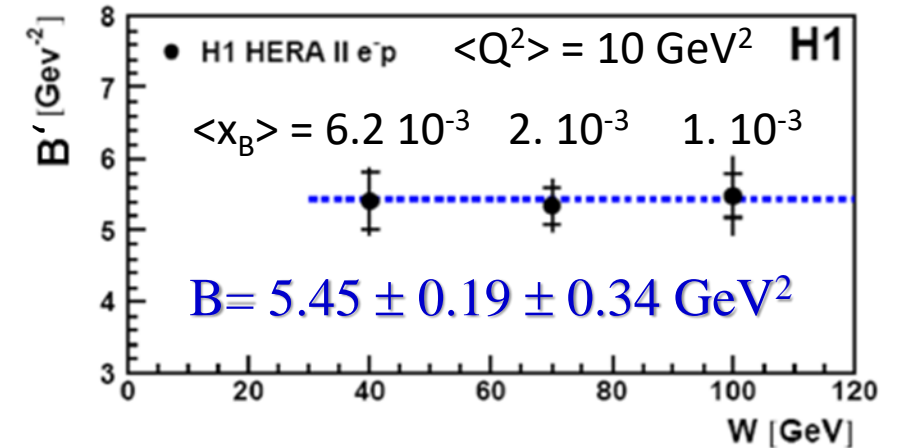
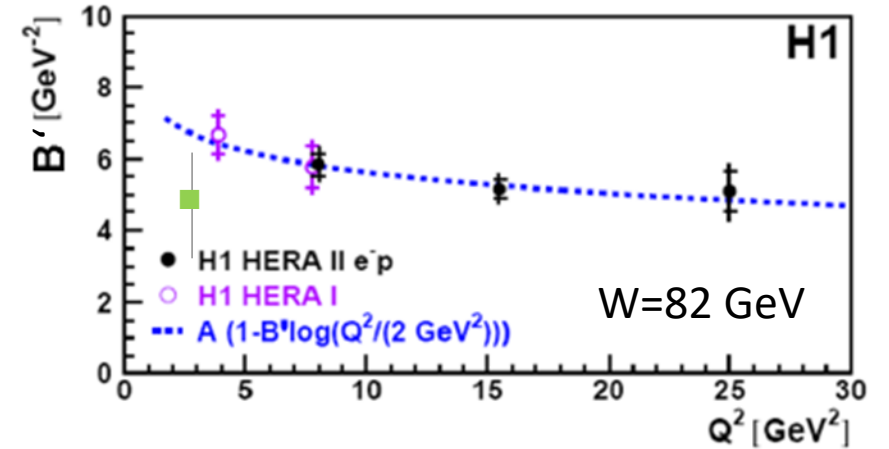
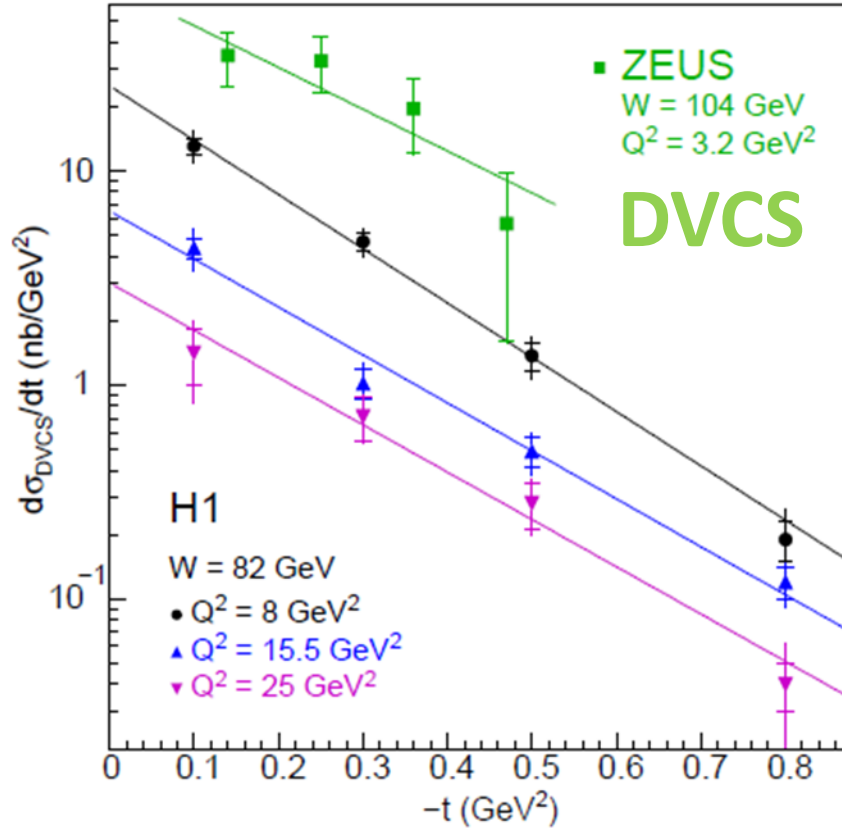
Dominance of  $Im\mathcal{H}$



**ZEUS-H1**

Data collected  
1995-2007

Aaron et al., H1 Coll, PLB659 (2008)



$$\langle r_{\perp}^2(x_B) \rangle \approx 2 B'(x_B)$$

$$\sqrt{\langle r_{\perp}^2 \rangle} = 0.65 \pm 0.02 \text{ fm}$$

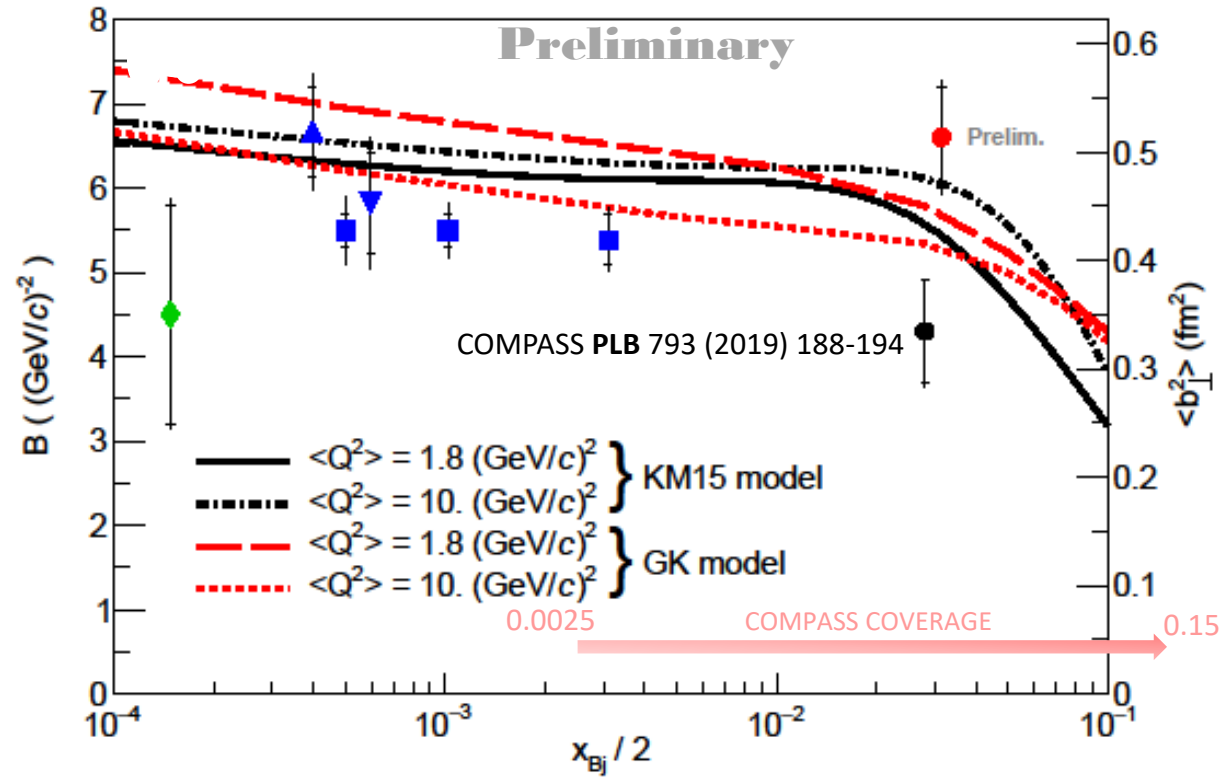
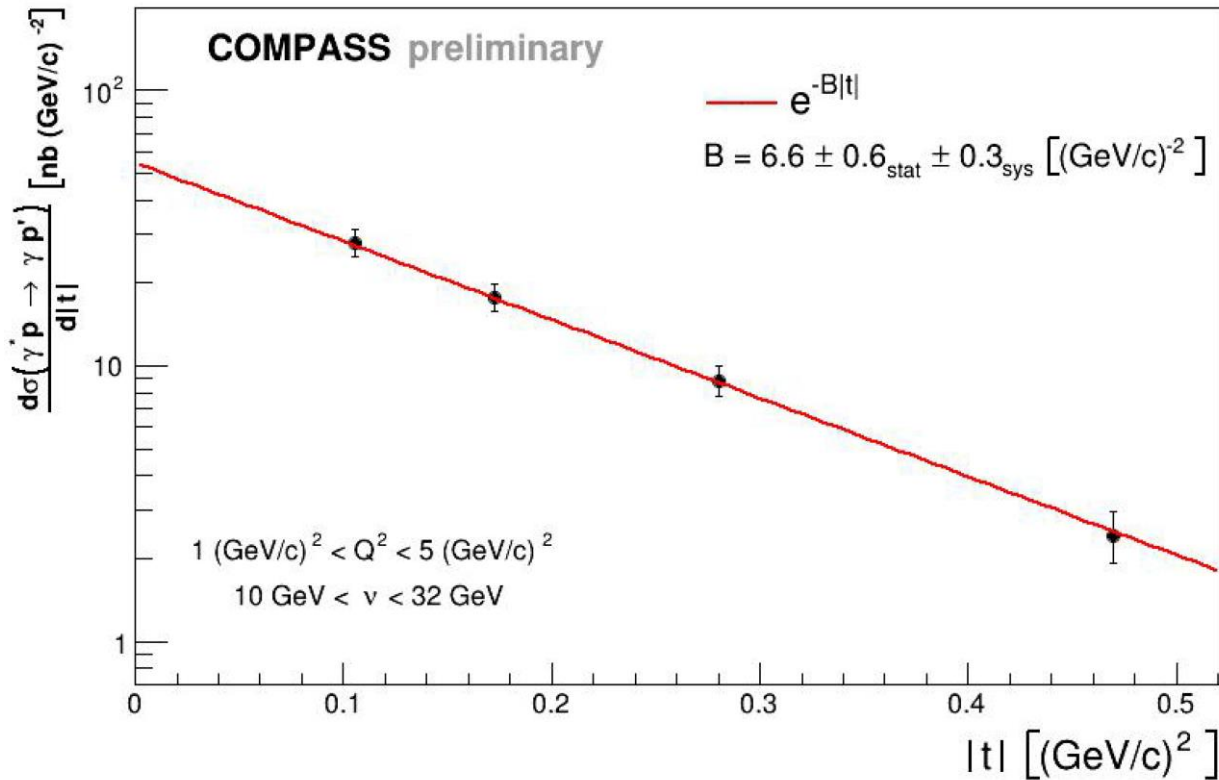


# Nucleon Tomography of COMPASS Preliminary Result

$$d\sigma^{DVCS}/d|t| \propto e^{-B|t|}$$

$$\langle r_{\perp}^2(x_B) \rangle \approx 2B(x_B) \text{ At small } x_B$$

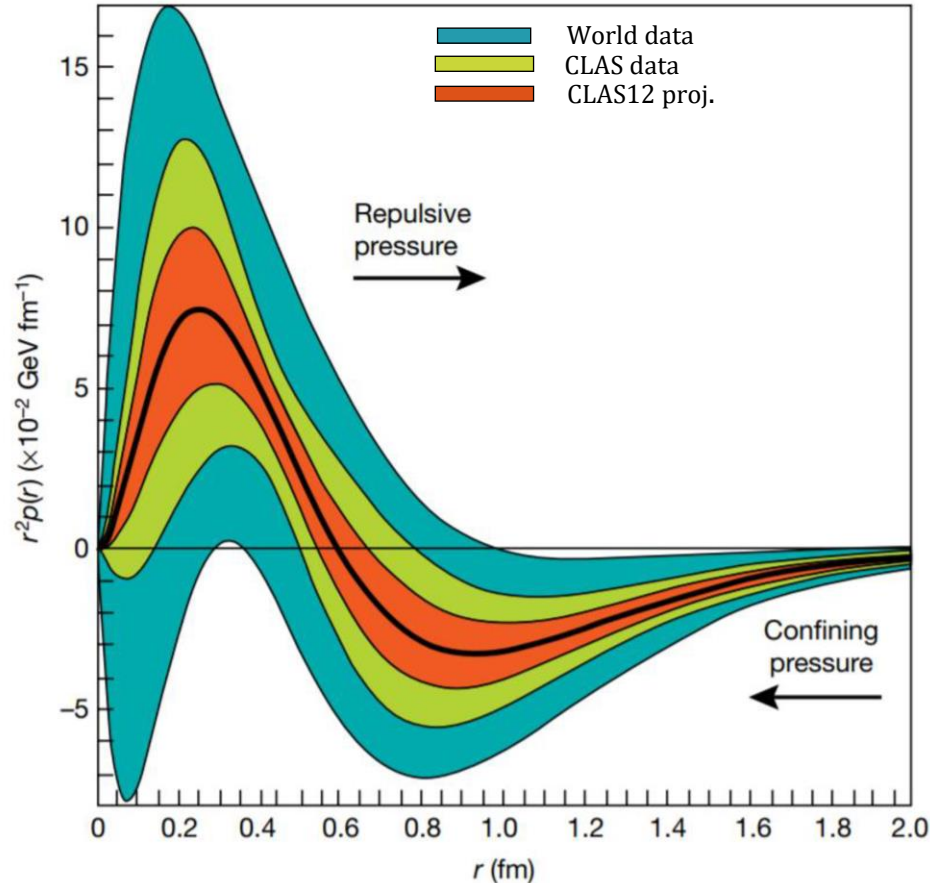
- COMPASS:  $\langle Q^2 \rangle = 1.8 \text{ (GeV/c)}^2$
- ◆ ZEUS:  $\langle Q^2 \rangle = 3.2 \text{ (GeV/c)}^2$
- ▲ H1:  $\langle Q^2 \rangle = 4.0 \text{ (GeV/c)}^2$
- ▼ H1:  $\langle Q^2 \rangle = 8.0 \text{ (GeV/c)}^2$
- H1:  $\langle Q^2 \rangle = 10. \text{ (GeV/c)}^2$



➤ The transverse-size evolution as a function of  $x_B \rightarrow$  Expect at least 3  $x_B$  bins from full 2016-17 data

# GPDs and Pressure Distribution

V. D. Burkert, L. Elouadrhiri, F. X. Girod  
*Nature* **557**, 396-399 (2018)



➤ **With all the data from beam spin sum and difference of CLAS at 6 GeV**

$$\overleftrightarrow{e} p \rightarrow e \gamma p$$

$$\int x H(x, \xi, t) dx = M_2(t) + \frac{4}{5} \xi^2 d_1(t)$$

$$d_1(t) \propto \int \frac{j_0(r\sqrt{-t})}{2t} p(r) d^3 r$$

$M_2(t)$  : Mass/energy distribution inside the nucleon

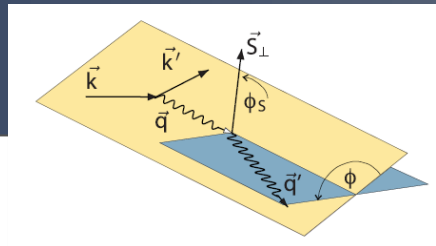
$d_1(t)$  : Forces and pressure distribution

Bessel Integral relates  $d_1(t)$  to the radial pressure  $p(r)$ .

- **Repulsive** pressure near center  
 $p(r=0) = 10^{35} \text{ Pa}$
- **Confining** pressure at  $r > 0.6 \text{ fm}$

**Atmospheric pressure:  $10^5 \text{ Pa}$**   
**Pressure in the center of neutron stars  $\leq 10^{34} \text{ Pa}$**

# GPDs and Nucleon Spin



$$\ell d \rightarrow \ell n \gamma (p)$$

$$\vec{\ell} \uparrow p \rightarrow \ell p \gamma$$

$$\Delta\sigma_{LU}^{\sin\phi} = \text{Im} (F_{1n} \mathcal{H} + \xi (F_{1n} + F_{2n}) \tilde{\mathcal{H}} + t/4m^2 F_{2n} \mathcal{E})$$

$$\Delta\sigma_{UT}^{\sin(\phi - \phi_s) \cos\phi} = -t/4m^2 \text{Im} (F_{2p} \mathcal{H} - F_{1p} \mathcal{E})$$

$$\Delta\sigma_{LT}^{\sin(\phi - \phi_s) \cos\phi} = -t/4m^2 \text{Re} (F_{2p} \mathcal{H} - F_{1p} \mathcal{E})$$

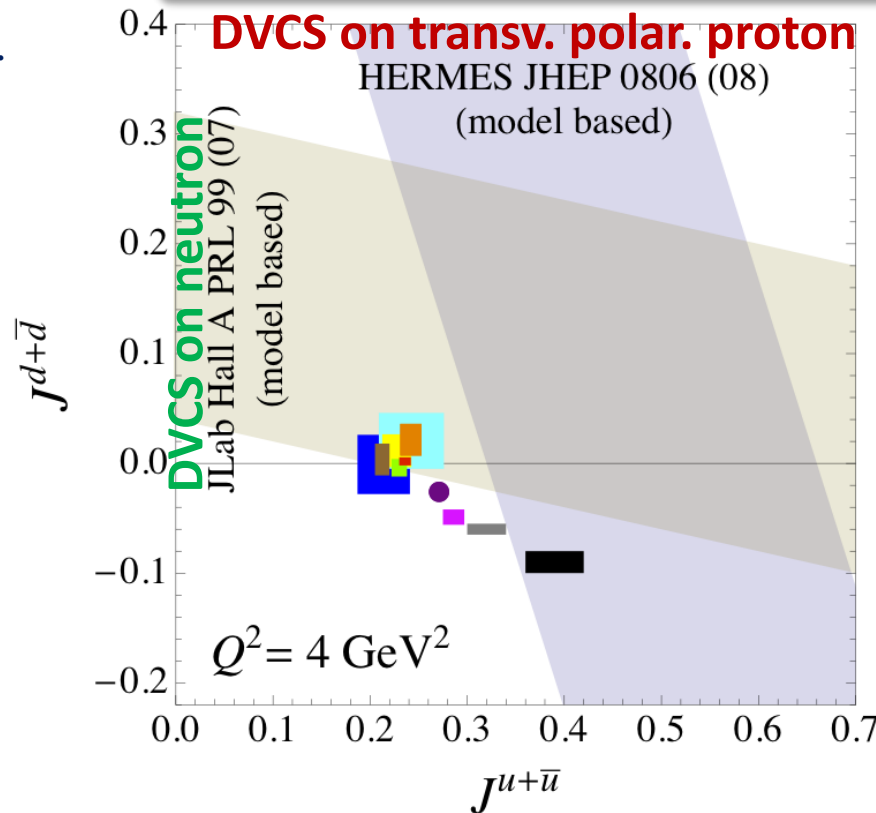
- First experimental constraint on  $E^q$  from neutron DVCS beam spin asymmetry at Hall A.

M. Mazouz *et al.*, PRL 99 (2007) 242501

- Provides constraints on orbital angular momentum of quarks

$$J_q = \frac{1}{2} \Sigma_q + L_q = \frac{1}{2} \int_{-1}^1 dx x [H^q(x, \xi, 0) + E^q(x, \xi, 0)]$$

## Model dependent extraction of $J^u$ and $J^d$

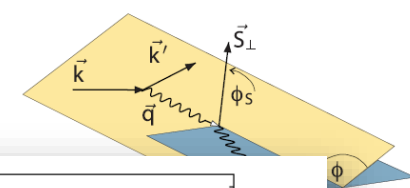


- Goloskokov & Kroll, EPJ C59 (09) 809
- Diehl *et al.*, EPJ C39 (05) 1
- Guidal *et al.*, PR D72 (05) 054013
- Liuti *et al.*, PRD 84 (11) 034007
- Bacchetta & Radici, PRL 107 (11) 212001
- LHPC-1, PR D77 (08) 094502
- LHPC-2, PR D82 (10) 094502
- QCDSF, arXiv:0710.1534
- Wakamatsu, EPJ A44 (10) 297
- Thomas, PRL 101 (08) 102003
- Thomas, INT 2012 workshop

Dudek *et al.*, EPJA48 (2012)

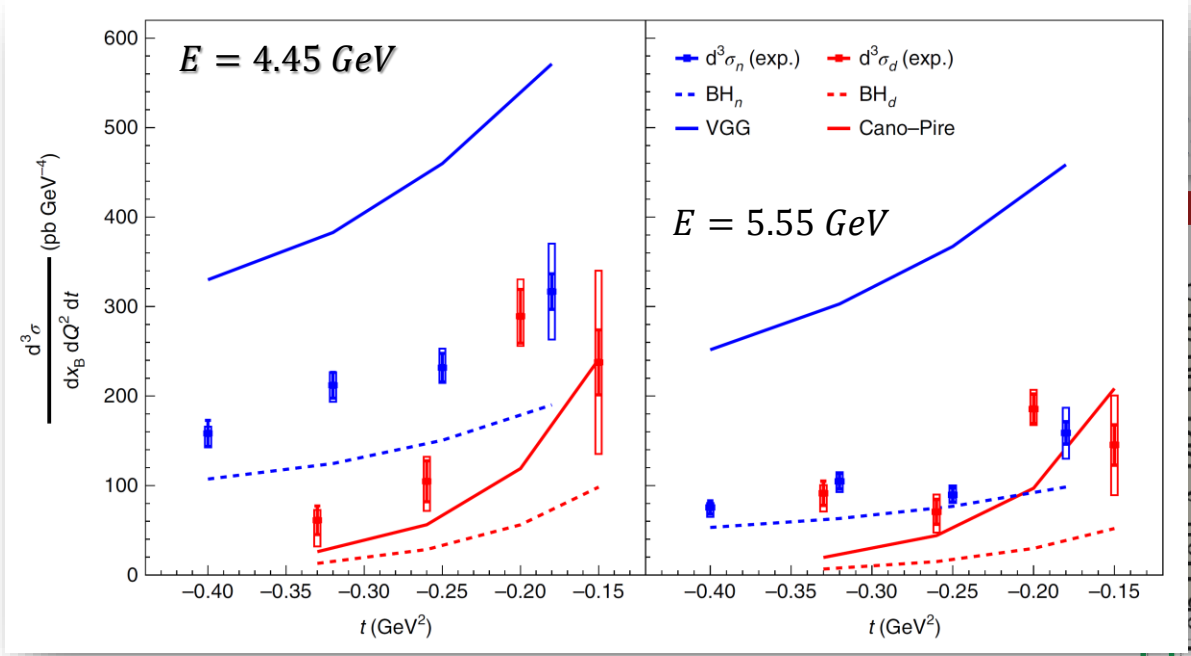
Lattice QCD

# GPDs and Nucleon Spin



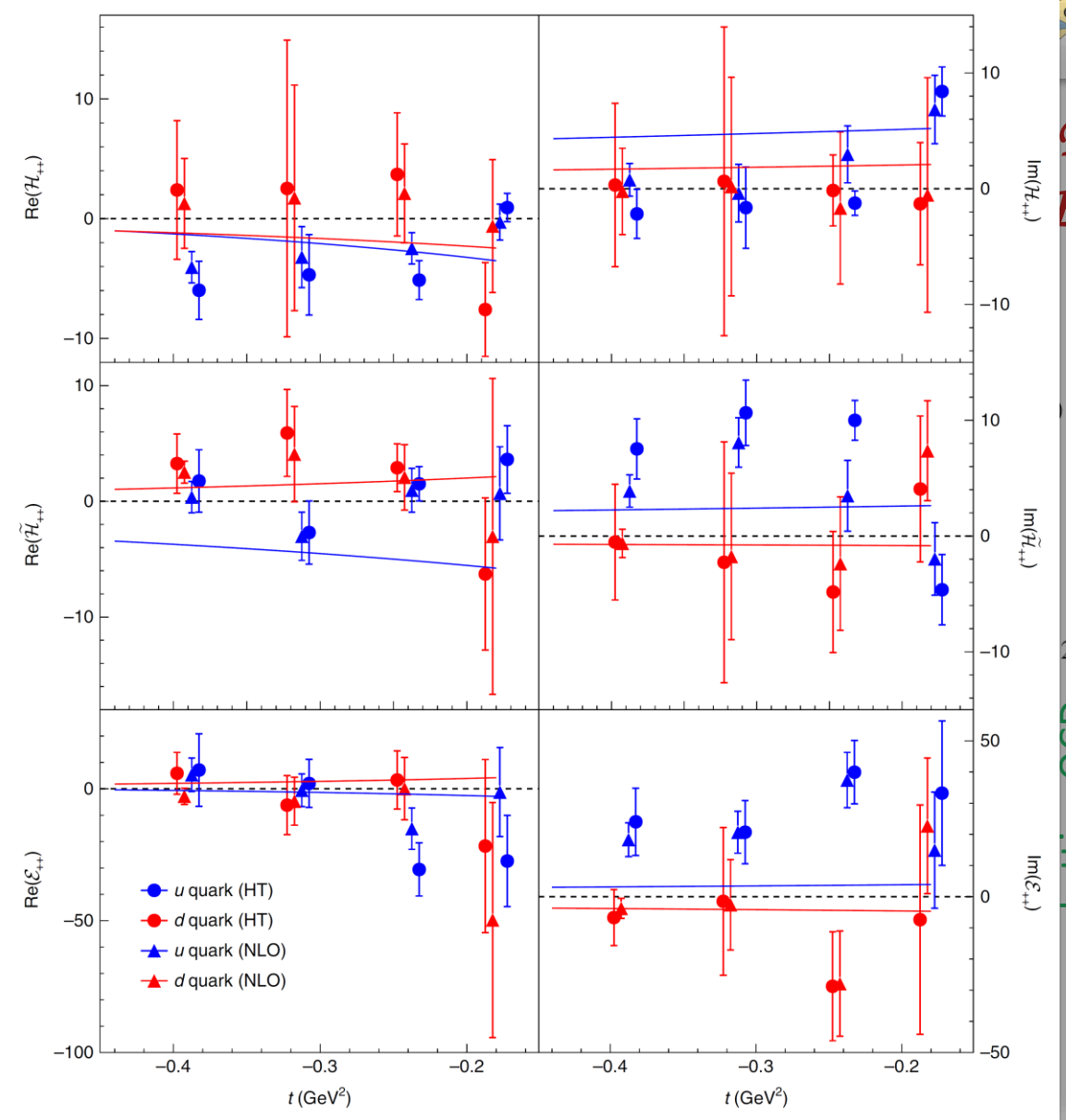
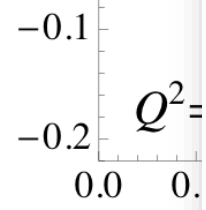
$$\ell d \rightarrow \ell n \gamma (p)$$

$$\Delta\sigma_{LU}^{\sin\phi} = \text{Im} (F_{1n}\mathcal{H} + \xi(F_{1n} + F_{2n})\tilde{\mathcal{H}} + t/4m^2 F_{2n}\mathcal{E})$$



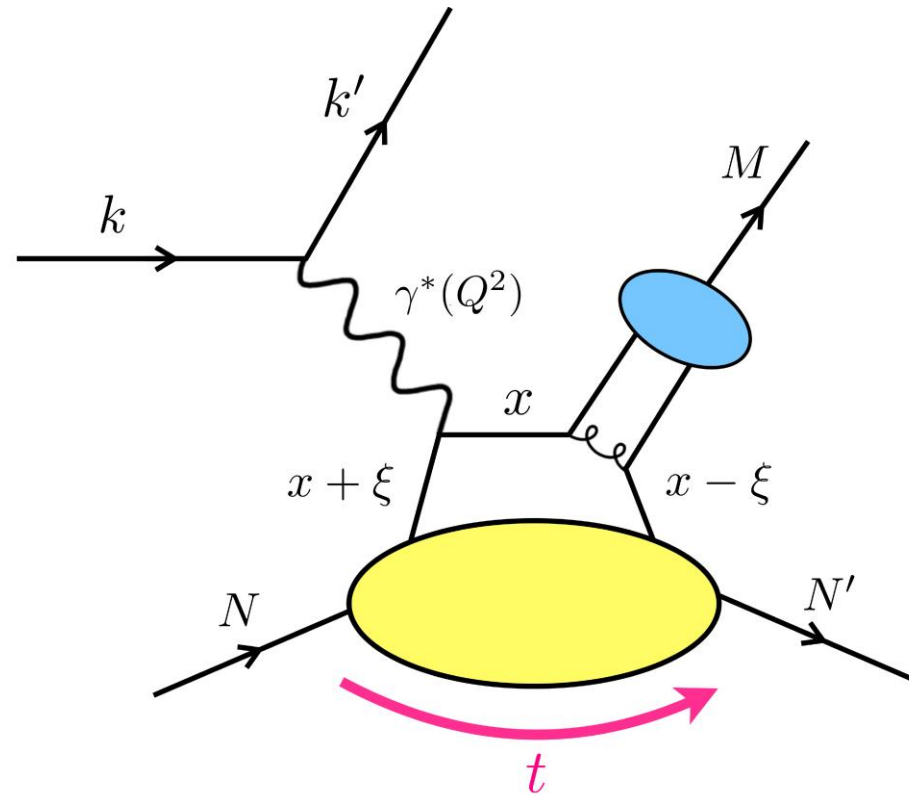
- Recent input from Result of neutron-DVCS at Hall A E08-025 ( done on 2010)
- with  $E_e = 4.5 \text{ \& } 5.5 \text{ GeV}$  on  $\text{LD}_2$  target.  $\langle Q^2 \rangle = 1.75 \text{ GeV}^2$ ,  $\langle x_B \rangle = 0.36$

M. Benali *et al.*, Nature Phys. 16(2), 191 (2020)



Lattice QCD

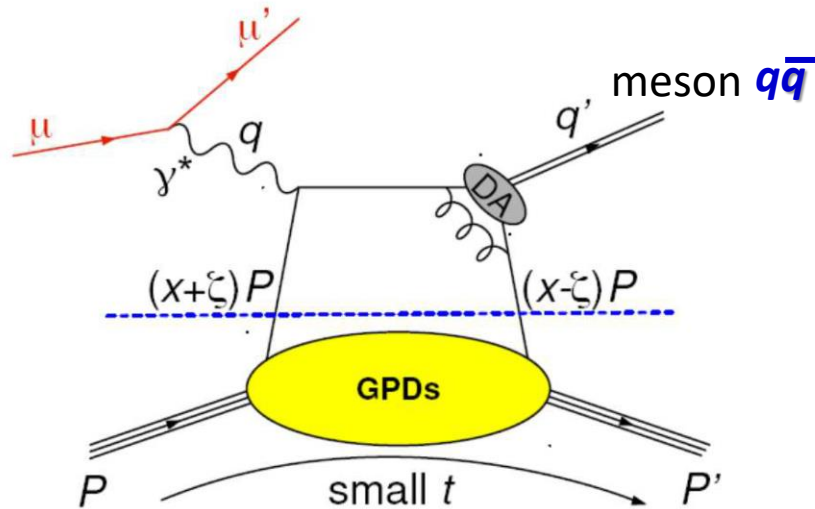
DVMP



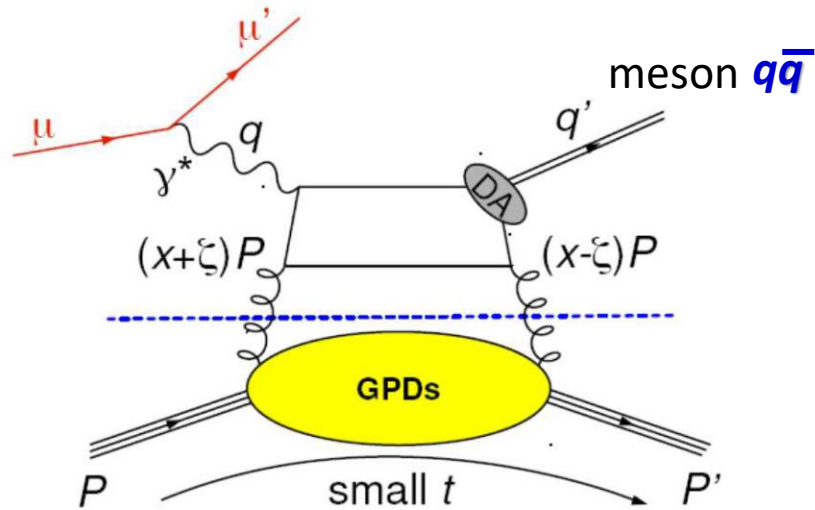


# Deeply Virtual Meson Production (DVMP)

quark contribution



gluon contribution



4 chiral-even GPDs: helicity of parton unchanged

$$\begin{matrix} \mathbf{H}^q(x, \xi, t) & \mathbf{E}^q(x, \xi, t) \\ \tilde{\mathbf{H}}^q(x, \xi, t) & \tilde{\mathbf{E}}^q(x, \xi, t) \end{matrix}$$

+ 4 chiral-odd or transversity GPDs: helicity of parton changed

$$\begin{matrix} \mathbf{H}_T^q(x, \xi, t) & \mathbf{E}_T^q(x, \xi, t) \\ \tilde{\mathbf{H}}_T^q(x, \xi, t) & \tilde{\mathbf{E}}_T^q(x, \xi, t) \end{matrix} \quad \bar{\mathbf{E}}_T^q = 2 \tilde{\mathbf{H}}_T^q + \mathbf{E}_T^q$$

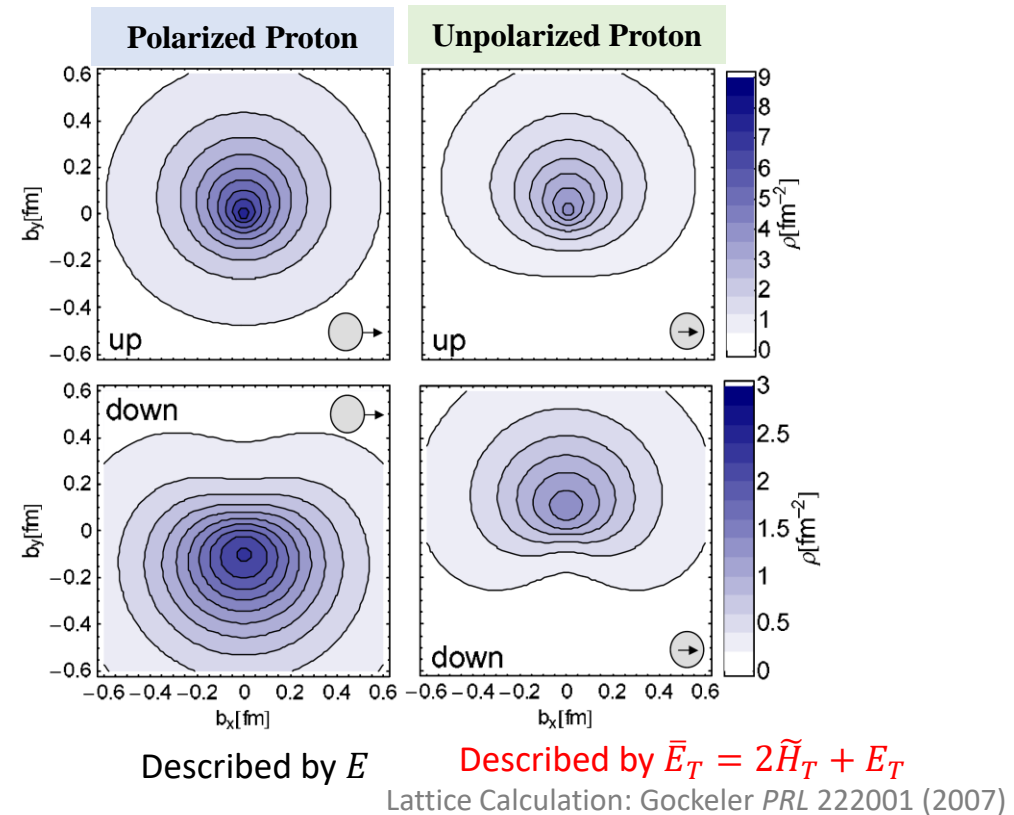
- Universality of GPDs, quark flavor filter
- Ability to probe the **chiral-odd GPDs**.
- Additional non-perturbative term from meson wave function → more difficult for GPD extraction
- In addition to nuclear structure, provide insights into reaction mechanism

# What Can We Learn from Chiral-GPDs

		Quark polarization		
		U	L	T
Nucleon polarization	U	$H$		$\bar{E}_T$
	L		$\tilde{H}$	$\tilde{E}_T$
	T	$E$	$\tilde{E}$	$H_T, \tilde{H}_T$

➤  $\bar{E}_T$  is related to the distortion of the polarized quark distribution in the transverse plane for an unpolarized nucleon

- Chiral-odd GPDs  $H_T$
- Generalization of transversity distribution  $h_1(x)$   
→ related to the transverse spin structure
  - Tensor charge



**GPDs parametrization:**

$H_T$

- tensor charge: T.Ledwig, A.Silva, H.C. Kim  
 $\int dx H_T(x, \xi, t)$
- transversity PDF: M.Anselmino  
 $H_T(x, \xi = 0, t = 0) = h_1$

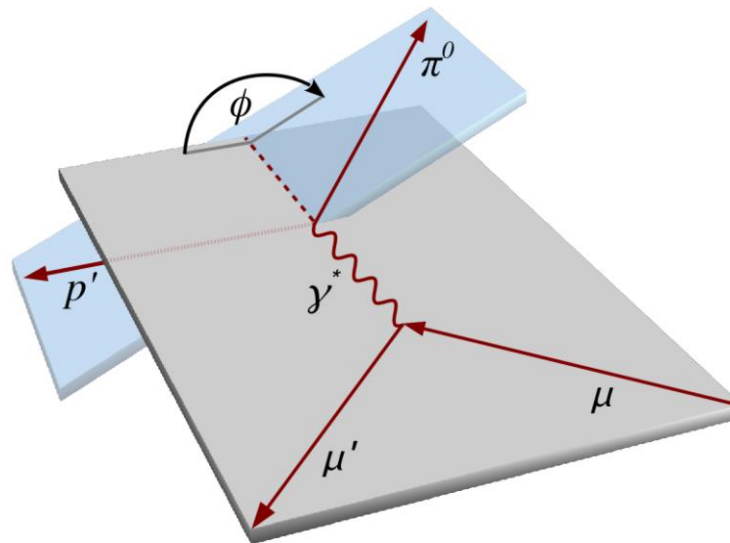
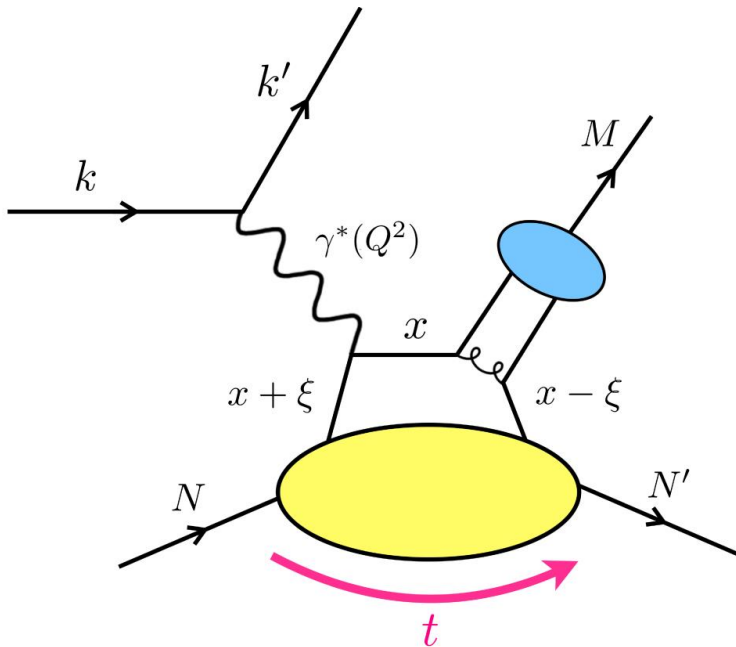
# DVMP Structure Functions with Longitudinally Polarized Beam & Target

$$\frac{2\pi}{\Gamma} \frac{d^4\sigma}{dQ^2 dx_B dt d\phi} = \sigma_T + \epsilon\sigma_L + \epsilon\sigma_{TT} \cos 2\phi + \sqrt{\epsilon(1+\epsilon)}\sigma_{LT} \cos \phi \quad \rightarrow \text{Unpolarized}$$

$$+ P_b \sqrt{\epsilon(1-\epsilon)}\sigma_{LT'} \sin \phi \quad \rightarrow \text{Longitudinally polarized beam}$$

$$+ P_{tg} \left( \sqrt{\epsilon(1+\epsilon)}\sigma_{UL}^{\sin \phi} \sin \phi + \epsilon\sigma_{UL}^{\sin 2\phi} \sin 2\phi \right) \rightarrow \text{Longitudinally polarized target}$$

$$+ P_b P_{tg} \left( \sqrt{1-\epsilon^2}\sigma_{LL} + \sqrt{\epsilon(1-\epsilon)}\sigma_{LL}^{\cos \phi} \cos \phi \right) \rightarrow \text{Longitudinally polarized beam and target}$$

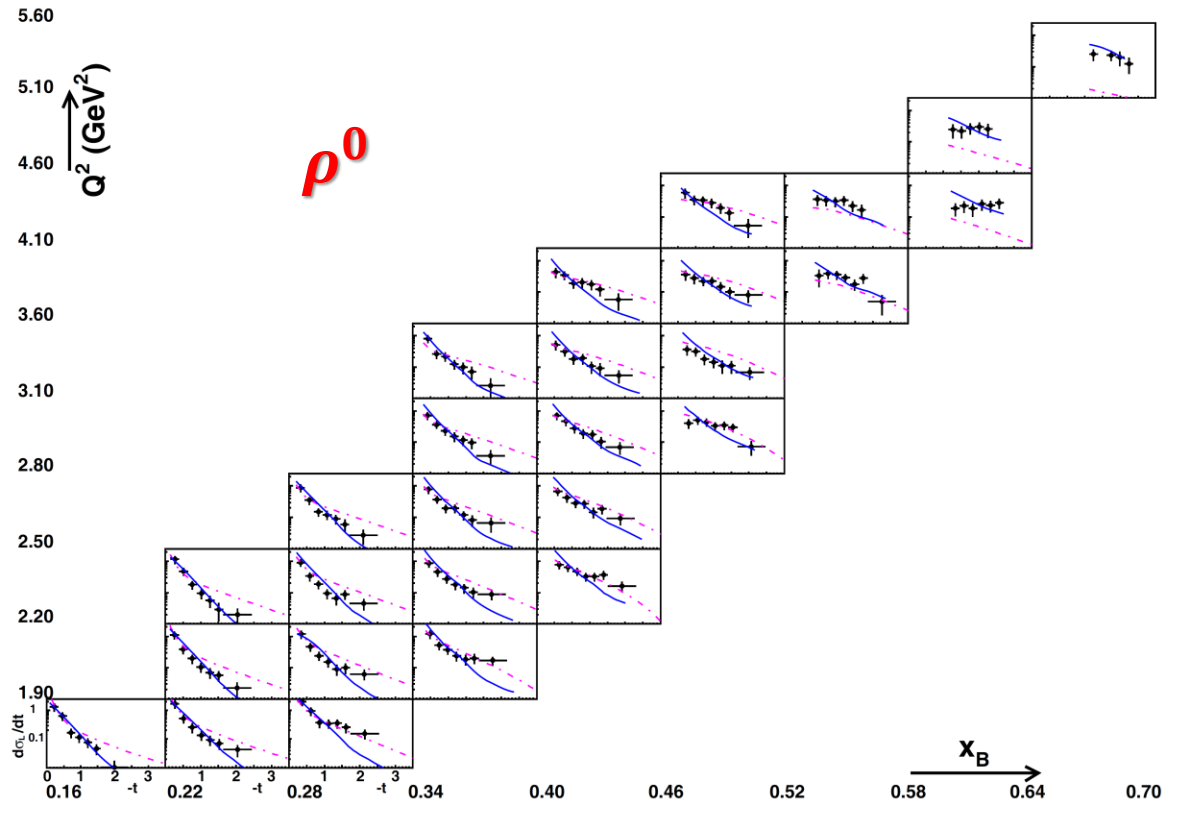
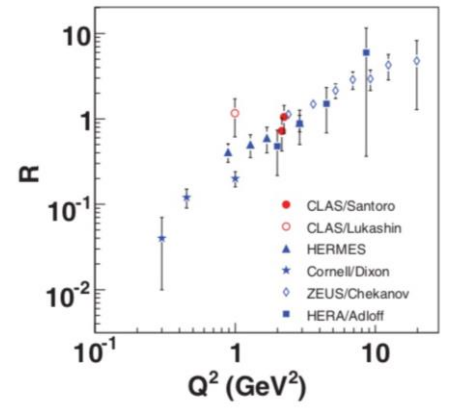
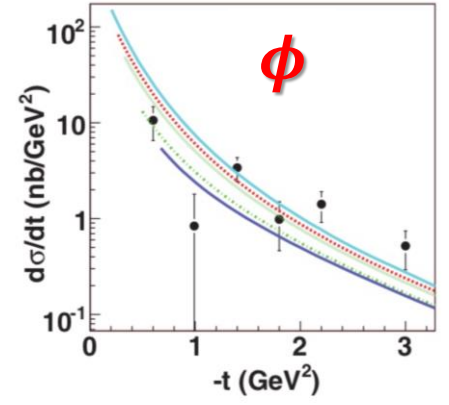
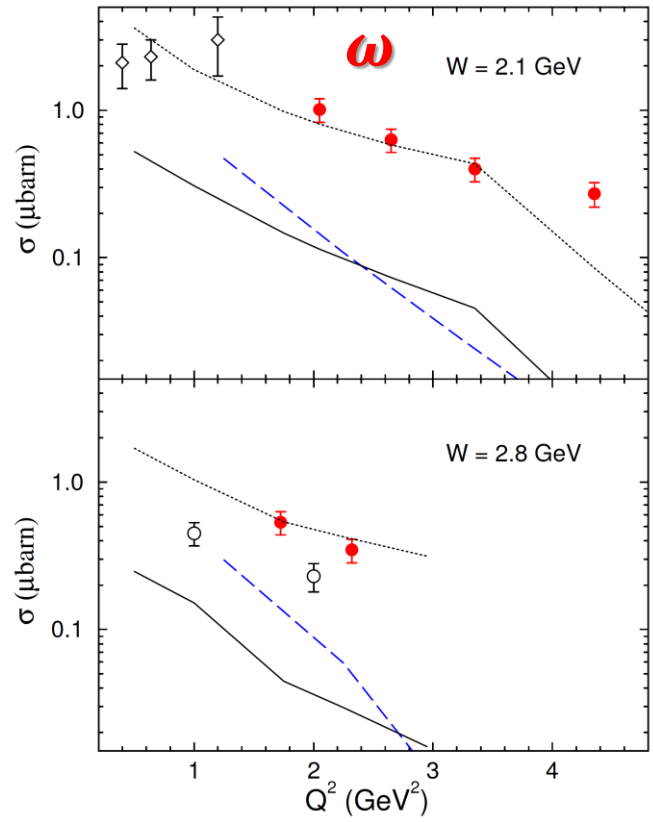
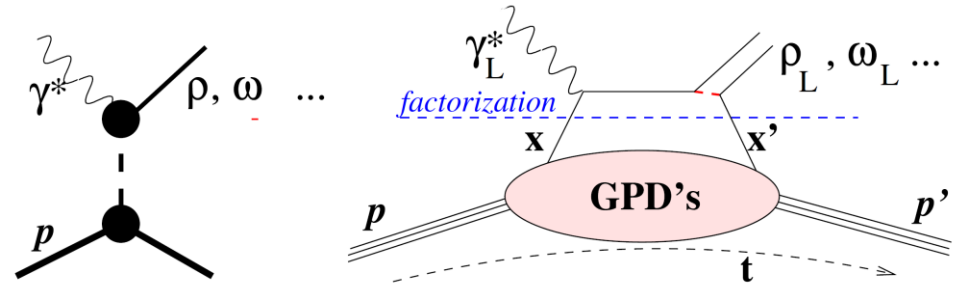


$\epsilon$  : degree of longitudinal polarization  
 $P_b$  : initial lepton polarization  
 $P_{tg}$  : initial target polarization

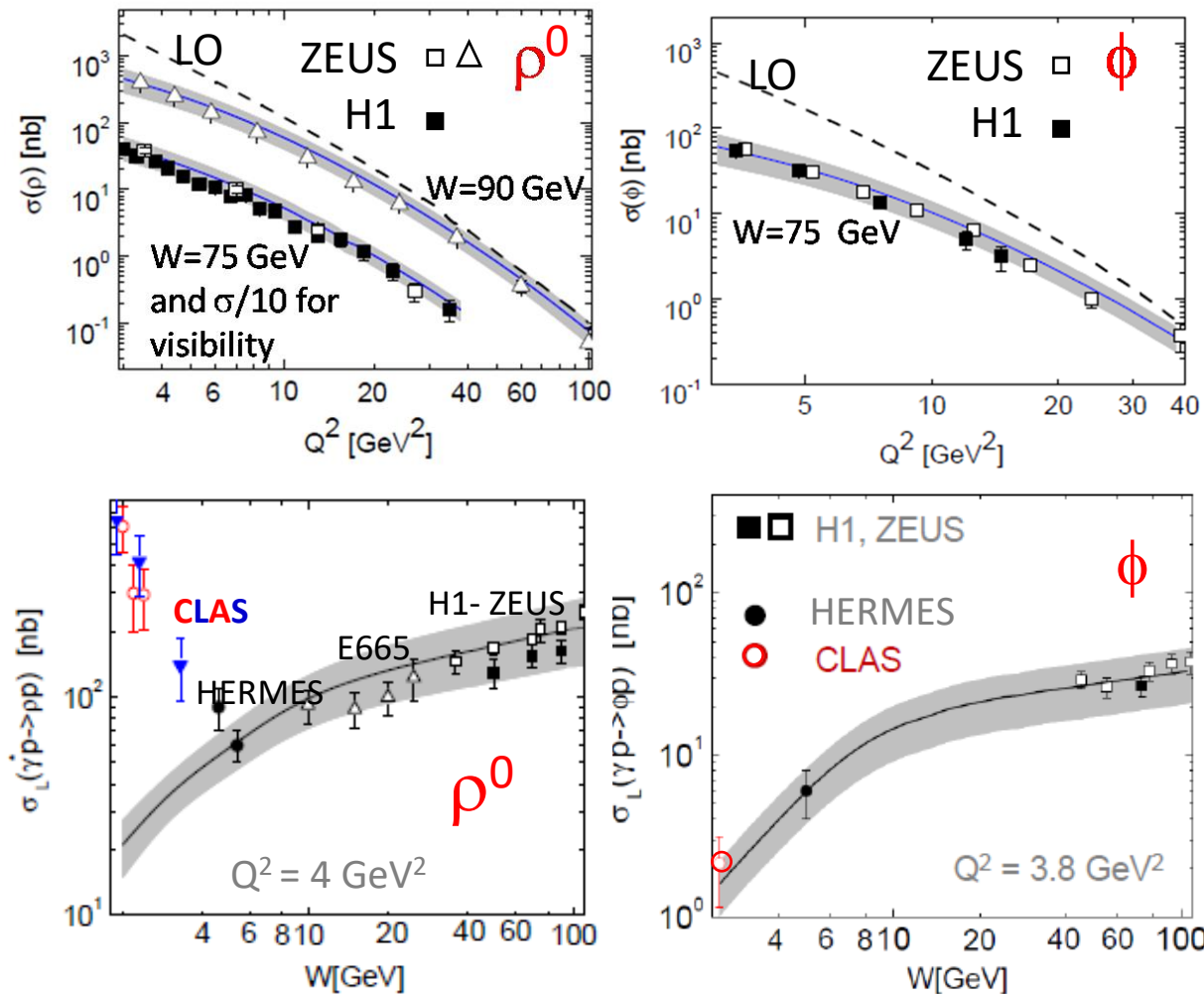
Fig: M.G. Alexeev et al. *Phys.Lett.B* 805 (2020)

# Vector Meson Production at CLAS

- Pilot analysis of exclusive  $\omega$ -electroproduction published in EPJ A **24**, 445 (2005), followed by analyses of  $\phi$ , Phys. Rev. C **78**, 025210 (2008), and  $\rho^0$ , EPJ A **39**, 5-31 (2009)
- Test two hypotheses  $\rightarrow$  t-channel Regge trajectory exchange on the hadronic level and the handbag diagram approach on the partonic level
- Regge Model favored by data in CLAS kinematics.

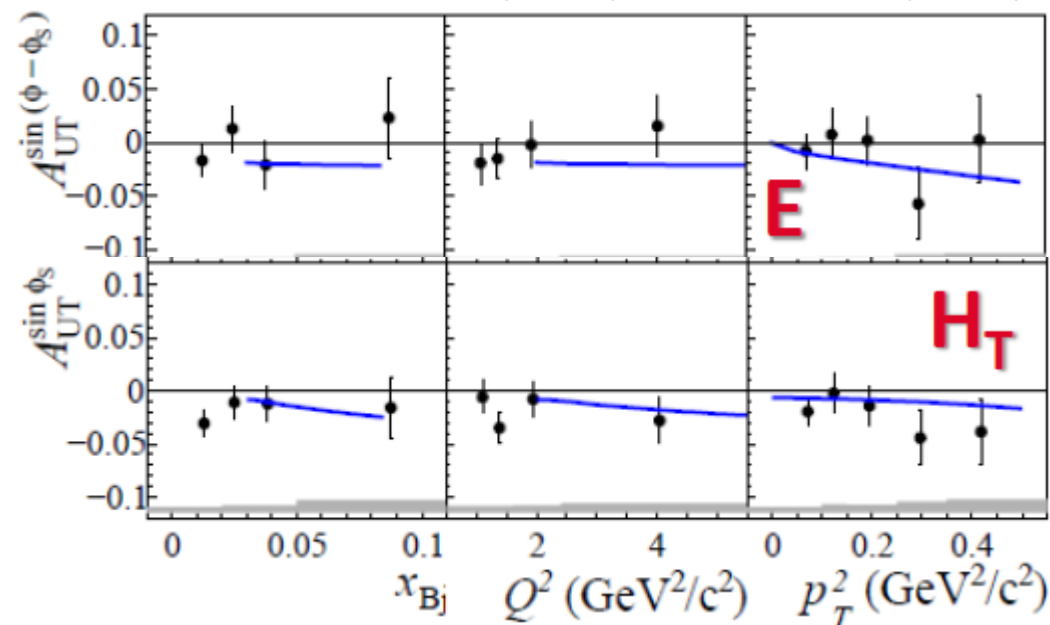


# GPDs with Vector Meson Production



$\rho^0$  ( $\rightarrow \pi^+\pi^-$ ) production at COMPASS with Transversely Polarized Target

COMPASS, NPB 865 (2012) 1-20, PLB731 (2014) 19



**GK Model** by Goloskokov, Kroll, constrained by DVMP at small  $x_B$  (or large  $W$ )

- leading-twist longitudinal  $\gamma_L^* p \rightarrow M p$  and transv. polar.  $\gamma_T^* p \rightarrow M p$
- quark and gluon contributions (GPDs  $H$ ,  $E$ ,  $H_T$ ) and beyond leading twist



# Exclusive $\pi^0$ Production

$$\ell p \rightarrow \ell \pi^0 p$$

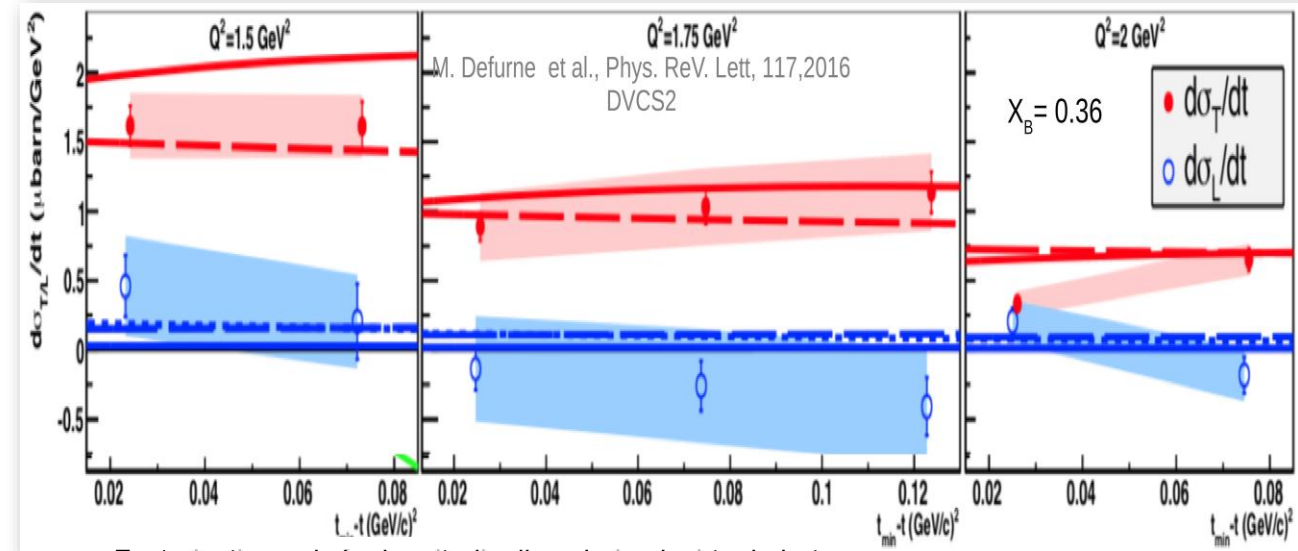
$$\frac{d^4\sigma}{dQ^2 dx_B dt d\phi} = \frac{1}{2\pi} \Gamma_\gamma(Q^2, x_B, E) \left[ \frac{d\sigma_T}{dt} + \epsilon \frac{d\sigma_L}{dt} + \sqrt{2\epsilon(1+\epsilon)} \frac{d\sigma_{TL}}{dt} \cos(\phi) + \epsilon \frac{d\sigma_{TT}}{dt} \cos(2\phi) + h \sqrt{2\epsilon(1-\epsilon)} \frac{d\sigma_{TL}}{dt} \sin(\phi) \right]$$

$$\bullet \frac{d\sigma_L}{dt} = \frac{4\pi\alpha}{k'} \frac{1}{Q^6} \left\{ (1-\xi^2) |\langle \tilde{H} \rangle|^2 - 2\xi^2 \text{Re} [\langle \tilde{H} \rangle^* \langle \tilde{E} \rangle] - \frac{t'}{4m^2} \xi^2 |\langle \tilde{E} \rangle|^2 \right\}$$

$$\bullet \frac{d\sigma_T}{dt} = \frac{4\pi\alpha}{2k'} \frac{\mu_\pi^2}{Q^8} \left[ (1-\xi^2) |\langle H_T \rangle|^2 - \frac{t'}{8m^2} |\langle \bar{E}_T \rangle|^2 \right]$$

$$\bullet \frac{\sigma_{LT}}{dt} = \frac{4\pi\alpha}{\sqrt{2}k'} \frac{\mu_\pi}{Q^7} \xi \sqrt{1-\xi^2} \frac{\sqrt{-t'}}{2m} \text{Re} [\langle H_T \rangle^* \langle \tilde{E} \rangle]$$

$$\bullet \frac{\sigma_{TT}}{dt} = \frac{4\pi\alpha}{k'} \frac{\mu_\pi^2}{Q^8} \frac{t'}{16m^2} |\langle \bar{E}_T \rangle|^2 \quad \bar{E}_T = 2\tilde{H}_T + E_T$$



- **Significant transverse contribution:**  
Coupling between chiral-odd (quark helicity flip) GPDs to the **twist-3** pion amplitude.

# GPDs and Hard Exclusive $\pi^0$ Production

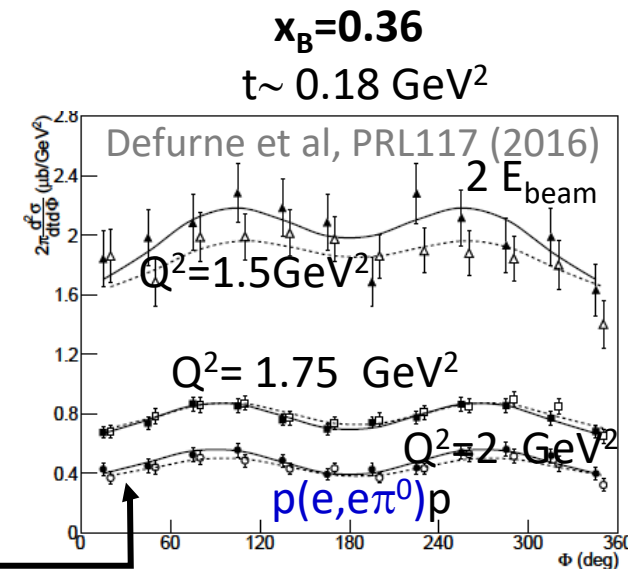
$$e p \rightarrow e \pi^0 p \quad \frac{d^2\sigma}{dt d\phi_\pi} = \frac{1}{2\pi} \left[ \left( \epsilon \frac{d\sigma_L}{dt} + \frac{d\sigma_T}{dt} \right) + \epsilon \cos 2\phi_\pi \frac{d\sigma_{TT}}{dt} + \sqrt{2\epsilon(1+\epsilon)} \cos \phi_\pi \frac{d\sigma_{LT}}{dt} \right]$$

$$\left| \langle \tilde{H} \rangle \right|^2 - \frac{t'}{4m^2} \left| \langle \tilde{E} \rangle \right|^2$$

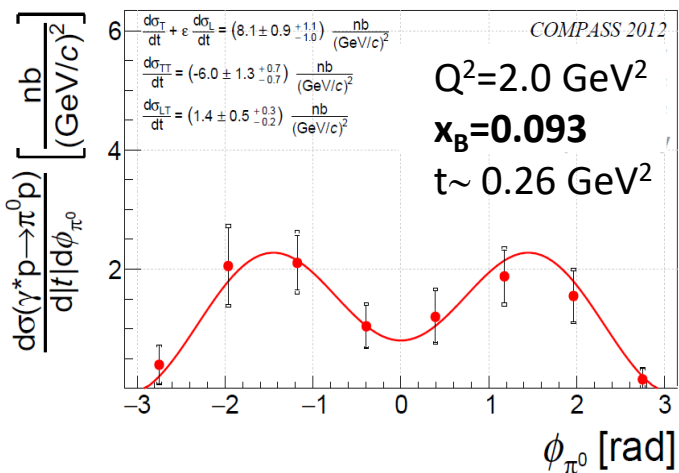
$$\left| \langle H_T \rangle \right|^2 - \frac{t'}{8m^2} \left| \langle \bar{E}_T \rangle \right|^2$$

$$\frac{t'}{16m^2} \left| \langle \bar{E}_T \rangle \right|^2$$

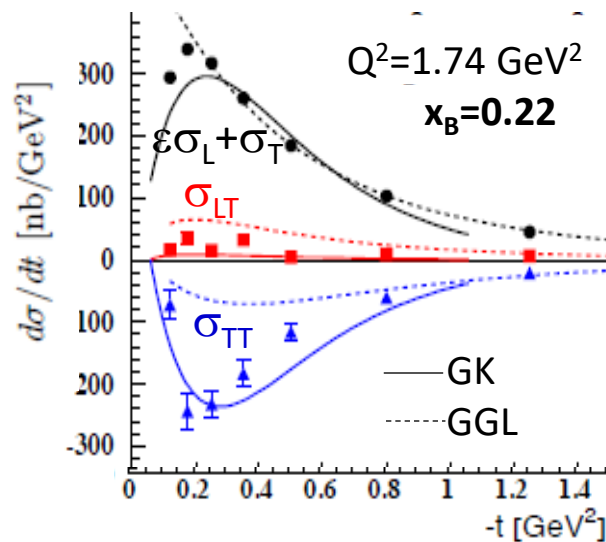
$$\frac{\sqrt{-t'}}{2m} \text{Re} \left[ \langle H_T \rangle^* \langle \tilde{E} \rangle \right]$$



**COMPASS 4 weeks 2012 pilot run**  
COMPASS, PLB 805 (2020) 135454



**JLab 6 GeV CLAS**  
Bedlinskiy et al,  
PRL109 (2012), PRC90 (2014)

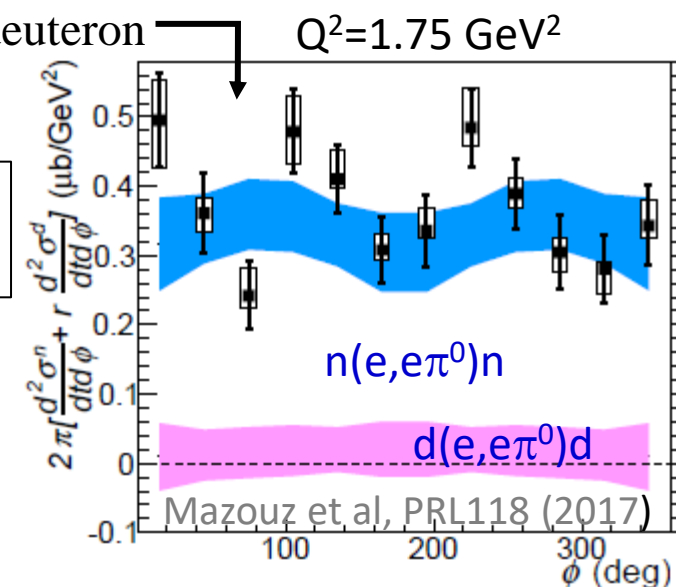


**JLab 6 GeV Hall-A**  
Different beam energies  
→ L/T separation

LH2 target → proton  
LD2 target → neutron+deuteron

$$D(e, e\pi^0)X - p(e, e\pi^0)p = n(e, e\pi^0)n + d(e, e\pi^0)d$$

➤ Flavor decomposition  
 $H_T^u$  and  $H_T^d$   
 $\bar{E}_T^u$  and  $\bar{E}_T^d$



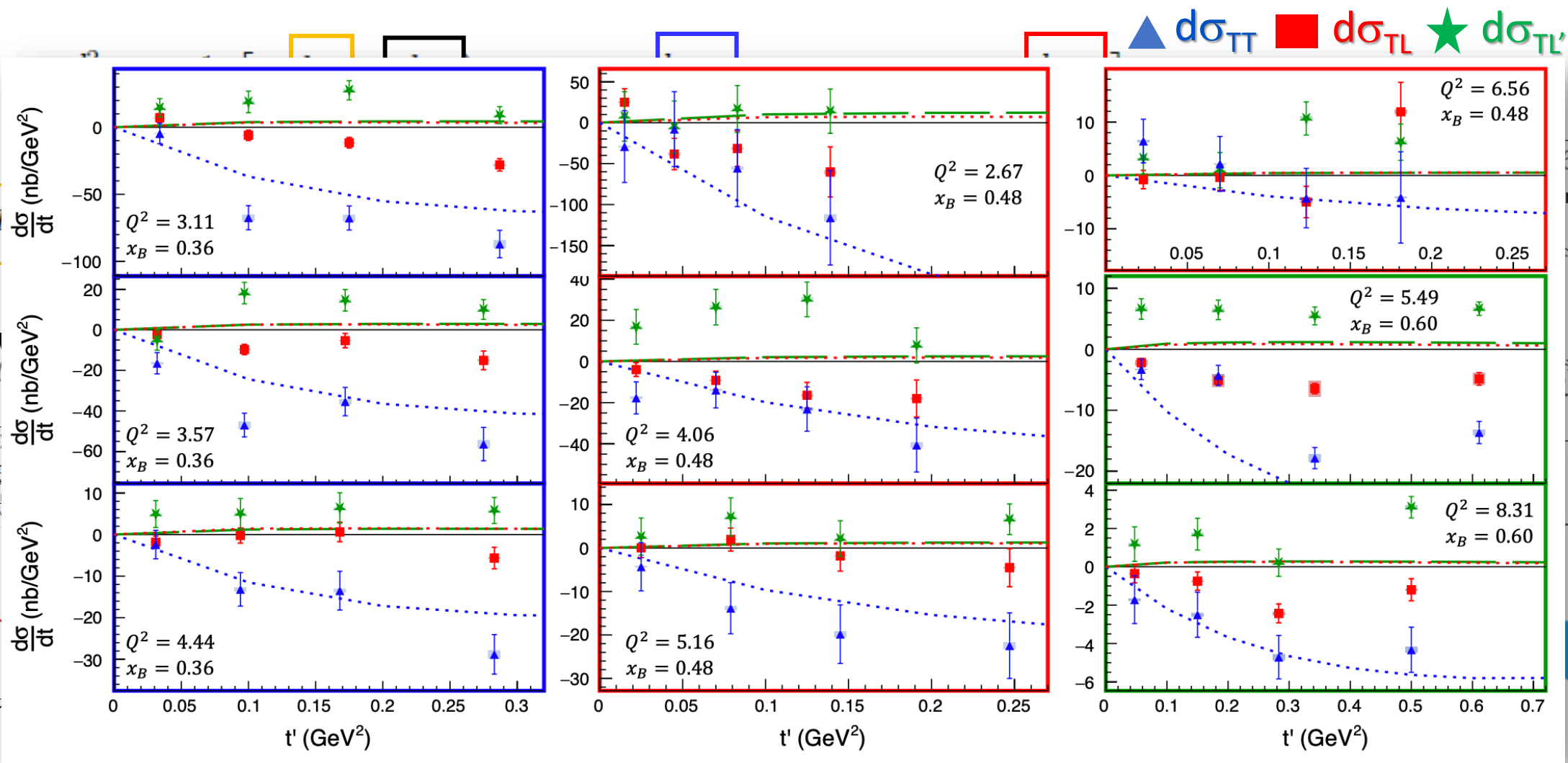
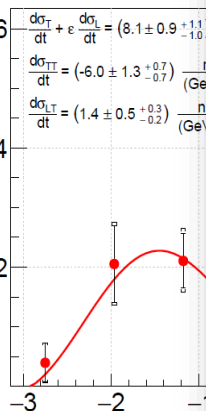
➤ Provide constraints on  $H_T$  and  $\bar{E}_T$

# GPDs and Hard Exclusive $\pi^0$ Production

$$e p \rightarrow e \pi^0 p$$

COMPASS 4 v  
COMPASS, PLB 805 (2015)

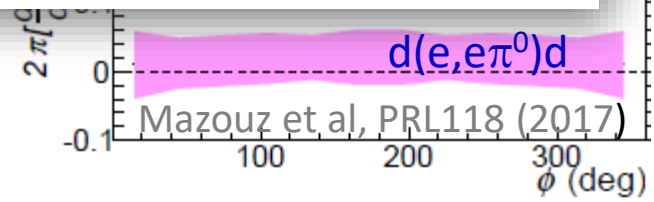
$$\frac{d\sigma(\gamma^* p \rightarrow \pi^0 p)}{d\phi d\phi_{\pi^0}} \left[ \frac{\text{nb}}{(\text{GeV}/c)^2} \right]$$



➤ Recent input from Hall-A E12-06-114, at high  $x_B$  over a large  $Q^2$  range

M. Dlamini et al, Phys. Rev. Lett 127, 152301 (2021)

$H_T^u$  and  $H_T^d$   
 $\overline{E}_T^u$  and  $\overline{E}_T^d$

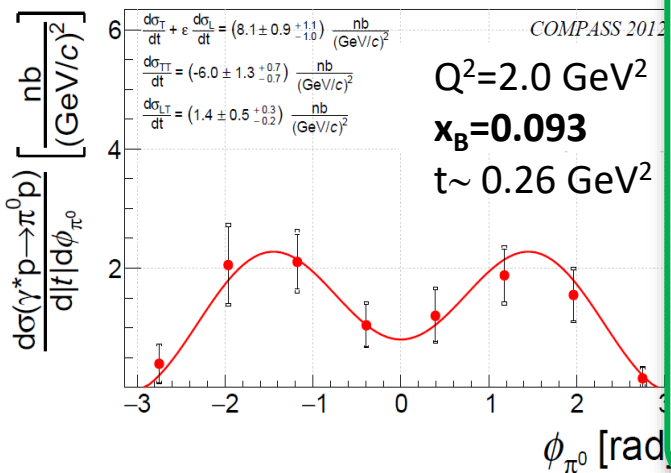


# GPDs and Hard Exclusive $\pi^0$ Production

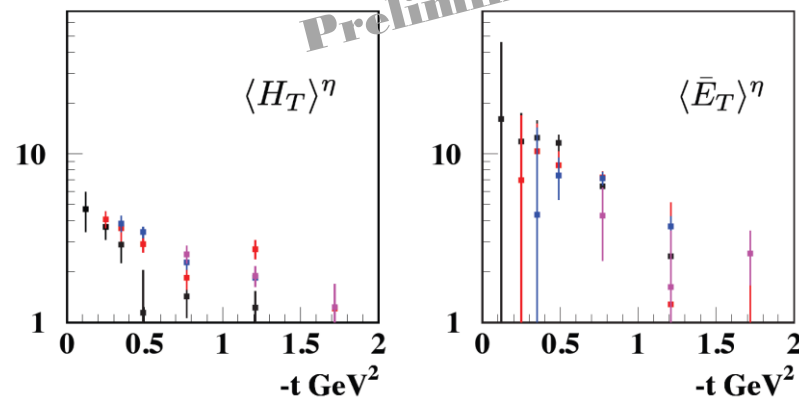
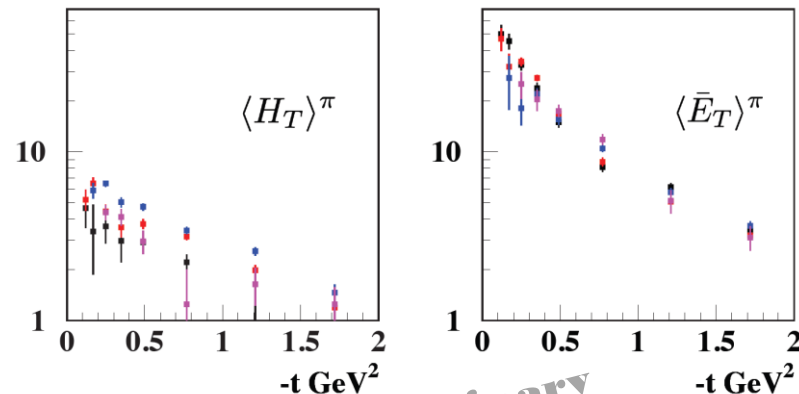
$$e p \rightarrow e \pi^0 p \quad \frac{d^2\sigma}{dt d\phi_\pi} = \frac{1}{2\pi}$$

$$\left| \langle \tilde{H} \rangle \right|^2 - \frac{t'}{4m^2} \left| \langle \tilde{E} \rangle \right|^2$$

COMPASS 4 weeks 2012 pilot run  
COMPASS, PLB 805 (2020) 135454

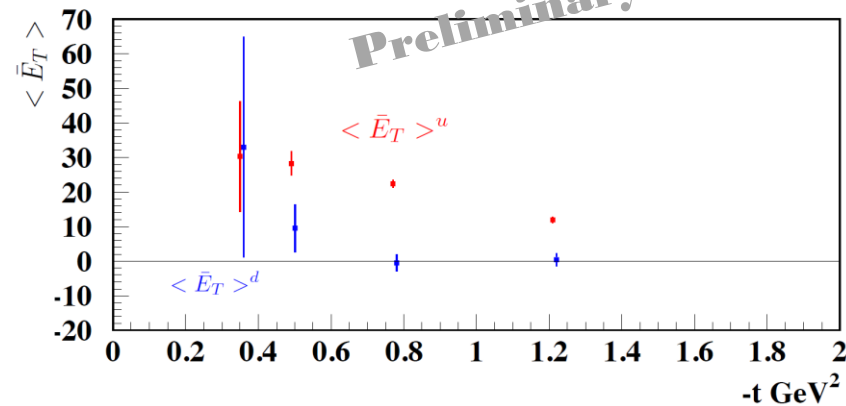
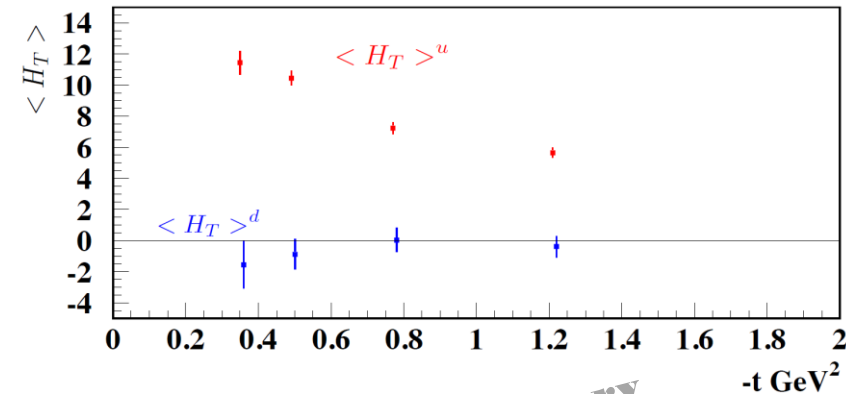


## ➤ Generalized Form Factors



Preliminary attempts using  $\pi^0$  &  $\eta$  data from CLAS

## ➤ Quark Flavor Decomposition



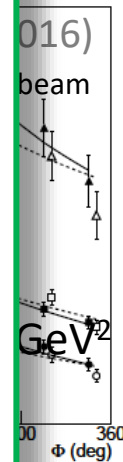
Valery Kubarovsky, arXiv:1601.04367v2

$H_T^u$  and  $H_T^d$   
 $\bar{E}_T^u$  and  $\bar{E}_T^d$

$d(e, e\pi^0)d$

Mazouz et al, PRL118 (2017)

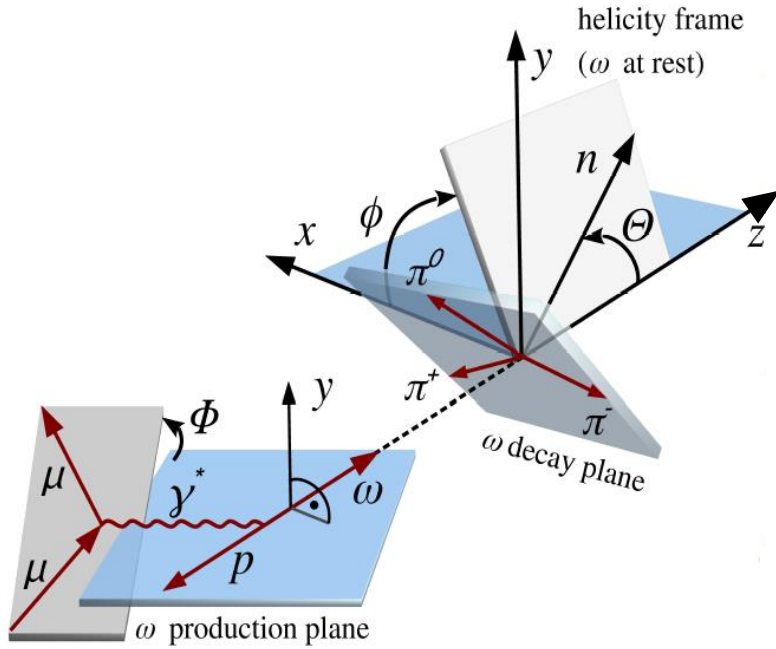
➤ Preliminary attempts using  $\pi^0$  &  $\eta$  data from CLAS



CLAS

# Vector Meson Production: Spin Density Matrix Elements

## Experimental angular distributions



$$\frac{d\sigma}{d\phi d\Phi d\Theta dQ^2 dx_B dt} = \Gamma(Q^2, x_B, E) \frac{1}{2\pi} \left\{ \frac{d\sigma_T}{dt} + \epsilon \frac{d\sigma_L}{dt} \right\} \mathcal{W}^{U+L}(\Phi, \phi, \cos \Theta)$$

$$\mathcal{W}^{U+L}(\Phi, \phi, \cos \Theta) = \mathcal{W}^U(\Phi, \phi, \cos \Theta) + P_b \mathcal{W}^L(\Phi, \phi, \cos \Theta)$$

15 unpolarized SDMEs in  $\mathcal{W}^U$  and 8 polarized in  $\mathcal{W}^L$

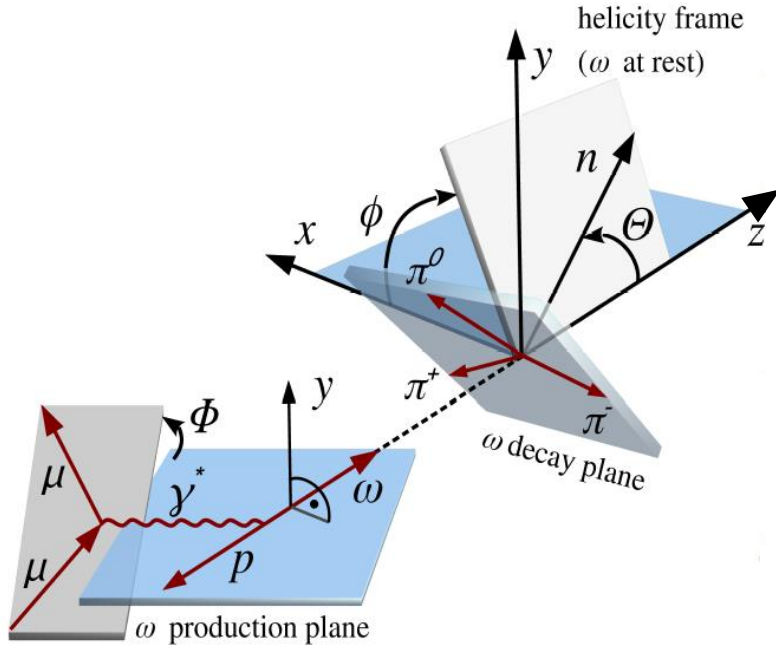
$$\begin{aligned} \mathcal{W}^U(\Phi, \phi, \cos \Theta) = & \frac{3}{8\pi^2} \left[ \frac{1}{2}(1 - r_{00}^{04}) + \frac{1}{2}(3r_{00}^{04} - 1) \cos^2 \Theta - \sqrt{2} \text{Re}\{r_{10}^{04}\} \sin 2\Theta \cos \phi - r_{1-1}^{04} \sin^2 \Theta \cos 2\phi \right. \\ & - \epsilon \cos 2\Phi \left( r_{11}^1 \sin^2 \Theta + r_{00}^1 \cos^2 \Theta - \sqrt{2} \text{Re}\{r_{10}^1\} \sin 2\Theta \cos \phi - r_{1-1}^1 \sin^2 \Theta \cos 2\phi \right) \\ & - \epsilon \sin 2\Phi \left( \sqrt{2} \text{Im}\{r_{10}^2\} \sin 2\Theta \sin \phi + \text{Im}\{r_{1-1}^2\} \sin^2 \Theta \sin 2\phi \right) \\ & + \sqrt{2\epsilon(1+\epsilon)} \cos \Phi \left( r_{11}^5 \sin^2 \Theta + r_{00}^5 \cos^2 \Theta - \sqrt{2} \text{Re}\{r_{10}^5\} \sin 2\Theta \cos \phi - r_{1-1}^5 \sin^2 \Theta \cos 2\phi \right) \\ & \left. + \sqrt{2\epsilon(1+\epsilon)} \sin \Phi \left( \sqrt{2} \text{Im}\{r_{10}^6\} \sin 2\Theta \sin \phi + \text{Im}\{r_{1-1}^6\} \sin^2 \Theta \sin 2\phi \right) \right], \end{aligned}$$

$$\begin{aligned} \mathcal{W}^L(\Phi, \phi, \cos \Theta) = & \frac{3}{8\pi^2} \left[ \sqrt{1-\epsilon^2} \left( \sqrt{2} \text{Im}\{r_{10}^3\} \sin 2\Theta \sin \phi + \text{Im}\{r_{1-1}^3\} \sin^2 \Theta \sin 2\phi \right) \right. \\ & + \sqrt{2\epsilon(1-\epsilon)} \cos \Phi \left( \sqrt{2} \text{Im}\{r_{10}^7\} \sin 2\Theta \sin \phi + \text{Im}\{r_{1-1}^7\} \sin^2 \Theta \sin 2\phi \right) \\ & \left. + \sqrt{2\epsilon(1-\epsilon)} \sin \Phi \left( r_{11}^8 \sin^2 \Theta + r_{00}^8 \cos^2 \Theta - \sqrt{2} \text{Re}\{r_{10}^8\} \sin 2\Theta \cos \phi - r_{1-1}^8 \sin^2 \Theta \cos 2\phi \right) \right] \end{aligned}$$



# Vector Meson Production: Spin Density Matrix Elements

## Experimental angular distributions



$$r_{00}^1 \sigma_0 \sim |\bar{E}_T|^2$$

$$r_{00}^5 \sigma_0 \sim \text{Re} [\langle \bar{E}_T \rangle \langle H \rangle + \langle H_T \rangle \langle E \rangle]$$

$$r_{00}^8 \sigma_0 \sim \text{Im} [\langle \bar{E}_T \rangle \langle H \rangle + \langle H_T \rangle \langle E \rangle]$$

$$\begin{aligned} \mathcal{W}^U(\Phi, \phi, \cos \Theta) = & \frac{3}{8\pi^2} \left[ \frac{1}{2}(1 - r_{00}^{04}) + \frac{1}{2}(3r_{00}^{04} - 1) \cos^2 \Theta - \sqrt{2} \text{Re}\{r_{10}^{04}\} \sin 2\Theta \cos \phi - r_{1-1}^{04} \sin^2 \Theta \cos 2\phi \right. \\ & - \epsilon \cos 2\Phi \left( r_{11}^1 \sin^2 \Theta + r_{00}^1 \cos^2 \Theta - \sqrt{2} \text{Re}\{r_{10}^1\} \sin 2\Theta \cos \phi - r_{1-1}^1 \sin^2 \Theta \cos 2\phi \right) \\ & \left. - \epsilon \sin 2\Phi \left( \sqrt{2} \text{Im}\{r_{10}^2\} \sin 2\Theta \sin \phi + \text{Im}\{r_{1-1}^2\} \sin^2 \Theta \sin 2\phi \right) \right. \\ & + \sqrt{2\epsilon(1 + \epsilon)} \cos \Phi \left( r_{11}^5 \sin^2 \Theta + r_{00}^5 \cos^2 \Theta - \sqrt{2} \text{Re}\{r_{10}^5\} \sin 2\Theta \cos \phi - r_{1-1}^5 \sin^2 \Theta \cos 2\phi \right) \\ & \left. + \sqrt{2\epsilon(1 + \epsilon)} \sin \Phi \left( \sqrt{2} \text{Im}\{r_{10}^6\} \sin 2\Theta \sin \phi + \text{Im}\{r_{1-1}^6\} \sin^2 \Theta \sin 2\phi \right) \right], \\ \mathcal{W}^L(\Phi, \phi, \cos \Theta) = & \frac{3}{8\pi^2} \left[ \sqrt{1 - \epsilon^2} \left( \sqrt{2} \text{Im}\{r_{10}^3\} \sin 2\Theta \sin \phi + \text{Im}\{r_{1-1}^3\} \sin^2 \Theta \sin 2\phi \right) \right. \\ & + \sqrt{2\epsilon(1 - \epsilon)} \cos \Phi \left( \sqrt{2} \text{Im}\{r_{10}^7\} \sin 2\Theta \sin \phi + \text{Im}\{r_{1-1}^7\} \sin^2 \Theta \sin 2\phi \right) \\ & \left. + \sqrt{2\epsilon(1 - \epsilon)} \sin \Phi \left( r_{11}^8 \sin^2 \Theta + r_{00}^8 \cos^2 \Theta - \sqrt{2} \text{Re}\{r_{10}^8\} \sin 2\Theta \cos \phi - r_{1-1}^8 \sin^2 \Theta \cos 2\phi \right) \right] \end{aligned}$$

# 2012 COMPASS Exclusive $\omega$ Prod. On Unpolarized Proton

SCHC ( $\lambda_\gamma = \lambda_V$ )

(S-Channel Helicity Conservation)

SCHC implies:

•  $r_{1-1}^1 + \text{Im} r_{1-1}^2 = 0$

=  $-0.010 \pm 0.032 \pm 0.047$  OK

•  $\text{Re} r_{10}^5 + \text{Im} r_{10}^6 = 0$

=  $0.014 \pm 0.011 \pm 0.013$  OK

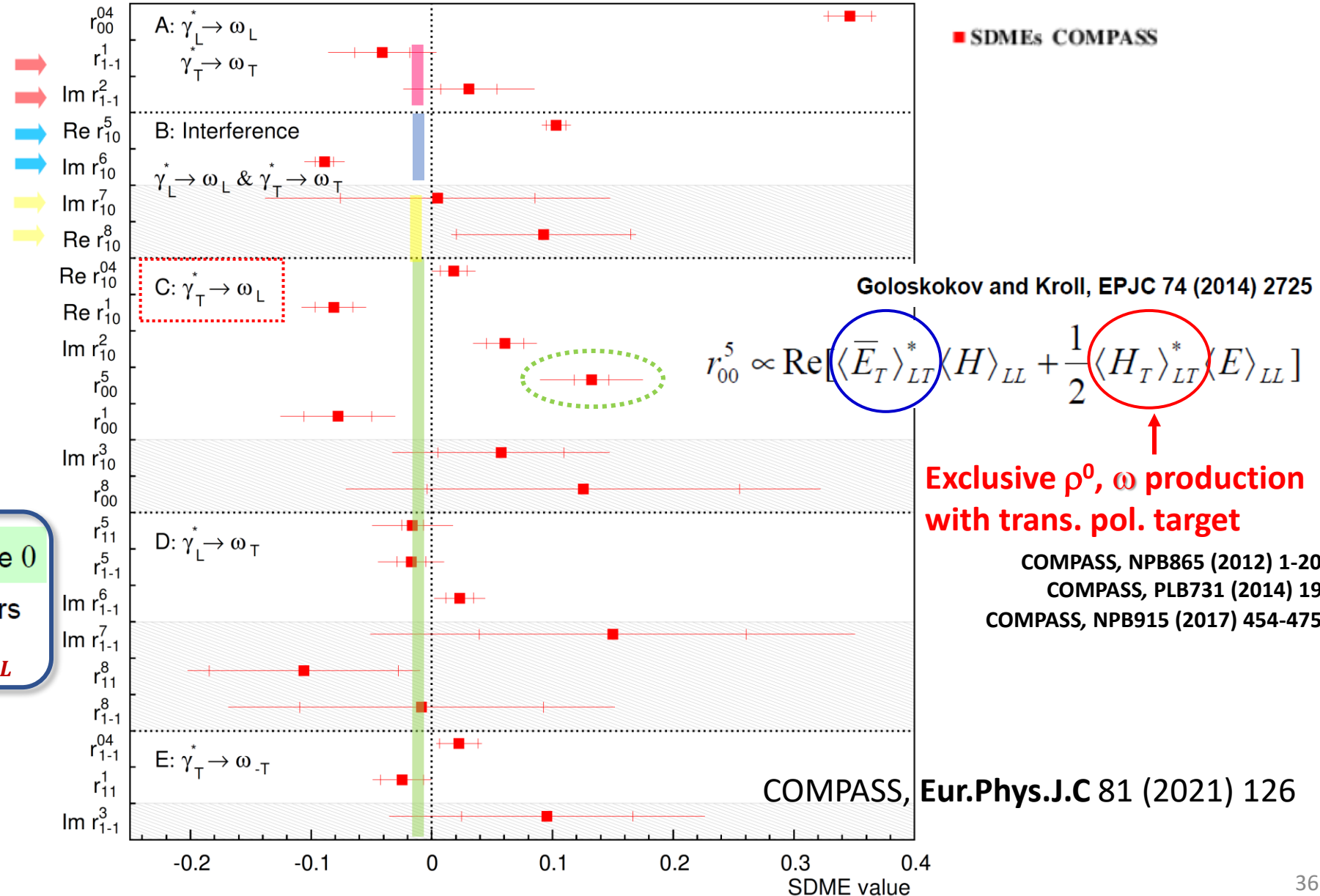
•  $\text{Im} r_{10}^7 - \text{Re} r_{10}^8 = 0$

=  $-0.088 \pm 0.110 \pm 0.196$  OK

• all elements of classes C, D, E should be 0

for  $\gamma_L^* \rightarrow \omega_T$  and  $\gamma_T^* \rightarrow \omega_T$  OK within errors

**NOT OBSERVED for transitions  $\gamma_T^* \rightarrow \omega_L$**



# 2012 COMPASS Exclusive $\rho^0$ Prod. On Unpolarized Proton

SCHC ( $\lambda_\gamma = \lambda_V$ )

(S-Channel Helicity Conservation)

SCHC implies:

•  $r_{1-1}^1 + \text{Im} r_{1-1}^2 = 0$  **OK**

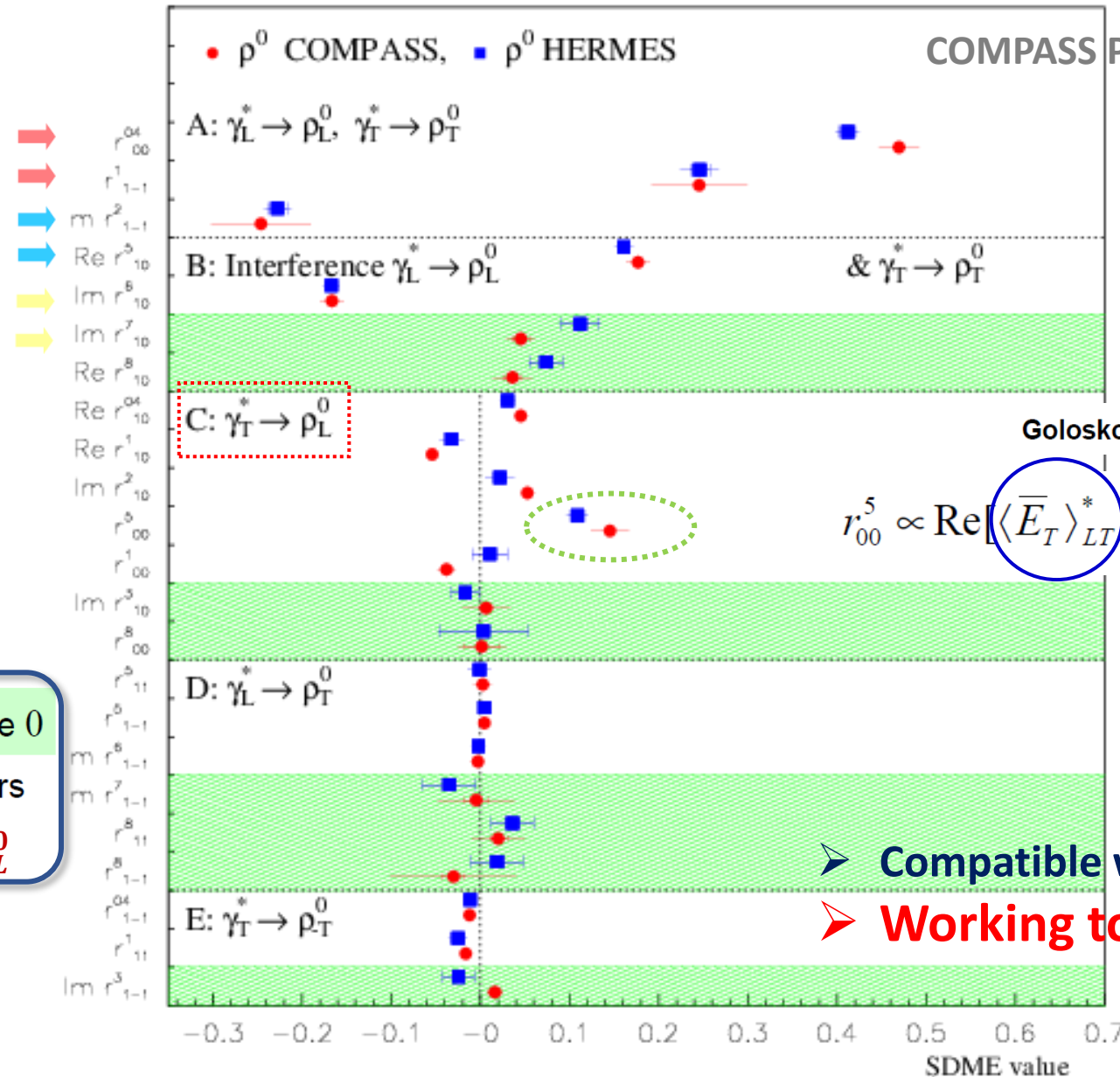
•  $\text{Re} r_{10}^5 + \text{Im} r_{10}^6 = 0$  **OK**

•  $\text{Im} r_{10}^7 - \text{Re} r_{10}^8 = 0$  **✓OK**

• all elements of classes C, D, E should be 0

for  $\gamma_L^* \rightarrow \rho_T^0$  and  $\gamma_T^* \rightarrow \rho_{-T}^0$  OK within errors

**NOT OBSERVED** for transitions  $\gamma_T^* \rightarrow \rho_L^0$



COMPASS Preliminary

Goloskokov and Kroll, EPJC 74 (2014) 2725

$$r_{00}^5 \propto \text{Re}[\langle \bar{E}_T \rangle_{LT}^* \langle H \rangle_{LL} + \frac{1}{2} \langle H_T \rangle_{LT}^* \langle E \rangle_{LL}]$$

**First term dominates**  
**→ Probes  $\bar{E}_T$**

➤ **Compatible with HERMES**  
 ➤ **Working towards publication!**

Other COMPTON Scatterings

# Timelike Compton Scattering (TCS)

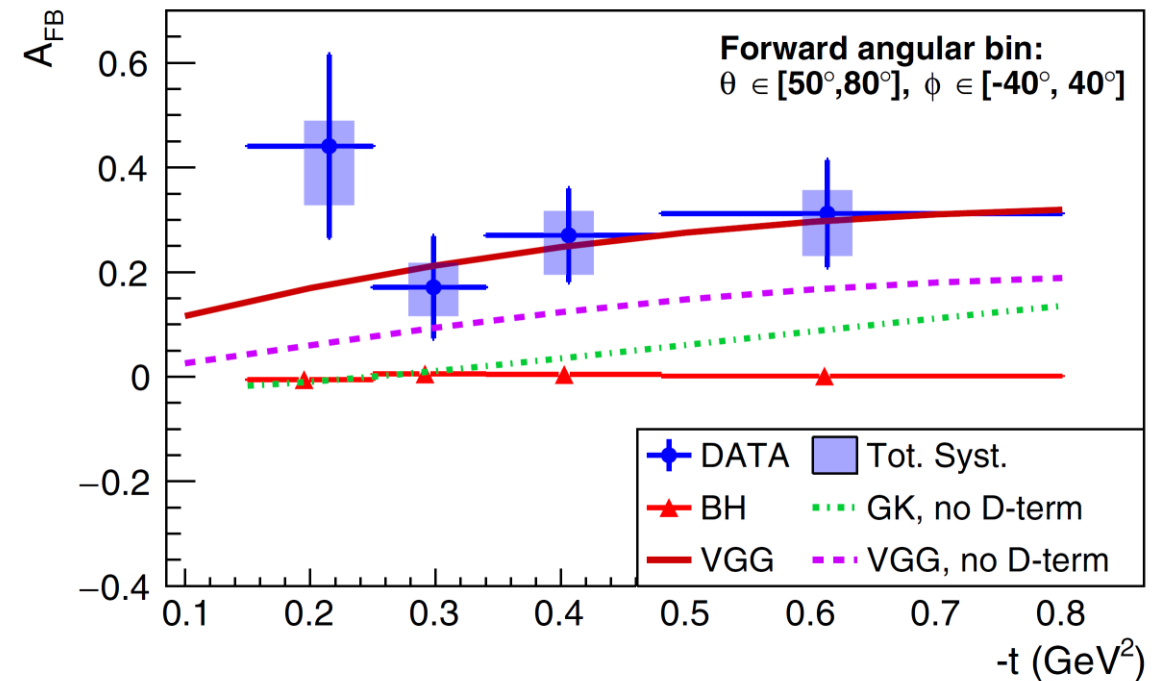
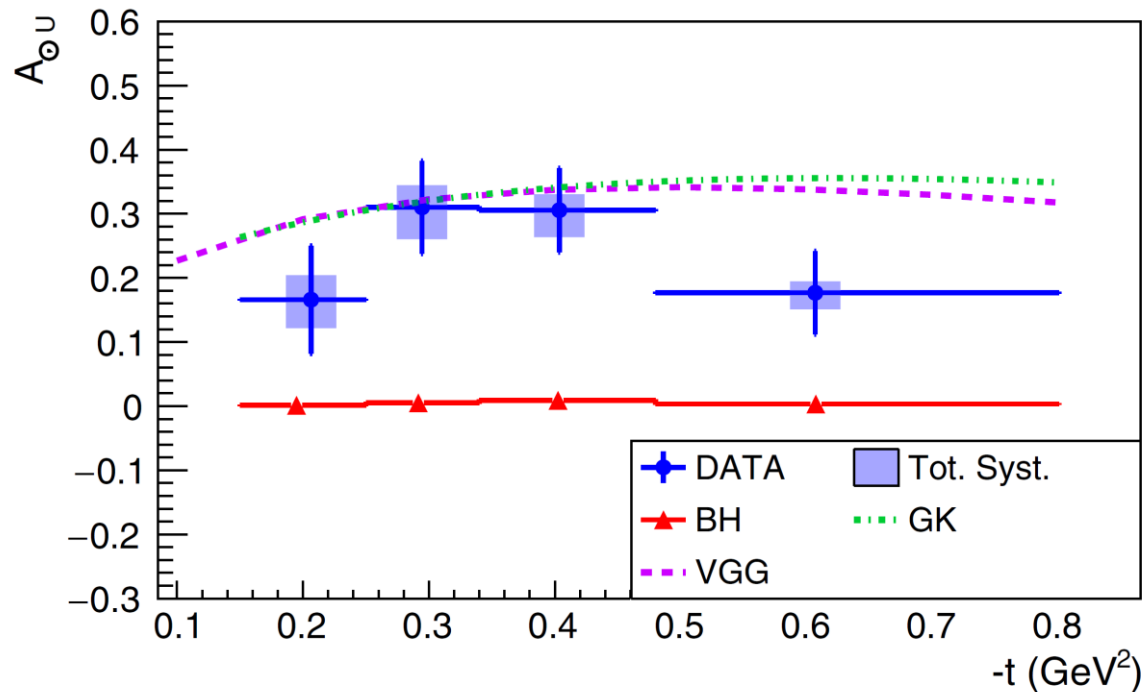
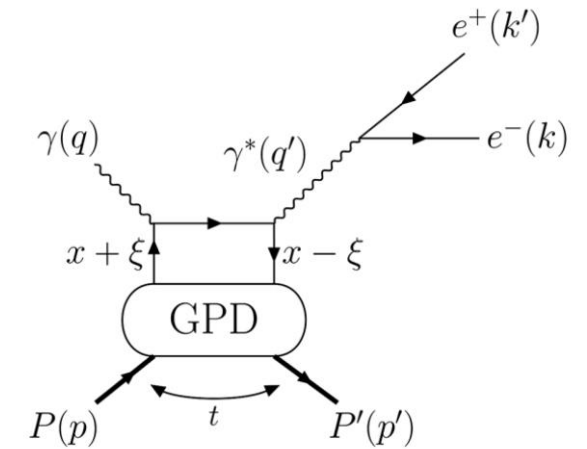
- First ever Timelike Compton Scattering Measurement at CLAS

*Phys. Rev. Lett. 127, 262501 (2021)*

- Photon polarization asymmetry  $A_{\odot U} \sim \sin\phi \cdot \text{Im}\tilde{M}^{--} \rightarrow$  **GPD universality**

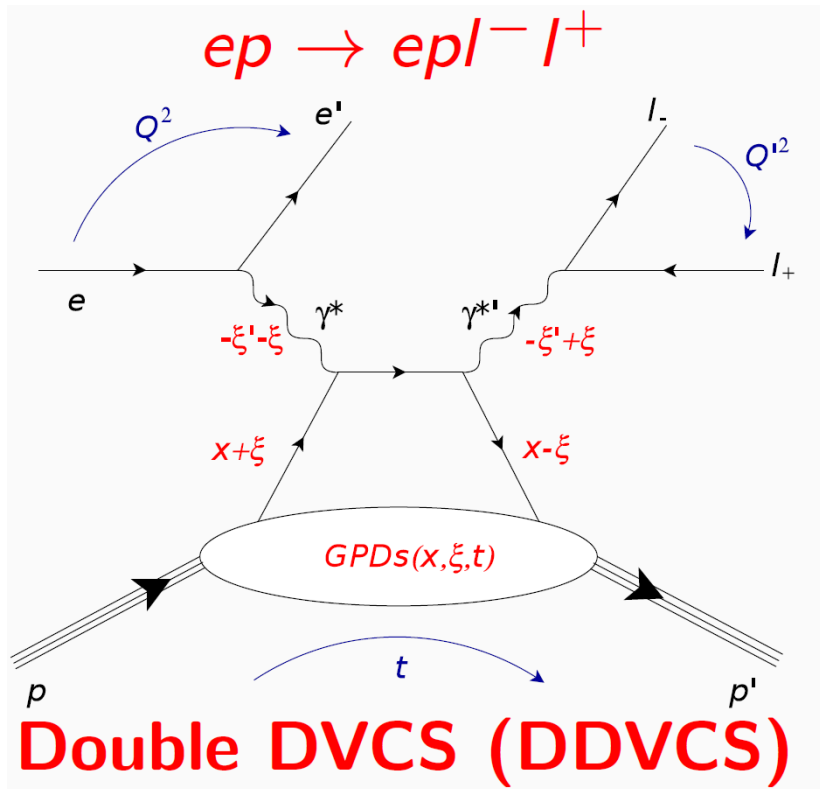
- Forward backward asymmetry  $A_{FB} \sim \cos\phi \cdot \text{Re}\tilde{M}^{--} \rightarrow$  **Access D-term**

$$\tilde{M}^{--} = \left[ \underline{F_1} \mathcal{H} - \xi(F_1 + F_2) \tilde{\mathcal{H}} - \frac{t}{4m_p^2} F_2 \mathcal{E} \right]$$





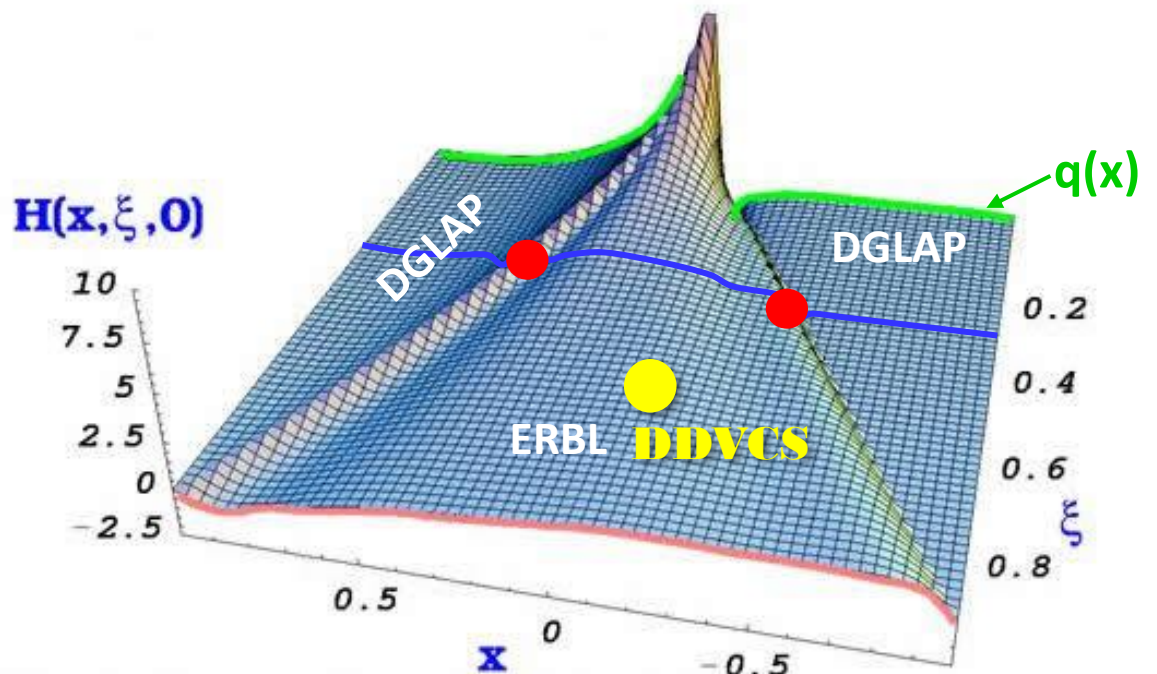
# Double DVCS (DDVCS)



- Both space-like and time-like photons can set the hard scale

$$\mathcal{H}(\xi', \xi, t) = \sum_q e_q^2 \left\{ \mathcal{P} \int_{-1}^1 dx H^q(x, \xi, t) \left[ \frac{1}{x - \xi'} + \frac{1}{x + \xi'} \right] - i\pi \left[ H^q(\xi', \xi, t) - H^q(-\xi', \xi, t) \right] \right\}$$

- Double DVCS gives access to phase space where  $x \neq \xi$
- VGG model: order of about 0.1 pb, about 100 to 1000 times smaller than DVCS
- **Interference term enhanced by BH**





A scenic landscape photograph featuring a vibrant turquoise lake in the center. The lake is framed by a dense forest of evergreen trees on both sides. In the background, majestic, rugged mountains with patches of snow rise against a clear blue sky with a few wispy clouds. The foreground shows a grassy clearing with some shadows cast by trees on the left.

**The view ahead  
– What do we expect?**

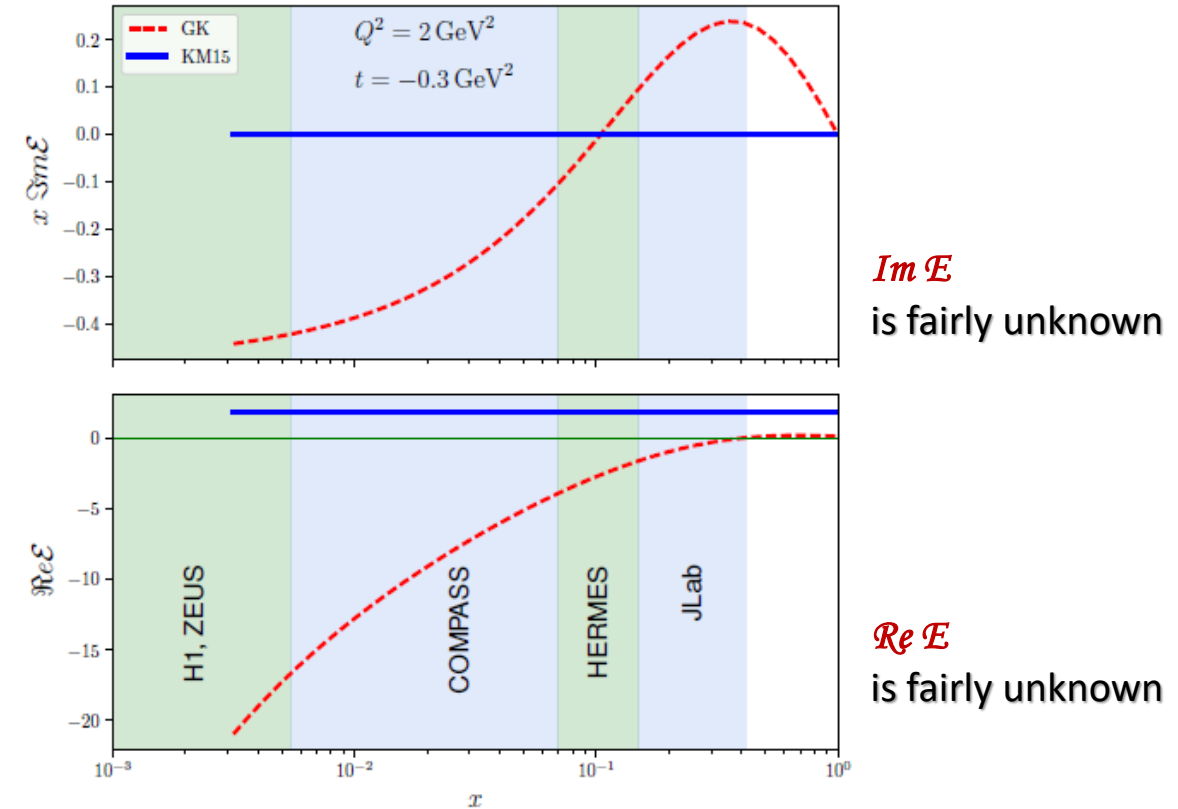
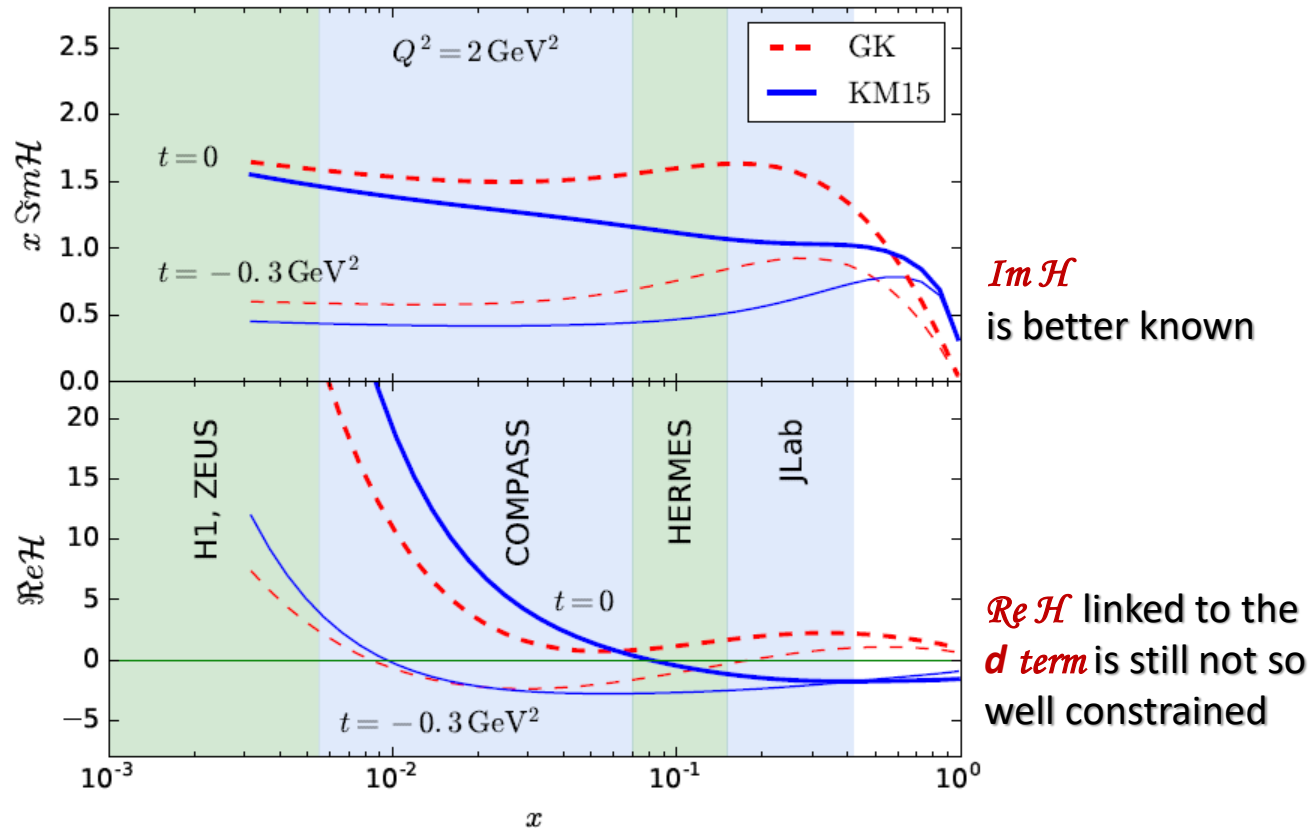


# Global Analysis

KM15 K Kumericki and D Mueller [arXiv:1512.09014v1](https://arxiv.org/abs/1512.09014v1)

GK S.V. Goloskokov, P. Kroll, EPJC53 (2008), EPJA47 (2011)

Figures made by D. Mueller and K. Kumericki



➤ Very little is known for chiral-odd GPDs as well.

➤ **We need more experimental inputs!**

- Various processes and precise data mapping, with high granularity and phase space wider than what has been covered, are required to fully constrain the entire set of GPDs

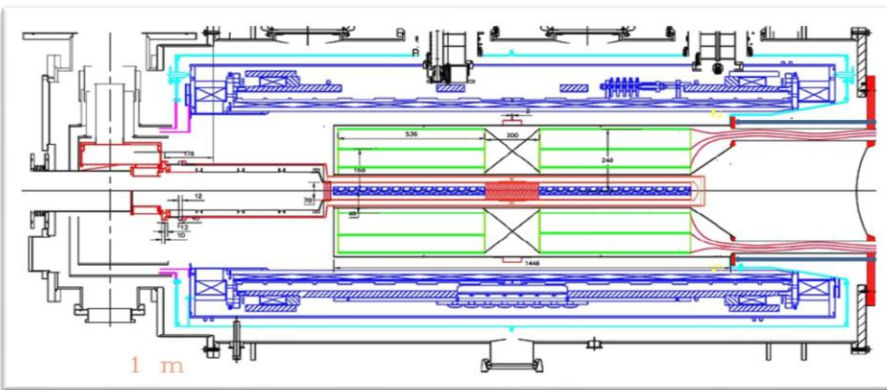
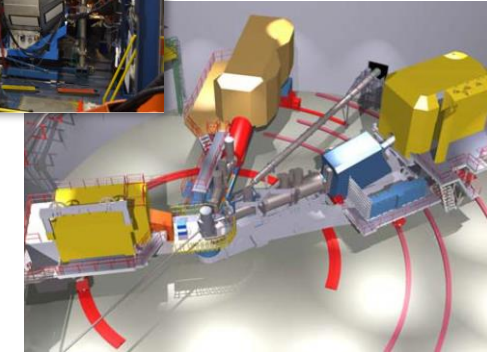
# Near Future

## ➤ Expect fruitful measurements coming from JLab-12

- Released: DVCS &  $\pi^0$  at Hall A, TCS at CLAS
- DVCS, nuclear DVCS, DVMP, TCS, even **DDVCS**?

## ➤ COMPASS/AMBER

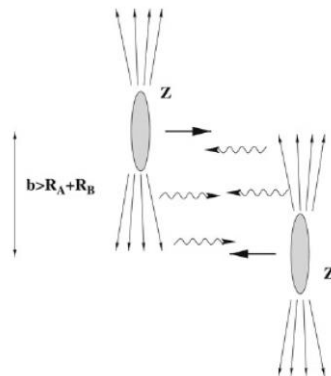
- DVCS  $\rightarrow$   $ReH$  with charge-spin asymmetry
- DVMP of  $\pi^0, \omega, \rho, J/\psi$
- Transversely polarized target in AMBER?



Silicone proton recoil detector between target & polarizing magnet

## ➤ Other possibilities at J-Parc, RHIC, FAIR, or LHC

- Exclusive Drell-Yan
- Ultra-peripheral collisions for TCS or exclusive  $J/\psi$  production for GPD E of the gluon



# The Ideal Experiment

## ➤ **High & variable beam energy**

- Large kinematic domain & hard regime → large  $Q^2$  span for evolution
- **Polarized** beams → various spin asymmetries
- Variable energy for:
  - Energy separation for DVCS<sup>2</sup> and DVCS-BH interferences
  - L/T separation for pseudo scalar meson production
- Availability of **positive** and **negative** leptons → real part of CFFs

## ➤ **H<sub>2</sub>, D<sub>2</sub>, and nuclear beams**

## ➤ **High luminosity**

- Small cross section
- Multi-dimensional binning for fully differential analysis ( $x_B, Q^2, t, \phi$ )

## ➤ **Hermetic detectors**

- Ensure exclusivity

***Does not exist (yet)***



# The Ideal Experiment – Challenges @ EIC

## ➤ High & variable beam energy

- Large
- Polarization
- Variable
- Average

### ➤ Beam polarization:

- For asymmetry measurements, statistical uncertainties inversely proportional to the degree of polarization achieved. → High polarization required.
- Longitudinal for  $e^-$ , transverse & longitudinal for polarizable nuclei → aim for ~70% polarization for both beams

## ➤ $H_2, I$

### ➤ Luminosity: one of the most demanding aspects of EIC

- Luminosity  $10^{33}$  to  $10^{34}$   $\text{cm}^{-1}\text{s}^{-1}$ . with  $10^{33}$   $\text{cm}^{-1}\text{s}^{-1}$ ,  $10 \text{ fb}^{-1}$  integrated luminosity achieved with 30 weeks of operation. GPD would ask for  $100 \text{ fb}^{-1}$  → needs higher luminosity of  $10^{34}$   $\text{cm}^{-1}\text{s}^{-1}$ .

## ➤ High

- Small
- Multiple

## ➤ Hermetic

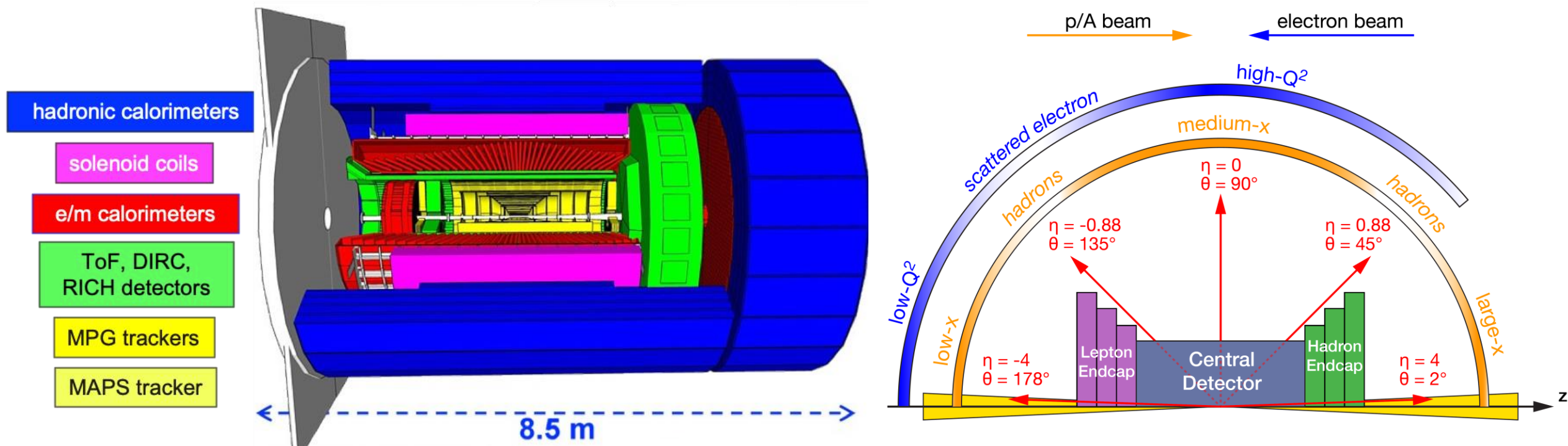
- Ensuring

➤  $0.03 < |t| < 1.6 \text{ GeV}^2$  → careful design of the interaction & hadron beam parameters

***Does not exist (yet)***

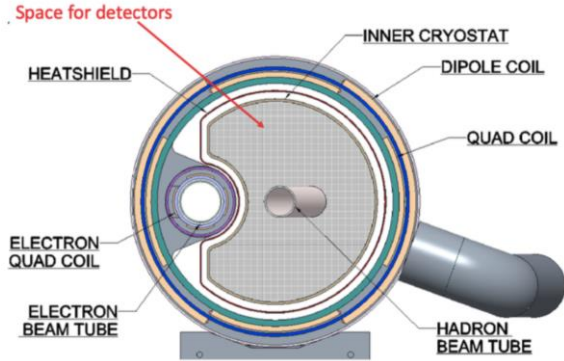
# The Electron Ion Collider

## Detector 1 $\rightarrow$ ePIC



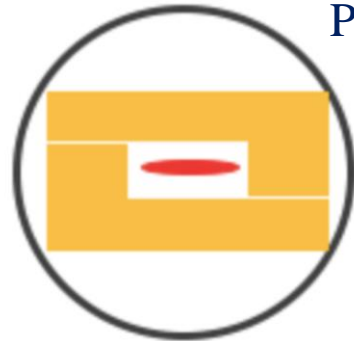
- **Auxiliary detectors** needed to tag particles with very small scattering angles both in the outgoing lepton and hadron beam direction.

# Far-Forward Detectors



B0 Spectrometer Configuration

Hadron beam pipe & Roman Pots in cross-section

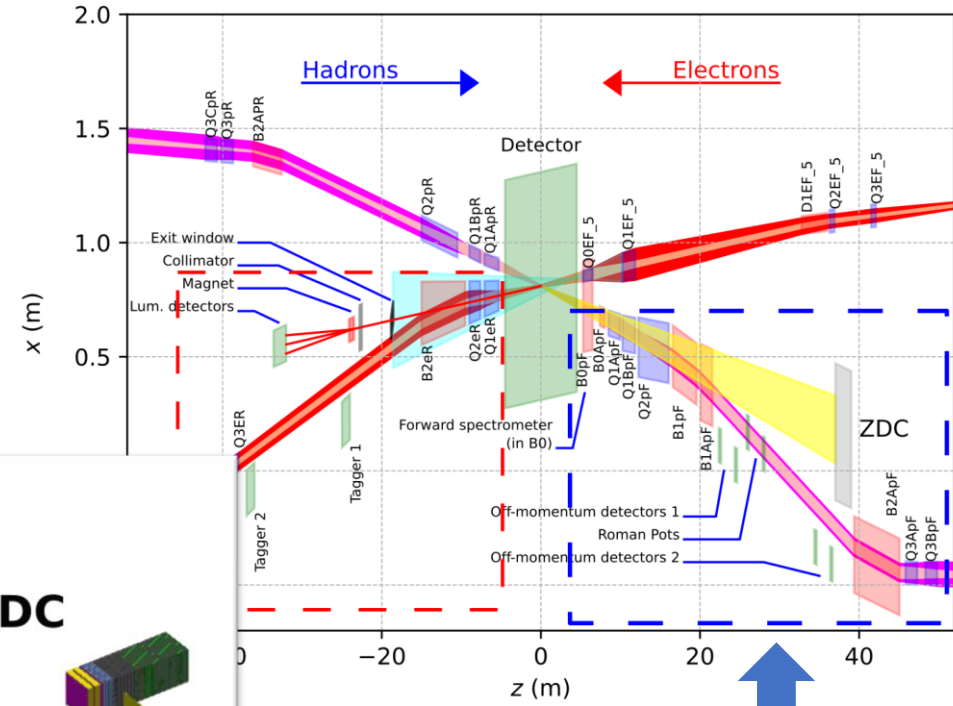
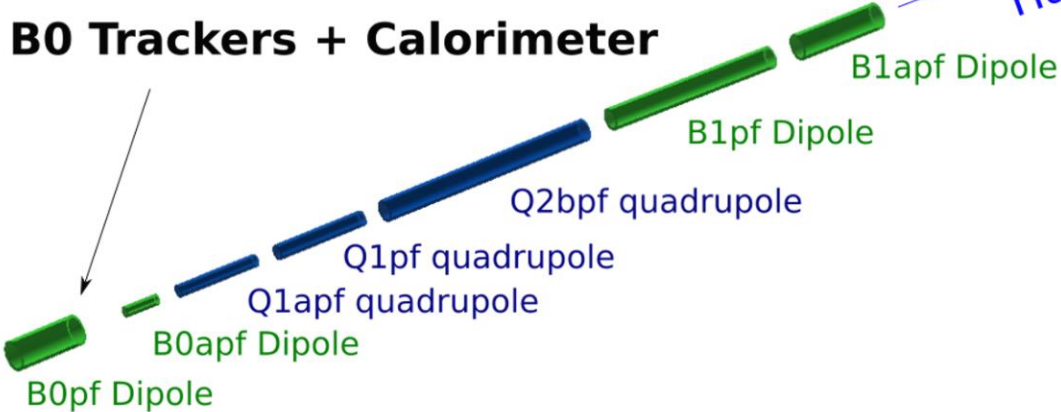


Roman Pots

Hadron Beam after IP

Off Momentum

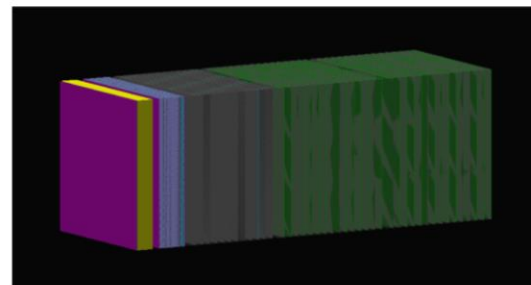
B0 Trackers + Calorimeter



➤ Forward detection particularly crucial in exclusive measurements - proton/ion measurement required

➤ B0 and/or Roman Pots are the critical forward detection regions

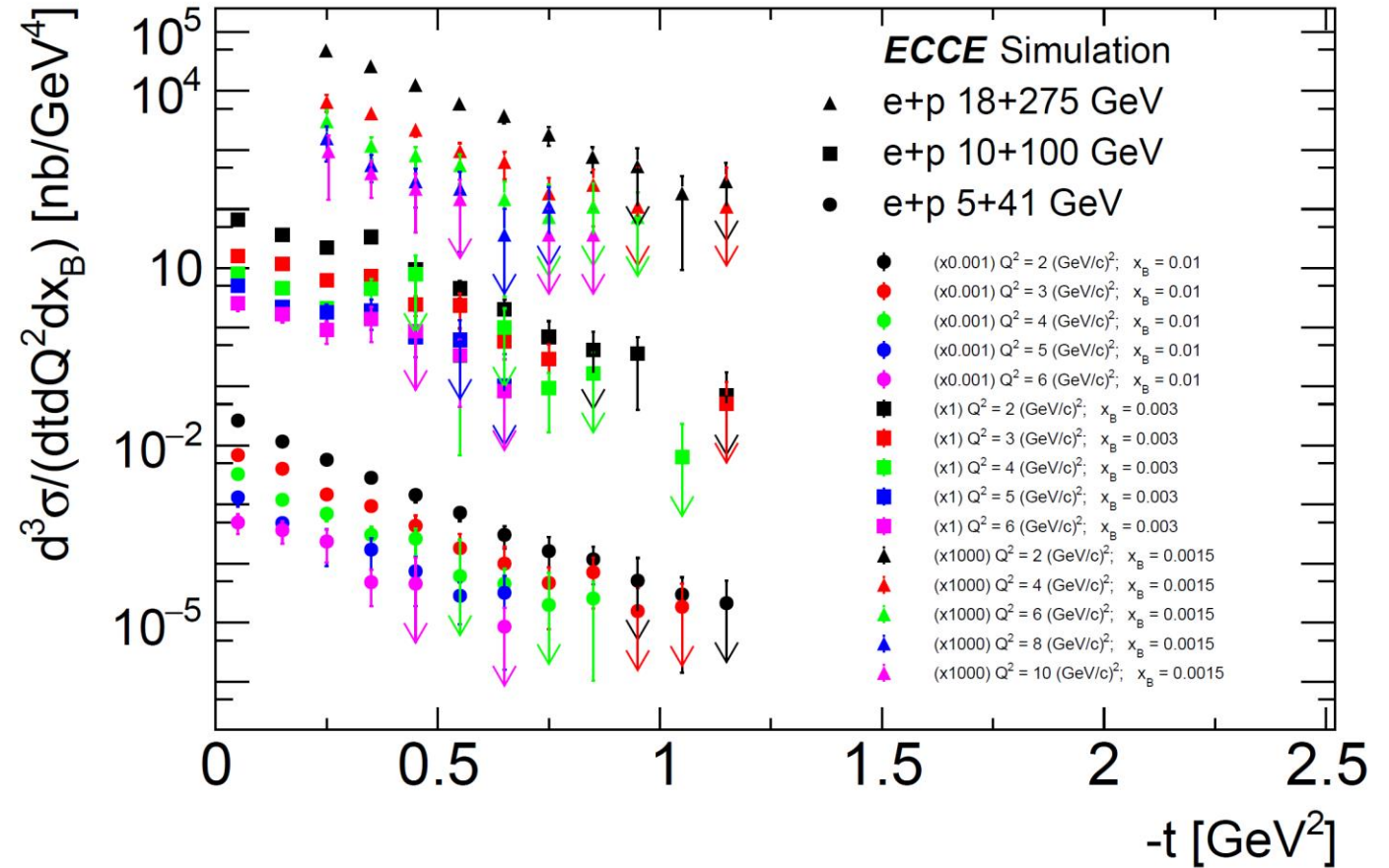
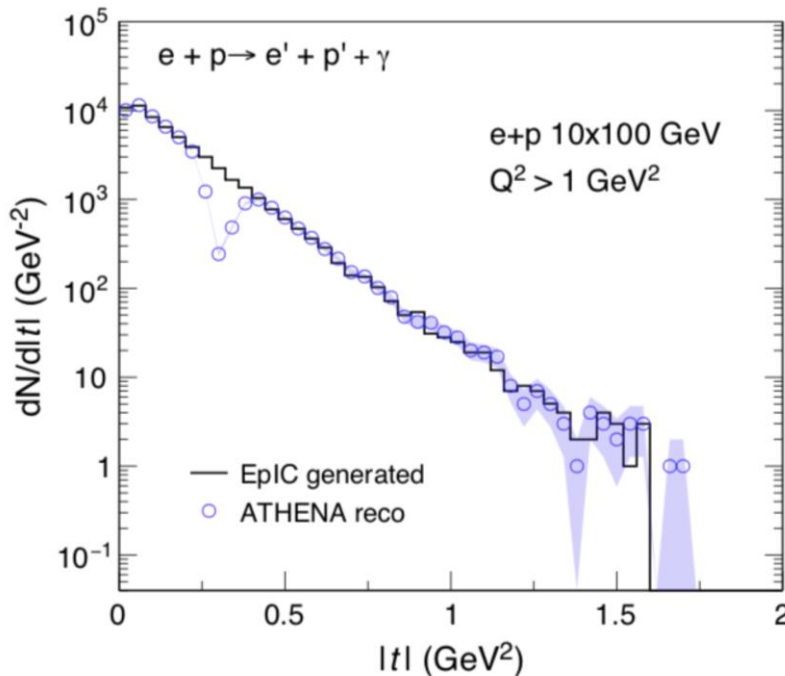
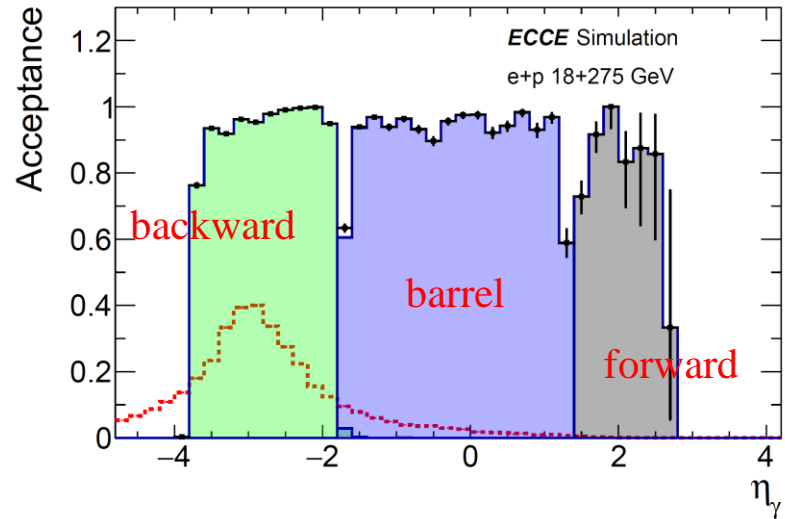
- Roman Pot: lowest values of  $t$
- B0: for higher values



ZDC

# DVCS Simulation

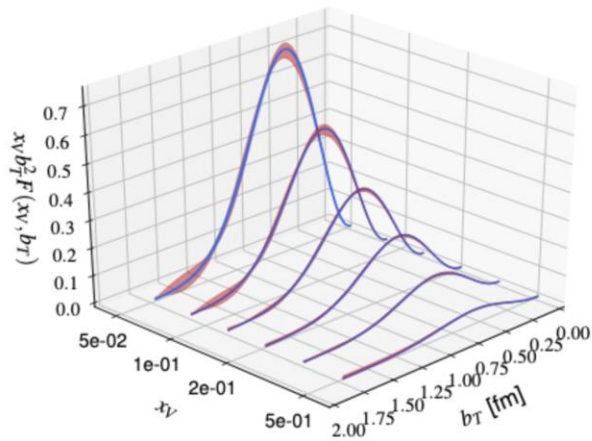
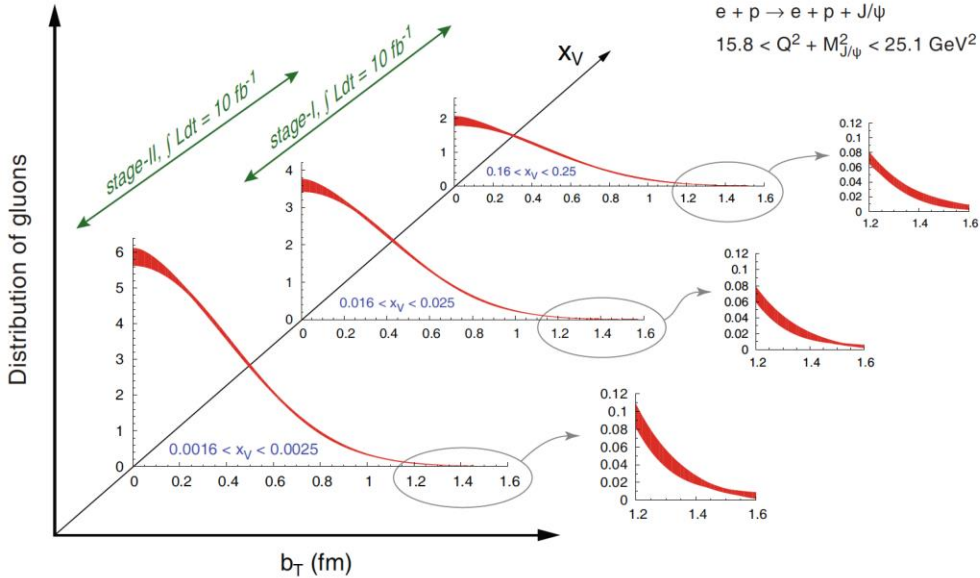
Plots: I. Korover (MIT), Kong Tu (BNL)



- Practically hermetic coverage for photons
- Wide range of  $t$
- Multi-dimensional binning possible

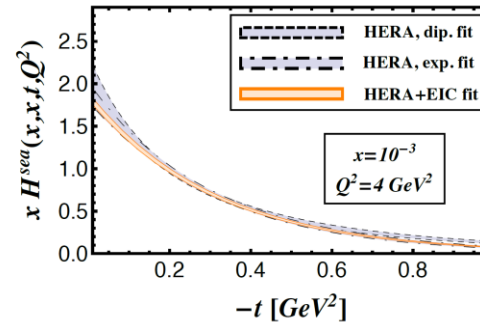


## Projected IPD from $J/\psi$

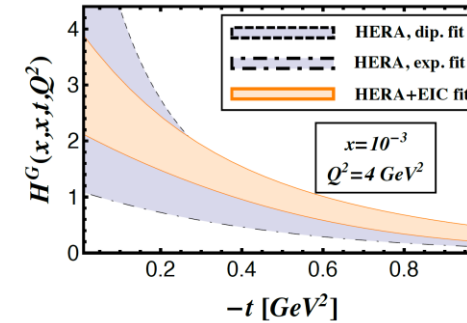


## Projected IPD from $\Upsilon$

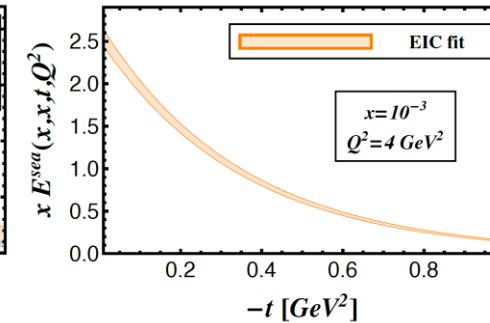
## GPD H - sea quarks



## GPD H - gluon



## GPD E - sea quarks



- Compton Scatterings – DVCS, TCS, DDVCS
  - GPD mapping, consistency of factorisation & universality test
- DVMP
  - Flavor separation, chiral-odd GPDs
  - heavy mesons ( $J/\psi$ ,  $\Upsilon$ )  $\rightarrow$  mechanism of saturation by gluon distribution from high to low  $x_B$
- New methods: diffractive process, charged-current processes of meson production...



# Summary

- A lot of interesting properties of proton can be revealed by GPDs and EIC can offer us unprecedented opportunity for a precise determination of GPDs.
- **Let's build it.**



# **Backup Slides**

# GPD Models

## ● VGG model (Vanderhaeghen, Guichon, Guidal 1999):

- Based on double distributions
- Includes a D-term to restore full polynomiality
- Includes a Regge inspired and a factorized t-ansatz
- Skewness depending on free parameters  $b_{val}$  and  $b_{sea}$
- Includes twist-3 contributions

## ● Dual model: (Guzey, Teckentrup 2006)

- GPDs based on an infinite sum of t-channel resonances
- Includes a Regge inspired and a factorized t-ansatz
- Does not include twist-3

**KM10a** — — — **(KM10 .....**) Kumericki, Mueller, NPB (2010) 841

Flexible parametrization of the GPDs based on both a Mellin-Barnes representation and dispersion integral which entangle skewness and t dependences

**Global fit on the world data ranging from H1, ZEUS to HERMES, JLab**

**VGG** Vanderhaeghen, Guichon, Guidal  
PRL80(1998), PRD60(1999), PPNP47(2001), PRD72(2005)

1st model of GPDs

improved regularly

**KMS12** Kroll, Moutarde, Sabatié, EPJC73 (2013)

using the **GK** model

Goloskokov, Kroll, EPJC42,50,53,59,65,74

for GPD adjusted on

the hard exclusive meson production at small  $x_B$

**“universality”** of GPDs

## Transversity in hard exclusive electroproduction of pseudoscalar mesons

S.V. Goloskokov<sup>1,a</sup> and P. Kroll<sup>2,3,b</sup>

- **UNPOLARIZED STRUCTURE FUNCTIONS:**

$$\sigma_L \sim \left\{ (1 - \xi^2) |\langle \tilde{H} \rangle|^2 - 2\xi^2 \text{Re} [\langle \tilde{H} \rangle^* \langle \tilde{E} \rangle] - \frac{t'}{4m^2} \xi^2 |\langle \tilde{E} \rangle|^2 \right\}$$

$$\sigma_T \sim \left[ (1 - \xi^2) |\langle H_T \rangle|^2 - \frac{t'}{8m^2} |\langle E_T \rangle|^2 \right]$$

$$\sigma_{TT} \sim |\langle \bar{E}_T \rangle|^2$$

- **POLARIZED OBSERVABLES:**

$$A_{LU}^{\sin \phi} \sigma_0 \sim \text{Im} [\langle H_T \rangle^* \langle \tilde{E} \rangle]$$

$$A_{UL}^{\sin \phi} \sigma_0 \sim \text{Im} [\langle \bar{E}_T \rangle^* \langle \tilde{H} \rangle + \xi \langle H_T \rangle^* \langle \tilde{E} \rangle]$$

$$A_{LL}^{\cos 0\phi} \sigma_0 \sim |\langle H_T \rangle|^2$$

$$A_{LL}^{\cos \phi} \sigma_0 \sim \text{Re} [\langle \bar{E}_T \rangle^* \langle \tilde{H} \rangle + \xi \langle H_T \rangle^* \langle \tilde{E} \rangle]$$

$$\bar{E}_T = 2\tilde{H}_T + E_T$$

$\langle F \rangle$ : Generalized Form Factor, convolution of hard subprocess with GPD F

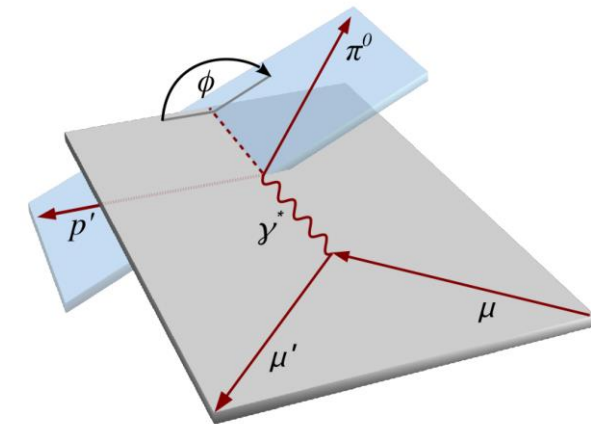
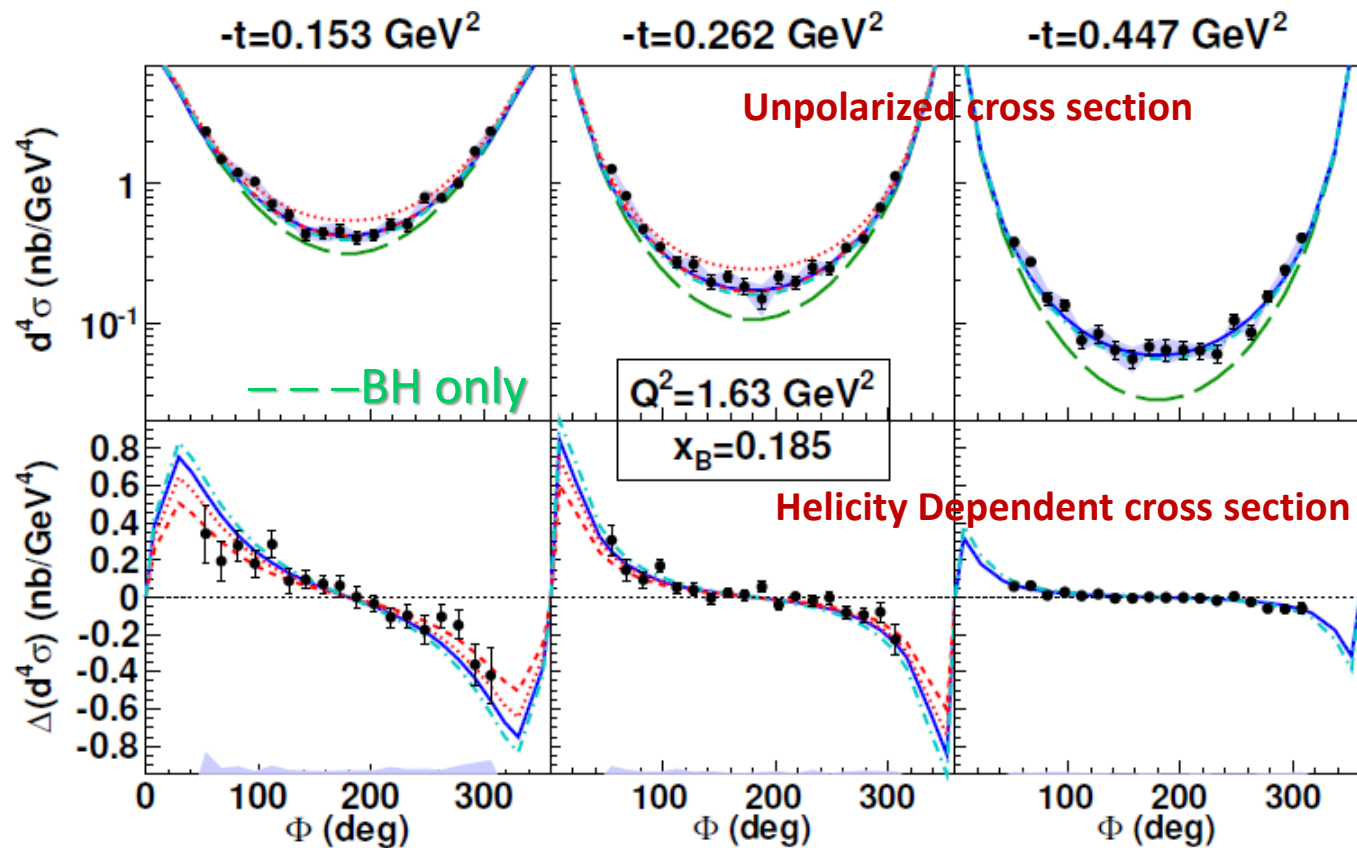


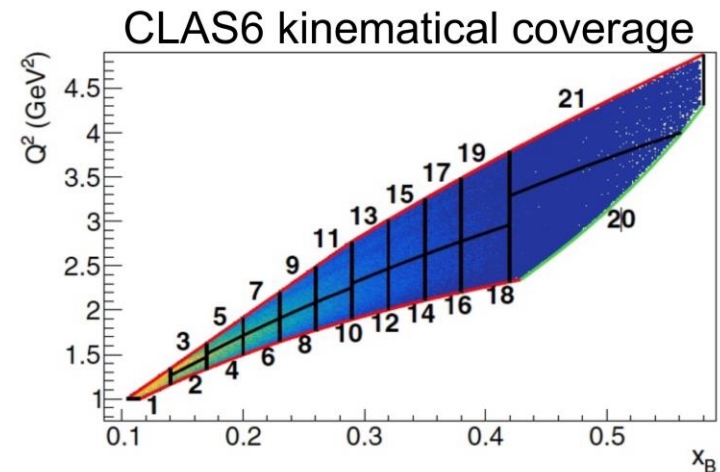
Fig: M.G. Alexeev et al. *Phys.Lett.B* 805 (2020)

# Beam Spin Sum and Diff of DVCS at CLAS

- Wide kinematic range → 21 bins in  $(x_B, Q^2)$  or 110 bins  $(x_B, Q^2, t)$  with 3 months data taken in 2005
- CFF constraints



$$\overleftarrow{e} p \rightarrow e \gamma p$$



- BH only
- VGG (Vanderhaeghen, Guichon, Guidal) - H only
- ⋯ KM10 (Kumericki, Mueller) includes strong  $\tilde{H}$
- - - KM10a (sets  $\tilde{H}$  to zero)
- - - KMS (Kroll, Moutarde, Sabatié, tuned on low  $x_B$  meson-production data)



# Nucleon Tomography in the Valence Domain

- Wide kinematic range → 21 bins in  $(x_B, Q^2)$  or 110 bins  $(x_B, Q^2, t)$  with 3 months data taken in 2005
- ➔ **Nucleon tomography in the valence domain**

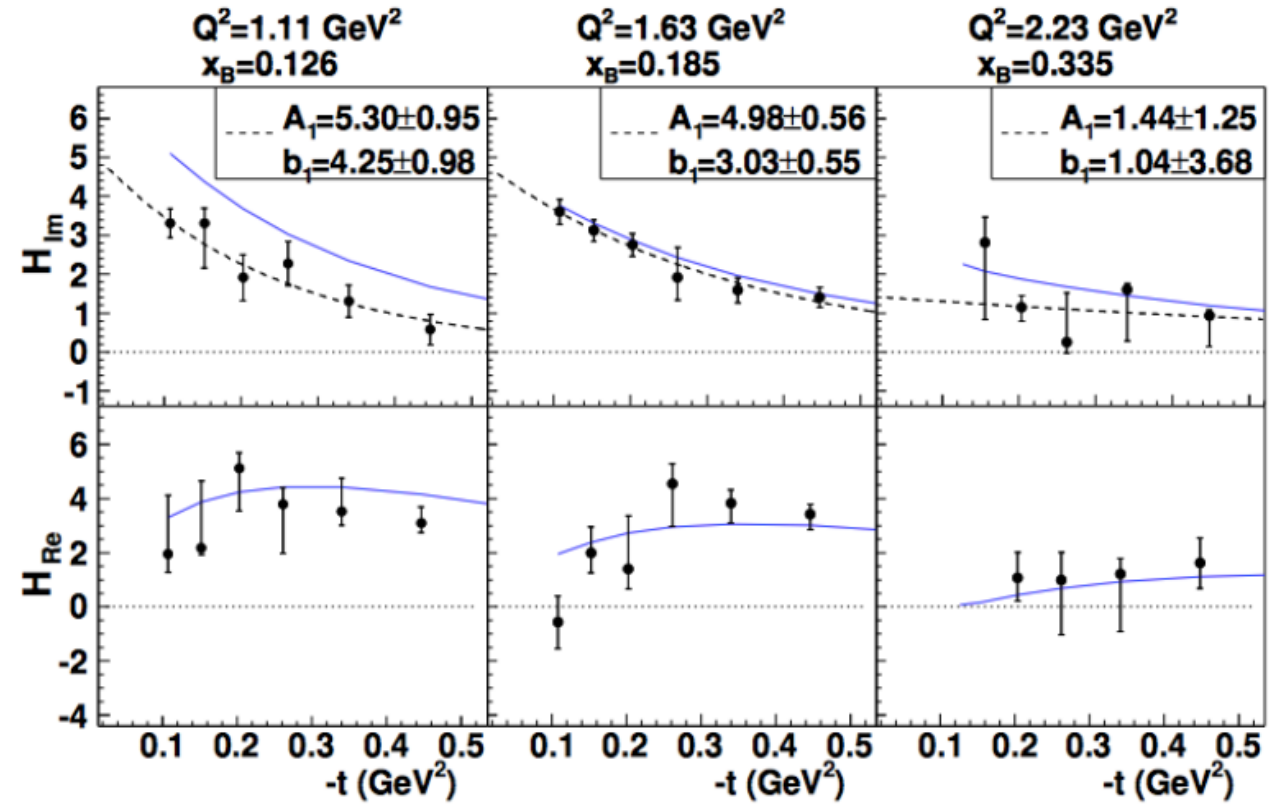
— VGG model  
 - - - Fit  $\text{Im}\mathcal{H} = A e^{-B|t|}$

Fit of 8 CFFs at **L.O.** and **L.T.**  
 ( $\text{Im}H$ ,  $\text{Re}H$ ,  $\text{Im}E$ ,  $\text{Re}E$ ,  $\text{Im}\tilde{H}$ ,  $\text{Re}\tilde{H}$ ,  $\text{Im}\tilde{E}$ ,  $\text{Re}\tilde{E}$ )

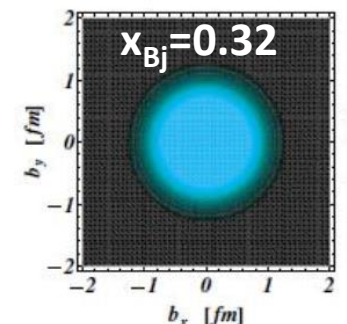
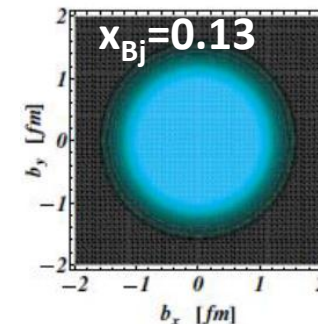
- Dominance of  $H$  in unpolarized cross-section.
- $H_{\text{Im}}$  slope  $B$  give information on the trasverse extension of the partons → becomes flatter at higher  $x_B$



Valence quarks at centre  
 Sea quarks spread out towards the periphery.



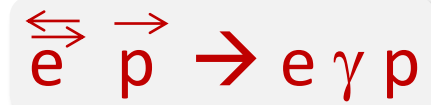
Guidal,  
 Moutarde,  
 Vanderhaeghen,  
 PNPP 76 (2013)



# Beam- and Target-spin asymmetries at CLAS

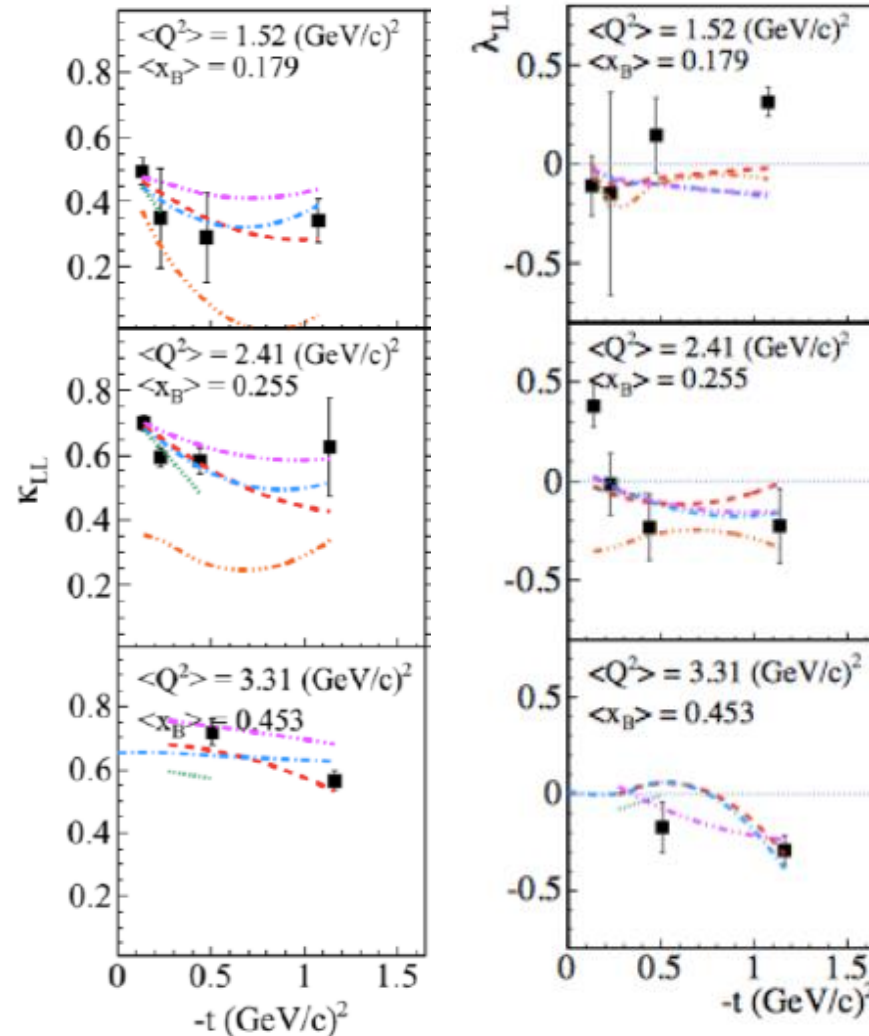
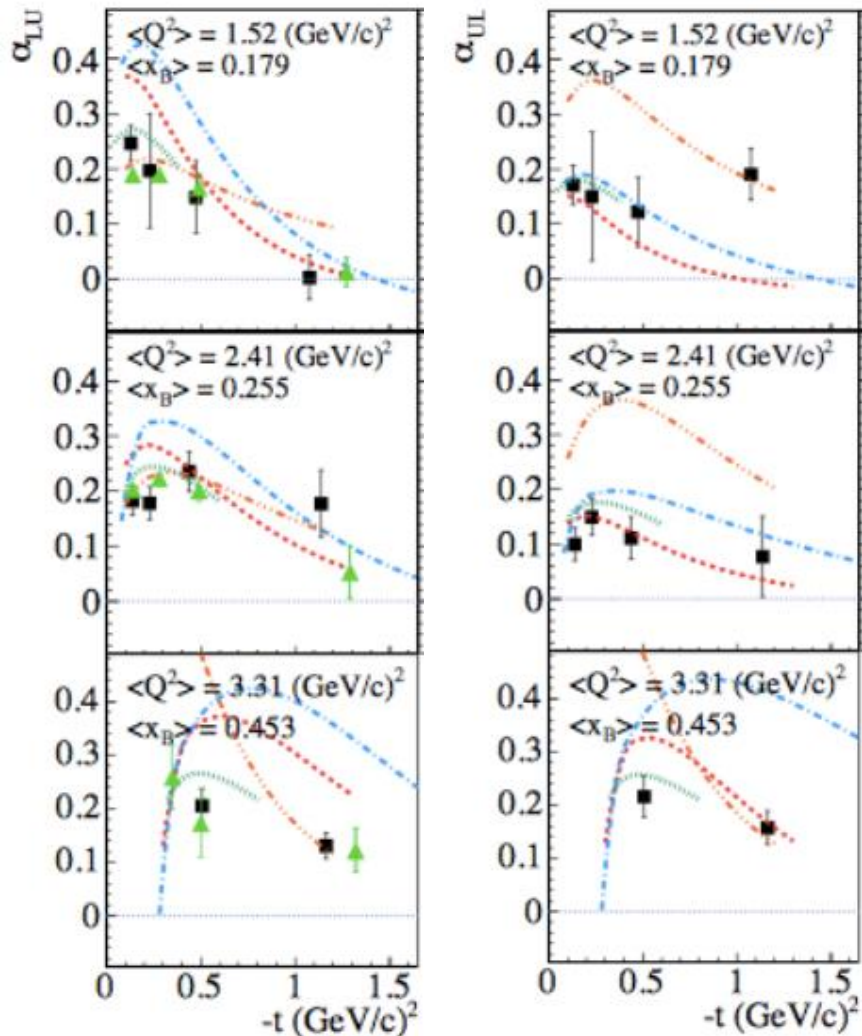
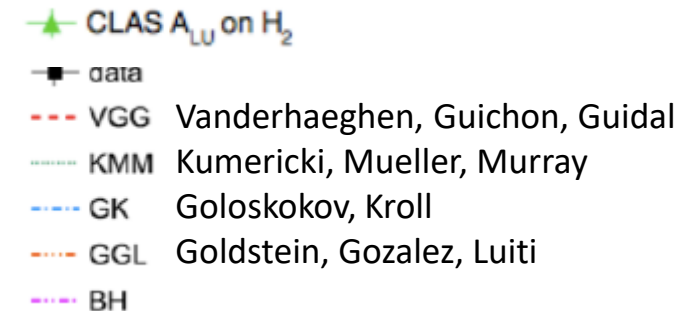
$$A_{LU(UL)} = \frac{\alpha_{LU(UL)} \sin \phi}{1 + \beta \cos \phi}$$

$$A_{LL} = \frac{\kappa_{LL} + \lambda_{LL} \cos \phi}{1 + \beta \cos \phi}$$



Longitudinally polarized NH<sub>3</sub> target on 2009

- LU consistent with previous data
- UL for parameterizing the  $t$ -dependence of  $H$  &  $\tilde{H}$
- Dominance of BH in  $A_{LL}$
- Simultaneous fit to BSA, TSA and DSA.



# Nucleon Tomography in the Valence Domain

Fit of 8 CFFs at L.O and L.T. Dupré, Guidal, Nicolai, Vanderhaeghen, PRD95, 011501(R)(2017) Eur.Phys.J. A53 (2017)

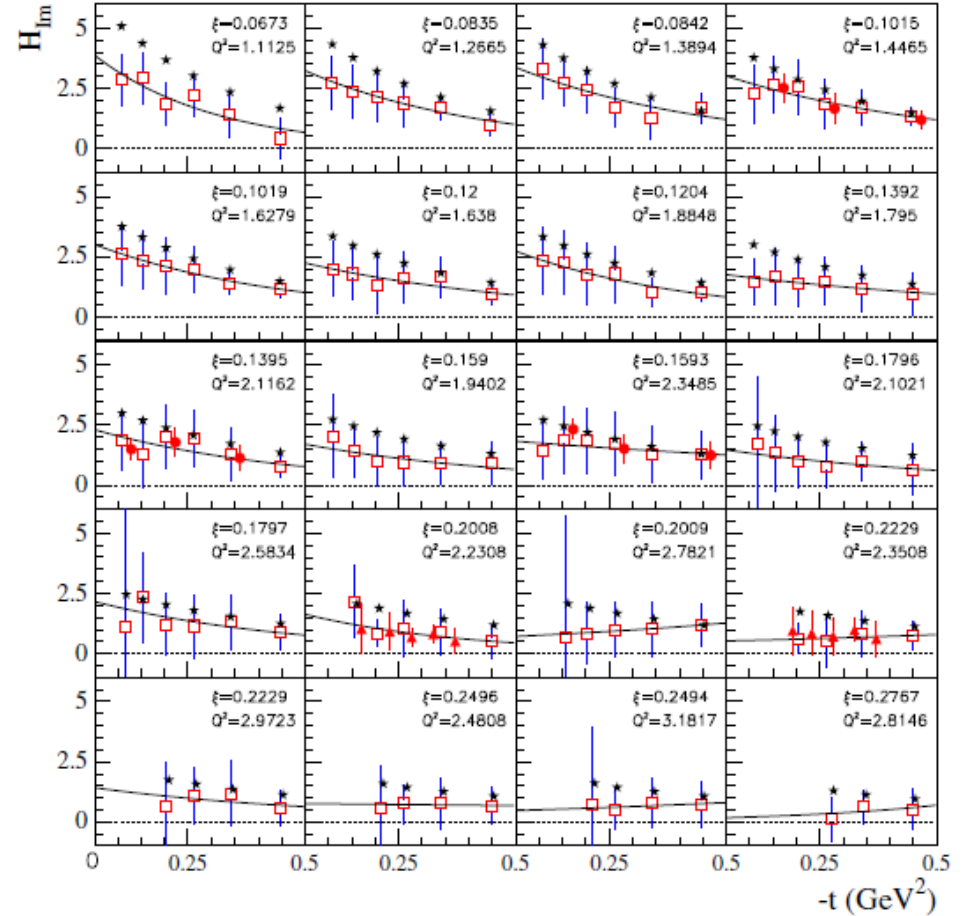
$s_1^I = \text{Im } F_1 \mathcal{H}$  is the best constrained

$$\rho^q(x, \mathbf{b}_\perp) = \int \frac{d^2 \Delta_\perp}{(2\pi)^2} e^{-i\mathbf{b}_\perp \cdot \Delta_\perp} H_-^q(x, 0, -\Delta_\perp^2).$$

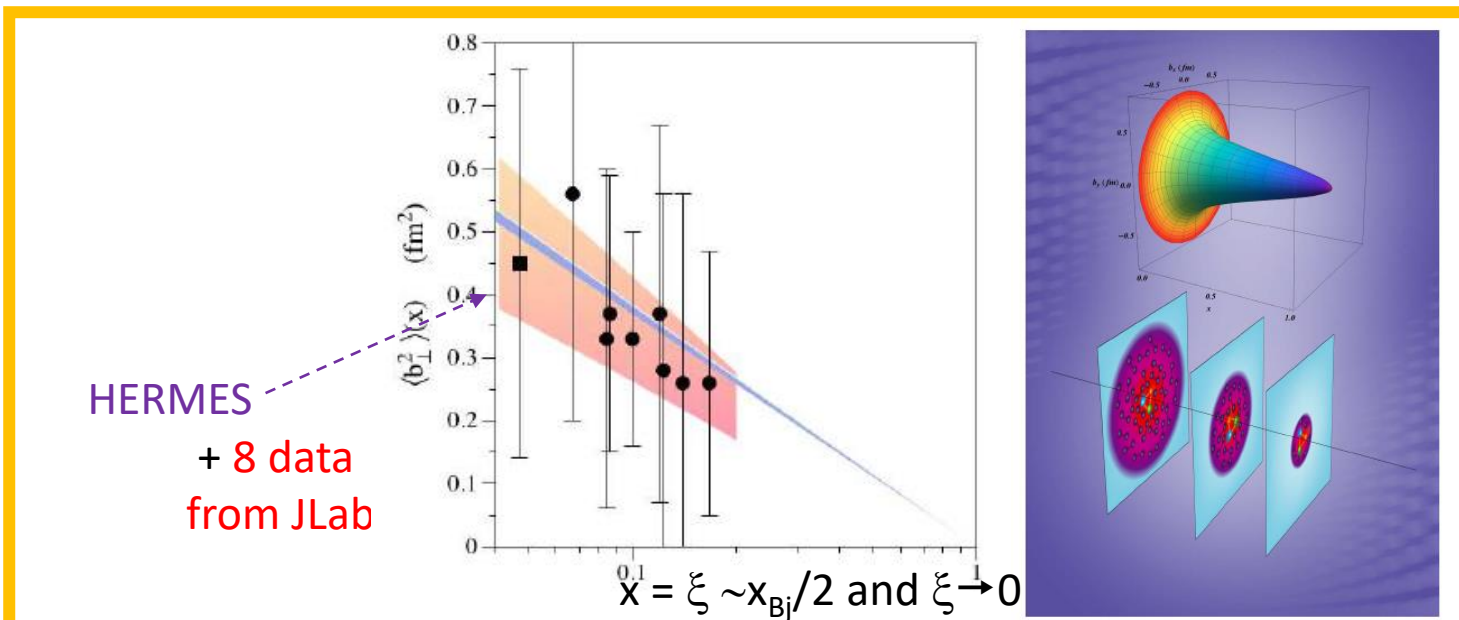
$$\langle b_\perp^2 \rangle^q(x) = -4 \frac{\partial}{\partial \Delta_\perp^2} \ln H_-^q(x, 0, -\Delta_\perp^2) \Big|_{\Delta_\perp=0}.$$

$$\langle b_\perp^2 \rangle \approx 4 B$$

— Fit  $A e^{-B|t|}$



- CLAS  $\sigma$  and  $\Delta\sigma$
- ▲ HallA  $\sigma$  and  $\Delta\sigma$
- CLAS  $A_{UL}$  and  $A_{LL}$
- ★ VGG model



HERMES  
+ 8 data  
from JLab